PHYSICAL MAP OF THE AUSTRALIAN CENTRAL BEARDED DRAGON (*Pogona vitticeps*) AND COMPARATIVE MAPPING AMONG DRAGONS (Squamata, Agamidae) AND AMNIOTES

By

MATTHEW JOHN YOUNG

B. Environmental Science

Institute for Applied Ecology

University of Canberra

Australia

A thesis submitted in partial fulfilment of the requirements for the degree of Bachelor of Applied Science (Honours) at the University of Canberra.

January 2011

Abstract

This study examines mechanisms of genome evolution among amniotes. Amniota comprises members of Sauropsida (reptiles and birds) and their sister taxa Synapsida (mammals). Within Sauropsida, squamate reptiles are phylogenetically placed in Lepidosauria (lizards, snakes and tuatara), the sister taxa of Archosauria (birds, crocodiles and turtles). As such, squamates hold a key phylogenetic position in elucidating the mechanisms of genome evolution among amniotes and provide critical contrast to the insights already gained from research on mammalian and avian genomes. However, decidedly few squamate genomes have been characterised and there are currently no physical maps spanning the entire karyotype of any squamate species. This study aims to address this knowledge gap by characterising the genome of a squamate reptile and examining mechanisms of genome evolution between squamates and among amniotes.

In this study I have constructed the first Bacterial Artificial Chromosome (BAC)-based physical map of an Australian reptile, the central bearded dragon, *Pogona vitticeps* (Agamidae). I used a cross-species approach to construct the first BAC-based agamid comparative map between *P. vitticeps* and the eastern water dragon (*Physignathus lesueurii*). Furthermore, I used these data to construct a comparative map between *P. vitticeps*, chicken (*Gallus gallus*) and human (*Homo sapiens*).

Seventy-three *P. vitticeps* BAC clones were mapped to *P. vitticeps* mitotic metaphase chromosomes using fluorescence *in situ* hybridisation (FISH) and end sequenced. The karyotype of *P. vitticeps* consists of 12 macrochromosomes and 10 microchromosomes. The *P. vitticeps* physical map has 71 diagnostic clones and 35 genic loci spanning all macrochromosomes and some microchromosomes. The genome-wide GC composition was estimated to be 42.3 percent, suggesting a similar composition to other squamates. Forty *P. vitticeps* clones were mapped by FISH to *P. lesueurii* chromosomes demonstrating the value of cross-species BAC mapping as a method for constructing low-resolution comparative maps among squamates. Mechanisms of genome evolution and ancestral syntenies are explored , including the evolution of *P. vitticeps* ZW sex chromosomes, the recent activity of retrotransposons in squamate genomes and the mechanism of

chromosome number reduction in Australian agamids. Indirect evidence of a shared origin between previously proposed non-orthologous sex chromosomes is presented.

In conclusion, this study has developed and demonstrated the value of a physical map of the model squamate *P. vitticeps* with a set of molecular anchor markers that with minimal further experimentation may prove to span the entire karyotype of this species. Once it is complete, it is envisioned that this genomic resource will contribute substantially to future research in the field of comparative genomics. Further, this study illustrates how cytogenetic research on squamate genomes can provide valuable insight into elucidating the mechanisms of genome evolution among all amniotes.

Certificate of Authorship of Thesis

Except where clearly acknowledged in footnotes, quotations and the bibliography, I certify that I am the sole author of the thesis submitted today entitled -

Physical map of the Australian central bearded dragon (*Pogona vitticeps*) and comparative mapping among dragons (Squamata, Agamidae) and amniotes

in terms of the Statement of Requirements for a Thesis issued by the University Research Degrees Committee.

……

Signature of Author

……..

Date

Acknowledgements

Firstly, I would like to thank my supervisors Asst Prof. Tariq Ezaz, Prof. Arthur Georges and Dr. Denis O'Meally for the opportunity to work on such a challenging and interesting project. Thank you for your advice, guidance, and enthusiasm throughout all aspects of my work. Special thanks must be given to Denis, who gave me my first introduction to FISH and who made sure I didn't get lost amongst the chromosomes or DNA sequence analysis.

To my family Annette, Peter and Belinda, thank you for your love and support throughout this demanding year.

For funding of this project, I would like to thank the University of Canberra, Institute for Applied Ecology and the Australian Research Council.

Thanks must also be given to the Wildlife Genetics Laboratory researchers for their advice, guidance and friendship, especially Juliet Ward for taking me under her wing.

And finally, a big thank you to everyone in the postgraduate room, the Wildlife Genetics Laboratory researchers, and staff from the Institute for Applied Ecology for providing great company and friendship and making the workplace an enjoyable place to be in. Special thanks to Kate Hodges for her great company on weekends, her shared passion for sliding in socks down newly polished corridors late at night and her helping hand when it came to a map of Australia.

Table of Contents

Abstract i

Acknowledgements iv

List of Figures viii

List of Tables x

Abbreviations xi

Chapter 1: Introduction 1

1.1 Overview 1

1.2 The development of physical maps 1

1.2.1 *Gene mapping* 1

1.2.2 *Attributes of physical maps* 2

1.2.3 *Fluorescent in situ hybridization (FISH) and gene mapping* 4

1.2.4 *Bacterial artificial chromosome (BAC) probes* 5

1.2.5 *Comparative genomics and gene mapping* 5

1.3 Amniote phylogeny 8

1.3.1 *Amniotes in the comparative genomics era* 11

1.3.2 *Significance of squamates in comparative genomics* 12

1.4 The development of a squamate model species .....**Error! Bookmark not defined.**

1.5 Aims and Objectives 19

1.5.1 *Specific research aims* 19

Chapter 2: Materials and Methods 20

2.1 Animals and cell suspensions 20

2.2 *Pogona vitticeps* BAC Library and Probe selection 21

2.3 Laboratory methods 22

2.3.1 *BAC DNA extraction* 22

2.3.2 *Fluorescence in situ hybridization (FISH), microscopy and image capture* 22

2.3.3 *Hybridisation of telomeric probe* 23

2.3.4 *DAPI banding* 24

2.3.5 *BAC end-sequencing* 24

2.4 Measurements and data analysis 24

2.4.1. *Chromosome nomenclature, sizes, banding, signal and centromere position* ... 24

2.4.3 *Sequence analysis, gene identification and comparative mapping* 26

2.4.3.1 *BLAST (Basic Local Alignment Search Tool) analyses* 26

2.4.3.2 *BLAT (BLAST-Like Alignment Tool) analyses* 27

Chapter 3: Results 28

3.1 Physical map of *Pogona vitticeps* 28

3.1.1 *Karyotype of Pogona vitticeps* 28

3.1.2 *DAPI banding Idiogram* 31

3.1.3 *18S rDNA localisation* 33

3.1.4 *Telomere localisation* 34

3.1.5 *BAC-based Physical map of Pogona vitticeps* 36

3.2 Molecular characterisation of *Physignathus lesueurii* chromosomes 45

3.2.1 *Karyotype of Physignathus lesueurii* 45

3.2.2 *18S rDNA localization* 48

3.2.3 *Telomere localization* 49

Chapter 4: Discussion ..... **Error! Bookmark not defined.**

4.1. Molecular characterisation of *Pogona vitticeps* chromosomes **Error! Bookmark not defined.**

4.1.1 *Karyotype of Pogona vitticeps* ..... **Error! Bookmark not defined.**

4.1.2 *DAPI ideograms and GC composition* ..... **Error! Bookmark not defined.**

4.1.3 *Telomeres* ..... **Error! Bookmark not defined.**

4.1.4 *Pogona vitticeps physical map* ..... **Error! Bookmark not defined.**

4.2 Comparing genomes between Australian agamids .....**Error! Bookmark not defined.**

4.2.1 *Molecular characterisation of Physignathus lesueurii chromosomes* ..... **Error! Bookmark not defined.**

4.2.2 *Australian agamid BAC-based comparative map* **Error! Bookmark not defined.**

4.3 Amniote comparative map .....**Error! Bookmark not defined.**

4.4 Future research directions .....**Error! Bookmark not defined.**

4.5 Conclusion .....**Error! Bookmark not defined.**

References 69

Appendices 76

List of Figures

Figure 1.1. Phylogeny of amniotes 22

Figure 1.2. Diploid chromosome number mapped onto a chronogram of a representative Australian agamid phylogeny 31

Figure 2.1. Map of Australia showing approximate species distribution of *P. vitticeps* and sampling locations.....33

Figure 3.1. Karyotype of *P. vitticeps* 41

Figure 3.2. Ideogram of P. vitticeps DAPI bands 45

Figure 3.3. 18S rDNA FISH on P. vitticeps metaphase chromosomes 46

Figure 3.4. Karyotype of *P. vitticeps* chromosomes showing hybridisation signals of telomeric probe $(TTAGGG)_5$ 48

Figure 3.5. Example FISH experiments in *P. vitticeps* 50

Figure 3.6. Physical map of *P. vitticeps* showing the location of diagnostic BAC clones mapped by FISH and orthology to chicken chromosomes 56

Figure 3.7. Karyotype of *P. lesueurii* 59

Figure 3.8. 18S rDNA FISH on *P. lesueurii* metaphase chromosomes 61

Figure 3.9. Hybridisation of telomeric sequences in *P. lesueurii* chromosomes 62

Figure 4.1. *P. vitticeps* and *P. lesueurii* comparative map 71

Figure 4.2. Chromosomal homologies among selected amniotes 76

Appendix 4. FISH images of BACs mapped to *P. vitticeps* mitotic metaphase spreads, data were used in the development of the *P. vitticeps* cytogenetic map (section 3.1.5) 96

Appendix 5. FISH images of each BAC mapped to *P. lesueurii* mitotic metaphase spreads 97

List of Tables

Table 3.1. Relative sizes, centromeric index, and proportional lengths of *P. vitticeps* chromosomes 43

Table 3.2. Gene contents and mapped locations of BAC clones in *P. vitticeps* and locations of chicken and human orthologues 51

Table 3.3. BAC clones that hybridise to multiple *P. vitticeps* chromosomes 22

Table 3.4. Relative sizes, centromeric index, and proportional lengths of *P. lesueurii* chromosomes 31

Table 4.1. Genome-wide GC content of *P. vitticeps* and representative amniotes 66

Appendix 1. Confidence levels in BLAST and BLAT analysis of identified *P. vitticeps* orthologues from end sequenced BAC clones.....91

Appendix 2. *P. vitticeps* microchromosome BAC two-colour FISH experiments 22

Appendix 3. *P. vitticeps* physical map data 31

Appendix 4. Male *P. lesueurii* comparative map data 22

Abbreviations

APTX	Aprataxin
ATP5A1	ATP synthase, H+ transporting, mitochondrial F1 complex, alpha subunit 1, cardiac muscle
BAC	Bacterial artificial chromosome
BCL6	B-cell CLL/lymphoma 6
BLAST	Basic local alignment search tool
BLAT	BLAST-like alignment tool
CA10	Carbonic anhydrase X
CHD1	Chromodomain helicase DNA binding protein 1
CTBP2	C-terminal binding protein 2
CTNNB1	Catenin (cadherin-associated protein), beta 1, 88kDa
DAPI	4′,6-diamidino-2-phenylindole
DDX58	DEAD (Asp-Glu-Ala-Asp) box polypeptide 58
DMRT1	Doublesex and mab-3 related transcription factor 1
dUTP	2′-Deoxyuridine 5′-triphosphate
EIF3H	Eukaryotic translation initiation factor 3, subunit H
FAM83B	Family with sequence similarity 83, member B
FBRSL1	Fibrosin-like 1
GHR	Growth hormone receptor
GMPPA	GDP-mannose pyrophosphorylase A
HCRTR2	Hypocretin (orexin) receptor 2
HMGCLL1	3-hydroxymethyl-3-methylglutaryl-CoA lyase-like 1
IBSP	Integrin-binding sialoprotein
IPO7	Importin 7
IQSEC3	IQ motif and Sec7 domain 3
KAT2B	K(lysine) acetyltransferase 2B
KLF6	Kruppel-like factor 6
MYST2	MYST histone acetyltransferase 2
NAV2	Neuron navigator 2
NPRL3	Nitrogen permease regulator-like 3
PSMA2	Proteasome (prosome, macropain) subunit, alpha type, 2
RAB5A	RAB5A, member RAS oncogene family

RRM1	Ribonucleotide reductase M1
SRY	Sex determining region Y
SUB1	SUB1 homolog (*S. cerevisiae*)
TAX1BP1	Tax1 (human T-cell leukemia virus type I) binding protein 1
TMEM41B	Transmembrane protein 41B
TNFRSF11B	Tumor necrosis factor receptor superfamily, member 11b
TTN	Titin
WAC	WW domain containing adaptor with coiled-coil
ZNF143	Zinc finger protein 143

Chapter 1: Introduction

1.1 Overview

This thesis presents the first physical map of an Australian reptile, the central bearded dragon (*Pogona vitticeps*) and demonstrates the value of this species as a model organism for comparative analyses of genome evolution among reptiles, birds and mammals (Amniota). A comparative gene mapping approach is used to investigate mechanisms of genome evolution at both narrow and wide phylogenetic focus. Cross-species comparative bacterial artificial chromosome (BAC)- mapping is used at a within closely related Australian dragon lizards (Agamidae), between *P. vitticeps* and the eastern water dragon (*Physignathus lesueurii*). Comparative gene mapping at a much broader phylogenetic scale is used to investigate the evolution of genome organisation among the broader amniote phylogeny, including species from both Synapsida (Mammalia) and Sauropsida (Archosauria): human (*Homo sapiens*) and the chicken (*Gallus gallus*), respectively.

The following chapter provides a theoretical context to the molecular characterisation and comparative investigation presented in this thesis and aims to define the significance and need for this study. Specifically, this chapter will discuss; gene mapping and the development of physical maps as a resource for investigating genome evolution, give a brief overview of the amniote phylogeny including the role certain amniote clades have played within the comparative genomics era, and discuss the significance of using reptiles in comparative genomic investigation. I also introduce my study species, including our current understanding of the phylogenetic relationships of Australian dragons and some of their genomic characteristics. This chapter concludes with an outline of the aims and objectives of this study.

1.2 The development of physical maps

1.2.1 Gene mapping

The purpose of gene mapping is to develop a comprehensive map of the entire genome of a particular species of interest. Maps can then be used as a resource for locating genes with specific functions and as a template to investigate the evolution of genome organisation (O'Brien *et al.*, 1999; Miller & Therman, 2000). Amniote genomes contain approximately

23, 000 genes (Hillier *et al.*, 2004) arranged in a linear order along double-stranded deoxyribonucleic acid (DNA) molecules called chromosomes. Knowledge of the structural changes in chromosomes and the mechanisms by which they occur is critical to understand patterns of genome evolution and speciation. Creating gene maps that depict the linear order and distance between genes on chromosomes is one of the main fields of cytogenetics. There are two broad types of gene maps; genetic maps and physical maps.

Genetic maps are based on linkage mapping, the calculation of recombination frequencies with distances between two loci defined in centiMorgans (cM). One cM is equal to a recombination frequency of 1%, the lower the recombination frequency the closer the loci are on the chromosome (Miller & Therman, 2000). In contrast, physical maps examine DNA molecules directly, with distances between loci defined in nucleotide base pairs (bp). Identifying the nucleotide sequence of DNA strands (sequencing) is one of the main techniques used in the development of physical maps, making them extremely accurate depictions of genomes. Featured within complete physical maps are the actual physical locations of every gene, functional and non-functional sequences of DNA for a particular organisms genome, giving these types of maps a much greater resolution over genetic maps (Miller & Therman, 2000). Both genetic and physical maps depict specific loci or genetic markers, of which there are three main types. Type I markers are functional coding sequences such as specific genes, Type II markers include non-coding repetitive elements such as microsatellites, also called short tandem repeats (STRs), and Type III markers include single nucleotide polymorphisms (SNPs) (O'Brien *et al.*, 1999).

1.2.2 Attributes of physical maps

Physical maps are diagrammatic representations of the genome and therefore are annotated with many of the structural features unique to the chromosomes of the particular species of interest. Karyotyping is the representation of the number and appearance of all chromosomes in a cell, and is fundamental for creating both physical and genetic maps. In a karyotype chromosomes are arranged following a standard classification system, featuring paired homologs ordered by size, shape and centromere position. The chromosomes in a karyotype are commonly observed at mitotic metaphase, that stage of the cell cycle when chromosomes can be easily visualised as they are in their most condensed

form (Sumner, 2003). A karyotype functions as a low resolution map of the entire genome, displaying the overall structure of each chromosome (Masabanda *et al.*, 2004).

There are two main structural features shared by all eukaryotic chromosomes: centromeres and telomeres. The centromere is the primary constriction of a chromosome and is the region involved in chromosome segregation during mitosis and meiosis (Sumner, 2003). The position of the centromere along the chromosome is commonly used as part of a chromosome classification system in karyotyping. There are four broad categories of chromosomes based upon this system: metacentric, submetacentric, acrocentric and telocentric (dos Santos, 1986). Telomeres are the physical ends of all linear chromosomes and contain a specific DNA sequences repeat (TTAGGG). This telomeric DNA sequence is conserved throughout most eukaryotes, as telomeres are required for chromosome replication and protection from degradation (Sandell & Zakian, 1993; Blackburn, 1994). Telomeric sequences are commonly mapped to chromosomes in physical mapping studies, as interstitial telomeric sequences may be indicative of ancestral chromosome fusions (Meyne *et al.*, 1990; Ruiz-Herrera *et al.*, 2008).

Other structural features often represented in physical maps include the position of the nucleolus organizer region(s) (NORs) and the distribution of isochores. NORs are specific loci on chromosomes consisting of a repeating unit of 18S, 5.8S and 28S genes that encode ribosomes (rRNA) (Shaw & Jordan, 1995). When chromosomes are observed at mitotic metaphase and appropriately stained, NORs form conspicuous secondary constrictions and are a common feature observed in the karyotypes of most eukaryotes (Shaw & Jordan, 1995). Isochores are bands observable in chromosomes after the application of cytogenetic staining techniques (Bernardi, 2000). The bands represent compositionally homogenous DNA segments above 300 kilo bases (kb), and are rich in either adenine (A) and thymine (T), or guanine (G) and cytosine (C) nucleotide bases (Bernardi, 2000). DAPI (4′,6 diamidino-2-phenylindole) is one of the most commonly used staining chemicals. It preferentially binds to AT rich sequences (Portugal & Waring, 1988) and frequently used as a counterstain for gene mapping using fluorescence *in situ* hybridization (FISH).

1.2.3 Fluorescent in situ *hybridization (FISH) and gene mapping*

The development of a comprehensive physical map requires that markers can be localised onto chromosomes with a high degree of accuracy. FISH is one of the main techniques employed in the development of physical maps. Early methods of *in situ* hybridization involved hybridising radioactively labelled specific DNA sequences (probes) onto metaphase chromosomes, and detecting signals through autoradiography (John *et al.*, 1969; Pardue & Gall, 1969). Since then, there have been many advances in these techniques resulting in improved resolution, mainly by the development of non-isotopic fluorescent labels that allow probes to be directly visualised on metaphase chromosomes using fluorescent microscopy (Trask, 1991). Probes can be either labeled directly or indirectly through nick translation, random priming or polymerase chain reaction (PCR) (Rigby *et al.*, 1977; Trask, 1991). Direct labelling involves incorporating fluorochromes already bound to nucleotides into probes. Indirect labelling involves incorporating nucleotides attached to molecules which are then detected by secondary molecules such as antibodies conjugated with fluorochromes.

The development of multi-colour FISH, whereby multiple probes can be labelled with separate fluorochromes and hybridised together onto the same metaphase has further increased the resolution of physical maps (Trask, 1991). Using multi-colour FISH on metaphase chromosomes loci can be reliably mapped to within 1 megabase (Mb) of each other (Trask, 1991). The use of multi-colour FISH on interphase chromosomes is another technique for increasing mapping resolution. As interphase chromatin is less condensed than at metaphase, the position of loci can be reliably determined when separated by as little as 50 kb (Trask, 1991). Other methods such as Fibre FISH can also be used to further increase the resolution of mapping in a particular chromosomal region of interest (Trask, 1991). At a much broader scale than mapping single loci, cross-species chromosome painting (Zoo-FISH) and comparative genomic hybridization (CGH) can map entire chromosomes or whole genomic DNA, respectively (Miller & Therman, 2000). These techniques can be used to assess chromosomal homology between species or differences in DNA sequence copy number between individuals of the same species (Shetty *et al.*, 1999; Miller & Therman, 2000; Ezaz *et al.*, 2005).

1.2.4 Bacterial artificial chromosome (BAC) probes

One of the many probe resources used in conjunction with FISH to develop physical maps is the bacterial artificial chromosome (BAC) library. A genomic BAC library consists of multiple *Escherichia coli* clones that each contain a specific DNA fragment (~100-200 kb) from the species of interest ligated to a vector molecule (Janes *et al.*, 2011). BAC libraries with a high depth of coverage may represent the entire genome of the species of interest, many times over, and therefore are an extremely useful resource for the development of comprehensive physical maps. Simultaneous sequencing and FISH mapping of BAC clones enables the identification of loci contained within the clone and the location of these loci on chromosomes (Zhang & Wu, 2001). Sequences derived from BAC clone DNA inserts can also be mapped *in silico* to the genomic sequences of other species for comparative analyses (Shedlock *et al.*, 2007; Chapus & Edwards, 2009). Sequenced and mapped BACs also function as molecular 'anchors', as they can be used to anchor the DNA sequences contained within contigs from whole-genome sequencing to chromosomes (Masabanda *et al.*, 2004; Alsop *et al.*, 2005). BAC libraries are also extremely versatile and can be screened for loci pr regions of interest, enabling mapping of these regions at high resolution (Zhang & Wu, 2001; Sankovic *et al.*, 2006; Deakin *et al.*, 2008; Ezaz *et al.*, 2009a). As in this study, BAC clones can be used to develop low resolution physical maps in non-model species through cross-species FISH mapping for comparative mapping analyses (Raudsepp *et al.*, 1999; Kasai *et al.*, 2003).

1.2.5 Comparative genomics and gene mapping

Genomic comparisons between species are fundamental to gaining insight into how genome organisation has evolved in particular lineages. Genomes evolve through mutation, which creates genetic diversity. This provides the raw material for evolutionary forces such as selection and genetic drift to act upon to promote change and adaptation. For example, selective pressure through purifying (negative) selection causes functional sequences to be maintained and change more slowly than non-functional sequences, or Darwinian (positive) selection that causes sequences to change at an increased rate (Miller *et al.*, 2004). Comparative gene mapping aims to answer questions concerning the mechanisms of genome evolution and changes in gene function through comparing molecular markers on physical maps between species (O'Brien *et al.*, 1993). For

comparative mapping purposes specific terminology has been developed to express the relationships of genes across multiple species. There are two main subcategories of homologous genes: orthologs; genes related via speciation, originating from a single ancestral gene in the last common ancestor of both species being compared, and paralogs; genes that are related via duplication of an ancestral gene (Koonin, 2005).

Comparative gene mapping of orthologs can be used to reconstruct ancestral syntenies and identify subsequent chromosome rearrangements that lead to genome organisation in extant species (Andersson *et al.*, 1996; O'Brien *et al.*, 1999; Nakatani *et al.*, 2007). Genes are said to be syntenic if they occur together on the same chromosome (Sumner, 2003). Segments of chromosomes are said to be conserved when the linear order of the syntenic genes is maintained in both species without rearrangements (Sumner, 2003). Many mechanisms change the organisation of genomes, both inter- and intrachromosomal and at small and large scales. Key small scale rearrangements include insertions and deletions (indels), amplification of STRs, activity and dispersal of mobile elements such as transposons and retrotransposons (Sumner, 2003). Amongst the most important large scale structural changes to genomes are chromosome fission, fusions, duplication, deletion, inversion, centromere repositioning (Sumner, 2003), and the presence of supernumerary chromosomes (Bertolotto *et al.*, 2004).

One of the main focuses of comparative mapping has been deducing the origins and evolution of sex chromosomes. Sex chromosomes are in all species that have genotypic sex determination (GSD), and are absent in species with environmental sex determination (ESD) (Bull, 1983). Sex chromosomes evolve when an allele on one chromosome of an autosomal pair evolves a sex-determining role (Ohno, 1967; Charlesworth, 1991). In GSD species, the sex-determining gene directs sexual differentiation to be either male or female (Charlesworth, 1991). In mammals, a primary male-determining gene *SRY* has been identified (Sinclair *et al.*, 1990), and in birds a dosage-dependent male determining gene *DMRT1* (Smith *et al.*, 2009). The sex chromosome pair may either be homomorphic and cytologically indistinguishable, or heteromorphic where one chromosome is degenerated and may lack entirely or possess only a small pseudoautosomal region where recombination still occurs. When males are the heterogametic sex, males possess one copy

of each type of sex chromosome, designated X and Y (XX female; XY male). Conversely, where females are the heterogametic sex, females possess one copy of each type of sex chromosome, designated Z and W (ZW female: ZZ male).

Comparative mapping of sex-linked genes from mammals, birds and non-avian reptiles has revealed that sex chromosomes have arisen from different autosomes of the amniote common ancestor. For example, comparative mapping of multiple chicken Z-linked genes revealed that the chicken Z chromosome is homologous to a region on chromosome 2 of the agamid lizard *P. vitticeps*, chromosome 2p of the Japanese four-striped rat snake (*Elaphe quadrivirgata*), chromosome 6 of the Chinese soft-shelled turtle (*Pelodiscus sinensis*), and regions on human chromosomes 5, 9 and 18 (Nanda *et al.*, 1999; Schmid *et al.*, 2000; Matsuda *et al.*, 2005; Ezaz *et al.*, 2009a). Z-linked genes of the turtle *P. sinensis* mapped to chicken chromosome 15 (Kawagoshi *et al.*, 2009). Snake Z-linked genes mapped to chicken chromosome 2p, and regions on human chromosomes 3, 7, 10 and 17 (Matsuda *et al.*, 2005; Matsubara *et al.*, 2006). While human X-linked genes mapped to a region on chromosome 4p and indistinguishable microchromosomes of *E. quadrivirgata*, and regions on chicken chromosome 1 and 4 (Schmid *et al.*, 2000; Matsuda *et al.*, 2005; Matsubara *et al.*, 2006; Srikulnath *et al.*, 2009b).

In contrast, comparative mapping has also identified homology between the sex chromosomes of some mammals, birds and squamates. For example, comparative mapping between a species of gecko (*Gekko hokouensis*) and the chicken revealed a syntenic region conserved on both avian and squamate Z chromosomes (Kawai *et al.*, 2009). Also, regions on four of the five X chromosomes and one Y chromosome of the platypus (*Ornithorhynchus anatinus*) are homologous to regions on the chicken Z (Veyrunes *et al.*, 2008). However, considering that *DMRT1* in birds is a dosage-dependent male-determining gene, the presence of *DMRT1* on both the Z and W of *G. hokouensis*, and on the X and Y chromosomes of the platypus implies that these orthologs cannot have retained the same sex-determining function (El-Mogharbel *et al.*, 2007; Veyrunes *et al.*, 2008; Kawai *et al.*, 2009). Comparative mapping between birds and snakes has also identified shared repetitive sequences in both sex chromosome systems that may elude to as yet

undetected ancestral synteny, or functional homology in sex chromosome degeneration (O'Meally *et al.*, 2010).

The identification of ancestral syntenies through comparative mapping coupled with a robust phylogeny and outgroup comparisons enables inference of approximately when and in which lineage certain chromosomes or gene arrangements arose. For example, comparative mapping between the snake Z chromosome, chicken chromosomes 2 and 27 and chromosome 6 of agamid lizards *P. vitticeps* and *Leiolepis reevesii rubritaeniata*, suggests that the synteny of snake Z-linked genes has been conserved for approximately 166 million years (O'Meally *et al.*, 2010), since the snake and lizard lineages diverged in the mid Jurassic Period (Hedges *et al.*, 2006). Furthermore, comparative mapping of orthologs from the turtle *P. sinensis* and the chicken revealed highly conserved linkage homology and that synteny of genes on chicken chromosomes 1, 2, 3, 5 and Z has been conserved for at least 210 million years (Matsuda *et al.*, 2005). Comparative mapping between *P. sinensis* and chicken suggested that the synteny of Z-linked genes in the turtle have been conserved for the past 250-290 million years, since archosaurs and lepidosaurs diverged (Kawagoshi *et al.*, 2009). However, as no outgroup species belonging to Lepidosauria was used as an outgroup comparison, this ancestral synteny may be no older than 243 million years, since the divergence of Aves and Testudines (Hedges *et al.*, 2006). Among many other examples, comparative gene mapping between chicken and human has shown that a contiguous block of chicken and human chromosome 4 are syntenic, conserved since sauropsids and synapsids diverged from an amniote common ancestor in the early Carboniferous Period some 324 million years ago (Mya) (Chowdhary & Raudsepp, 2000; Hedges *et al.*, 2006).

1.3 Amniote phylogeny

Amniotes were the first group of vertebrates to permanently colonise terrestrial habitats in the early Carboniferous Period, some ~330 million years ago (Hedges, 2009). This was facilitated by major adaptations that allowed reproduction to take place independently of an aquatic environment. One of the key adaptations making this possible was the evolution of the amniote egg, which comprises a series of extra-embryonic membranes that protect the developing embryo from the dry terrestrial environment (Reisz, 1997). Amniotes have

since colonised every continent and are found in a variety of terrestrial, aquatic and marine habitats, portraying astonishing ecological, phenotypic and genotypic diversity.

Extant amniotes belong within two broad groups: Synapsida (mammals) and Sauropsida (birds and non-avian reptiles), that diverged from a common ancestor in the mid Carboniferous Period approximately 324 Mya, (Hedges *et al.*, 2006). Within these two lineages there are approximately 23, 000 extant species, comprising taxa from three distinct clades (Shedlock & Edwards, 2009). Representing members of Synapsida, there are approximately 5, 200 extant species of mammals (Mammalia) (Janes *et al.*, 2010) that belong to one of three sub-clades: Prototheria (monotremes), Metatheria (marsupials) and Eutheria (placental mammals) (Shedlock & Edwards, 2009). Sauropsida include members of Lepidosauria and Archosauria, numbering approximately 18, 000 extant species, roughly three quarters of all amniotes. Lepidosauria is comprised of two sub-clades, Squamata (Gekkota, Scinciformata, Toxicofera and Laterata), and Rhynchocephalia (tuatara). Archosauria is comprised of three sub-clades, including Testudines (Cryptodira and Pluerodira: turtles), Crocodylia (alligators and crocodiles) and Aves (Palaeognathae and Neognathae: birds) (Figure 1.1.).

Figure 1.1. (following page) Phylogeny of amniotes. Branch lengths are proportional to divergence dates from http://timetree.org (Hedges *et al.*, 2006) and references therein. Dotted line represents uncertain placement of turtles in phylogeny. Numbers in parentheses represent approximate number of species in each clade. MYA: millions of years ago. * denotes the presence of microchromosomes within extant members of clade.

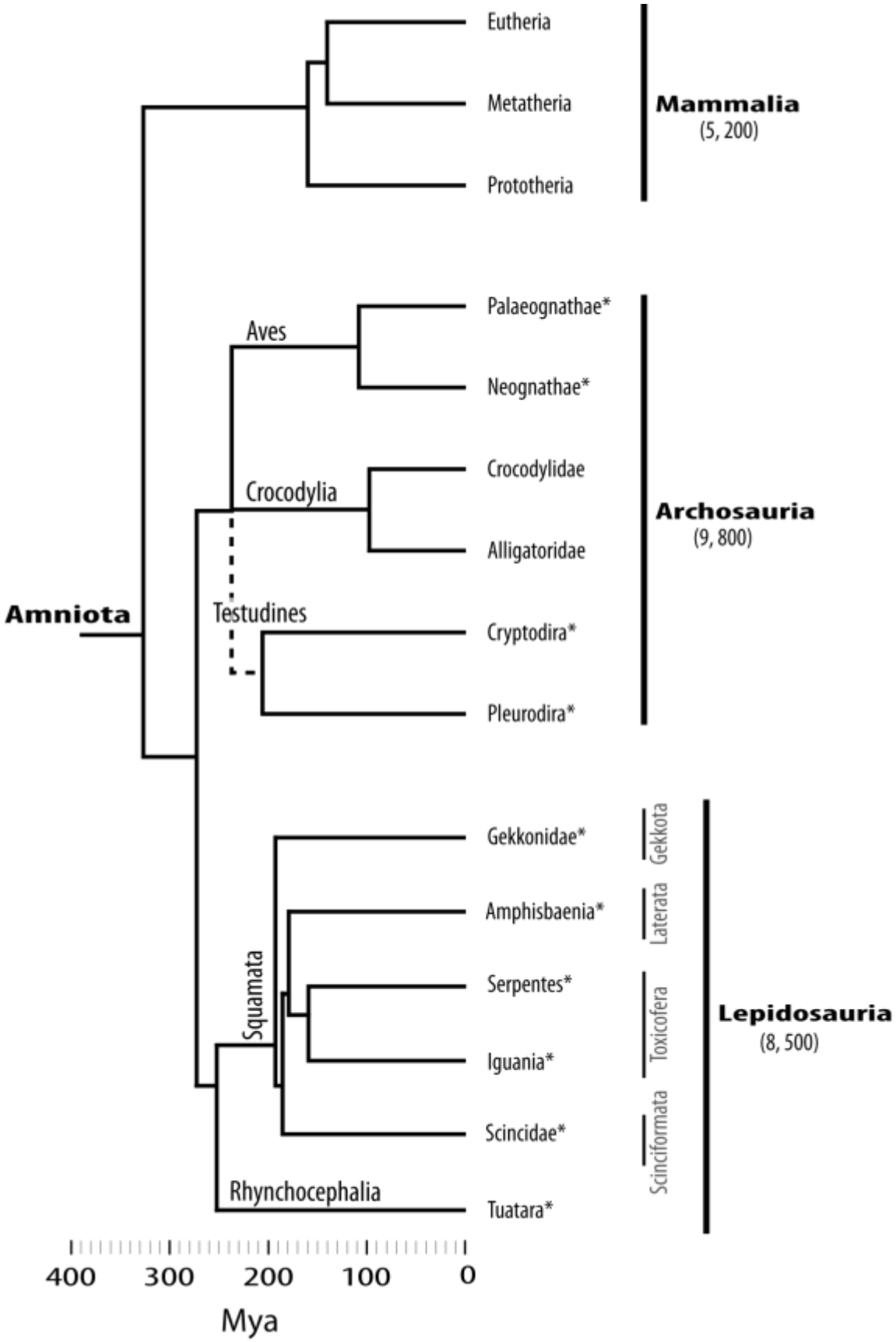
Eutheria
Metatheria
Prototheria
Mammalia
(5, 200)
Palaeognathae*
Aves
Neognathae*
Crocodylidae
Crocodylia
Alligatoridae
Archosauria
(9, 800)
Amniota
Testudines
Cryptodira*
Pleurodira*
Gekkonidae*
Gekkota
Amphisbaenia*
Laterata
Serpentes*
Toxicofera
Squamata
Iguania*
Lepidosauria
(8, 500)
Scincidae*
Scinciformata
Rhynchocephalia
Tuatara*
400
300
200
100
0
Mya

1.3.1 Amniotes in the comparative genomics era

Amniotes have featured extensively in comparative genomic analyses, with 226 genome sequencing projects either currently in progress or complete (NCBI, 2011) in conjunction with numerous physical and comparative maps. Of these 226 projects, 208 are mammalian, with representative species from all three clades Eutheria, Metatheria and Prototheria. Sixteen projects are of birds, including representative species from both Palaeognathae and Neognathae, and two projects are of squamate reptiles, both representing lineages within Toxicofera, Serpentes: Indian python (*Python molurus*) and Iguania: green anole (*Anolis carolinensis*). Many important insights into gene function and the mechanisms of genome evolution are emerging from these extensive genomic resources.

One of the major advances in the study of comparative genomics was the online publishing of sequence data from multiple genome sequencing projects and corresponding physical maps. This allowed the karyotype reconstruction of an amniote common ancestor using an *in silico* approach (Nakatani *et al.*, 2007). This reconstruction suggests that whole genome duplications shaped the early vertebrate karyotype followed by a number of fusions in the common amniote ancestor, prior to the rise of Synapsida and Sauropsida (Nakatani *et al.*, 2007). More recent changes were also inferred, such as fission events occurring in Aves, fusions in Crocodylia, and intensive fusions within Squamata and Metatheria (Nakatani *et al.*, 2007). This reconstruction analysis could not have been undertaken nor its findings tested if it were not for the increase in genomic resources from phylogenetically distant vertebrates, including from sauropsids, synapsids.

In comparative mapping analysis, the phylogenetic distance at which comparisons are made has implications for the types of information and insight that can be acquired. For example, finding sequences that are highly conserved in phylogenetically distant species can give great insight into genes that have critical functions (Miller *et al.*, 2004). Non- or neo-functional sequences will likely have acquired mutations through selection or drift resulting in their homology no longer being apparent (Miller *et al.*, 2004). Clearly, as more genomic resources become available from phylogenetically distant species, new insights will be gained to the mechanisms of early genome evolution and subsequent lineage-specific evolution in all amniotes. However, the focus of comparative genomics so far has

primarily been on mammals, accounting for at least 90 percent of all amniote sequencing projects. While this focus has dramatically improved our understanding of genome organisation and established much of what is known about the mechanisms of genome evolution, to truly gain insight into how amniote genomes evolved physical maps, genome sequencing and comparative analyses must be integrated systematically from all major amniote groups.

1.3.2 Significance of squamates in comparative genomics

Squamates fall within Lepidosauria, the sister group of Archosauria. Together they comprise Sauropsida, the sister group of Synapsida (mammals). As such, they hold a key phylogenetic position in elucidating the mechanisms of genome evolution among amniotes and provide critical contrast to the insights already gained from research on mammalian and avian genomes.

Comparative genomic analyses undertaken within mammalian, and recently within avian and squamate genomes, have shown that there are many genomic characteristics that are intrinsic to certain amniote clades. These include genome size, karyotype, sex-determining mechanisms and GC content among others. For example, genome size is highly variable within mammals, squamates and turtles, while avian genomes are less variable (Janes *et al.*, 2010). Variation in chromosome size is also much greater in sauropsids that synapsids, owing to the large number of microchromosomes present in most sauropsid karyotypes (Janes *et al.*, 2010; Uetz, 2011). Avian genomes are also relatively small compared to mammals and squamates, a trait which is thought to be associated with increased metabolic demands required for flight (Hughes & Hughes, 1995; Hughes & Piontkivska, 2005), but also due to unknown factors that began to reduce genome size in this lineage before flight evolved (Organ *et al.*, 2007). Archosaurs are also characterised by smaller introns than have been observed in most mammalian clades (Waltari & Edwards, 2002).

Microchromosomes from both birds and turtles are structurally and functionally different from mammalian macrochromosomes, possessing a higher GC content and gene density (Auer *et al.*, 1987; Hillier *et al.*, 2004; Kuraku *et al.*, 2006), which is also correlated with a higher recombination rate (Hillier *et al.*, 2004; Freudenberg *et al.*, 2009).

Microchromosomes are present in most lizards, snakes, geckos, turtles and birds but are absent in all crocodiles, alligators (Olmo & Signorino, 2005) and mammals. As microchromosomes are present in many sauropsid karyotypes but not in mammals, it has been suggested that microchromosomes first appeared after the divergence of sauropsids and synapsids from a common ancestor (Burt, 2002; Griffin *et al.*, 2007), some 324 million years ago (Hedges *et al.*, 2006). Since microchromosomes are present in most sauropsid karyotypes, this also raises questions about the level of conservation of these microchromosomes across sauropsids. The development of a comprehensive physical map of a squamate species that includes all chromosomes could be used in comparative analyses with the chicken genome to gain insight into the level of microchromosome conservation between Archosauria and Lepidosauria.

Another genomic characteristic that differs between major amniote clades is the activity, class and abundance of mobile elements (Waltari & Edwards, 2002; Hillier *et al.*, 2004; Kordis, 2009). Mobile elements are DNA sequences that are able to integrate into new sites within the genome. They have important functions as a source of mutation, promoting novel genomic variation (Kazazian, 2004; Kordis, 2009) and the evolution of differentiated sex chromosomes (Steinmann & Steinmann, 2005). There are two main classes of mobile elements distinguished by the mechanisms of transposition. DNA transposons are mobile elements that are excised and integrated at new sites within the genome, while retrotransposons are mobile elements that proliferate throughout the genome through duplication via an RNA intermediate (Kazazian, 2004; Capy, 2005). Long interspersed nuclear elements (LINEs) and short interspersed nuclear elements (SINEs) are the two main sub-classes of retroelements that make up a large percentage of mammalian genomes (Lander *et al.*, 2001; Waterston *et al.*, 2002).

Comparisons between species within Mammalia, Archosauria and Lepidosauria using BAC end sequences, have demonstrated that the common ancestor of sauropsids and synapsids had a diverse array of microsatellites and mobile elements, that have been recently active in both lineages (Shedlock *et al.*, 2007). In contrast, birds have very few mobile elements, none of which has been active in the past 50 million years (Hillier *et al.*, 2004). Avian genomes therefore have a derived condition of mobile element and microsatellite loss

without further retroelement activity. This explains their relatively small genome size in comparison to mammals (Hillier *et al.*, 2004; Shedlock *et al.*, 2007). In contrast to Aves, retroelements are abundant and show evidence of recent activity in Crocodylia, Testudines and Squamata, indicating that genomic characteristics vary among sauropsids and even between clades within Archosauria (Shedlock *et al.*, 2007). Analysis of the recently sequenced *A. carolinensis* genome suggests that horizontal gene transfer has played a role in the distribution of retroelements between synapsid and sauropsid genomes (Novick *et al.*, 2010).

Extant Sauropsida includes two evolutionary, phenotypically and genomically divergent lineages. The genomic characteristics outlined above integrate with many other characteristic phenotypic, behavioural and life-history traits that separate birds and reptiles from mammals. For example, birds and reptiles have extremely diverse modes and mechanisms of sex determination. Many reptiles, including squamates (Harlow, 2004; Ezaz *et al.*, 2005; Ezaz *et al.*, 2009c; Gamble, 2010) and turtles (Ewert *et al.*, 2004; Ezaz *et al.*, 2006; Kawagoshi *et al.*, 2009) have GSD with either XY or ZW modes, or have temperature-dependent sex determination (TSD), a form of ESD where incubation temperature during embryo development influences offspring sex (Bull, 1983). In contrast all crocodilians (Deeming, 2004) and the monotypic tuatara (Cree *et al.*, 1995) have TSD, and all birds (Ellegren, 2000) and snakes (Becak, 1964; Matsubara *et al.*, 2006) have GSD with a fixed ZW mode.

The inherent variability in mechanisms and modes of sex determination among sauropsids has lead to the proposal that GSD and TSD systems are not separate mechanisms but rather function as a continuum, ranging from strict GSD systems, to systems based upon interactions between GSD and TSD, to strict TSD systems (Sarre *et al.*, 2004), a view which has been evidenced in squamates (Quinn *et al.*, 2007; Radder *et al.*, 2008). Also, squamates are the only vertebrates that exhibit true naturally occurring parthenogenesis (Fujita & Moritz, 2009). As all mammals have a conserved GSD system with male heterogamety (Graves, 2008), it is only possible to gain insight into these varied and diverse mechanisms by studying the genomes of reptiles (Sarre *et al.*, 2004). Clearly, developing genomic resources for squamate species to join those that have already been

developed for synapsid and avian species will provide great insight into genome evolution and organisation amongst amniotes.

Comparisons between the genomes of mammals, archosaurs and squamates have increased our understanding of amniote genome organisation and evolution substantially. These insights have lead to initiatives to sequence the genomes of a wide range of representative species from within Archosauria and Lepidosauria (Haussler *et al.*, 2009). However, a present set-back for comparative analyses is the lack of physical maps for squamate species, including those which are the focus for current genome sequencing efforts such as *A. carolinensis* and *P. molurus*. This has meant that the contigs generated from whole-genome sequencing are not assembled onto chromosomes (as has been achieved for the chicken and many mammalian species). Incomplete squamate physical maps are starting to emerge to fill this void, such as the snake *E. quadrivirgata* (Matsuda *et al.*, 2005; Matsubara *et al.*, 2006), turtle *P. sinensis* (Matsuda *et al.*, 2005) and the recently mapped Asian agamid lizard *L. r. rubritaeniata* (Srikulnath *et al.*, 2009a). Through comparative mapping analyses, these physical maps have produced insights into genome evolution and organisation among squamates and also among amniotes. The field of comparative genomics would benefit largely from the development of a comprehensive physical map of a squamate that spanned all chromosomes. This would allow for comparative mapping among squamates, between Lepidosauria and Archosauria, and between sauropsids and synapsids. This would reveal the mechanisms of genome evolution and novel genome organisation that set these species apart, and to provide a focus for genome sequencing efforts in Squamata.

1.4 The development of a squamate model species

The central bearded dragon, *P. vitticeps*, is an endemic Australian squamate that is emerging as a model reptilian species in both comparative genomic (Ezaz *et al.*, 2005; Ezaz *et al.*, 2009a; Ezaz *et al.*, 2009b; Patel *et al.*, 2010; Quinn *et al.*, 2010), and sex determination research (Quinn *et al.*, 2007). This reptile is broadly distributed over much of the arid and semi-arid interior of the Australian continent and belongs within the family Agamidae (dragon lizards). There are currently 410 recognised species of agamid in at least 52 genera worldwide, distributed across Australia, Africa, Europe, central and

southeast Asia and New Guinea (Uetz, 2011). Agamids are phylogenetically nested within Toxicofera, a group that includes snakes and iguanid lizards.

Phylogenetic analysis of multiple Asian and Australian agamids has revealed that the Australian agamids diverged from an Asian common ancestor approximately 30 Mya following multiple dispersals from the forest biomes of Papua New Guinea across Torres Strait and immigration to Australia (Hugall *et al.*, 2008). Within the Australian agamids, the rainforest dragons belonging to the genus *Hypsilurus* and the water dragon *P. lesueurii* emerged as basal members of the Australasian radiation, while the Indo-Chinese water dragon (*Physignathus cocincinus*) emerged as the sister taxon of all Australian agamids (Hugall *et al.*, 2008) (Figure 1.2.). Following initial cladogenesis in the Australian mesic rainforests of the early Miocene around 22 Mya, changes in climate resulting in aridification and rainforest habitat loss approximately 15 Mya (McGowran *et al.*, 2004), promoted adaptive radiations into newly formed xeric habitats (Hugall *et al.*, 2008).

Australian agamids currently include 70 recognised species (Wilson & Swan, 2008), which show substantial ecological, phenotypic and genotypic diversity. Since colonisation of the Australian continent, agamids have evolved both GSD and TSD (Harlow, 2004; Ezaz *et al.*, 2005; Doody *et al.*, 2006), the haphazard distribution across the genera suggesting multiple and independent transitions between mechanisms (Ezaz *et al.*, 2009b). The development of a female-specific DNA marker (Quinn *et al.*, 2007) has recently enabled investigation into the origins of Australian agamid sex chromosome systems. (Ezaz *et al.*, 2009b) showed that the sex chromosomes of *P. vitticeps* and *Ctenophorus fordi* are not homologous and therefore have been independently derived since their divergence from a common ancestor 19 Mya (Ezaz *et al.*, 2009b).

Figure 1.2. (following page) Diploid chromosome numbers mapped onto a chronogram of a representative Australian agamid phylogeny (modified from Hugall *et al.* (2008)). Numbers inside parentheses represent the diploid number of macrochromosomes and number of microchromosomes, respectively. Numbers outside of parentheses denote references for diploid number: 1) Witten, 1983; 2) Uetz, 2005. Mya: millions of years ago.

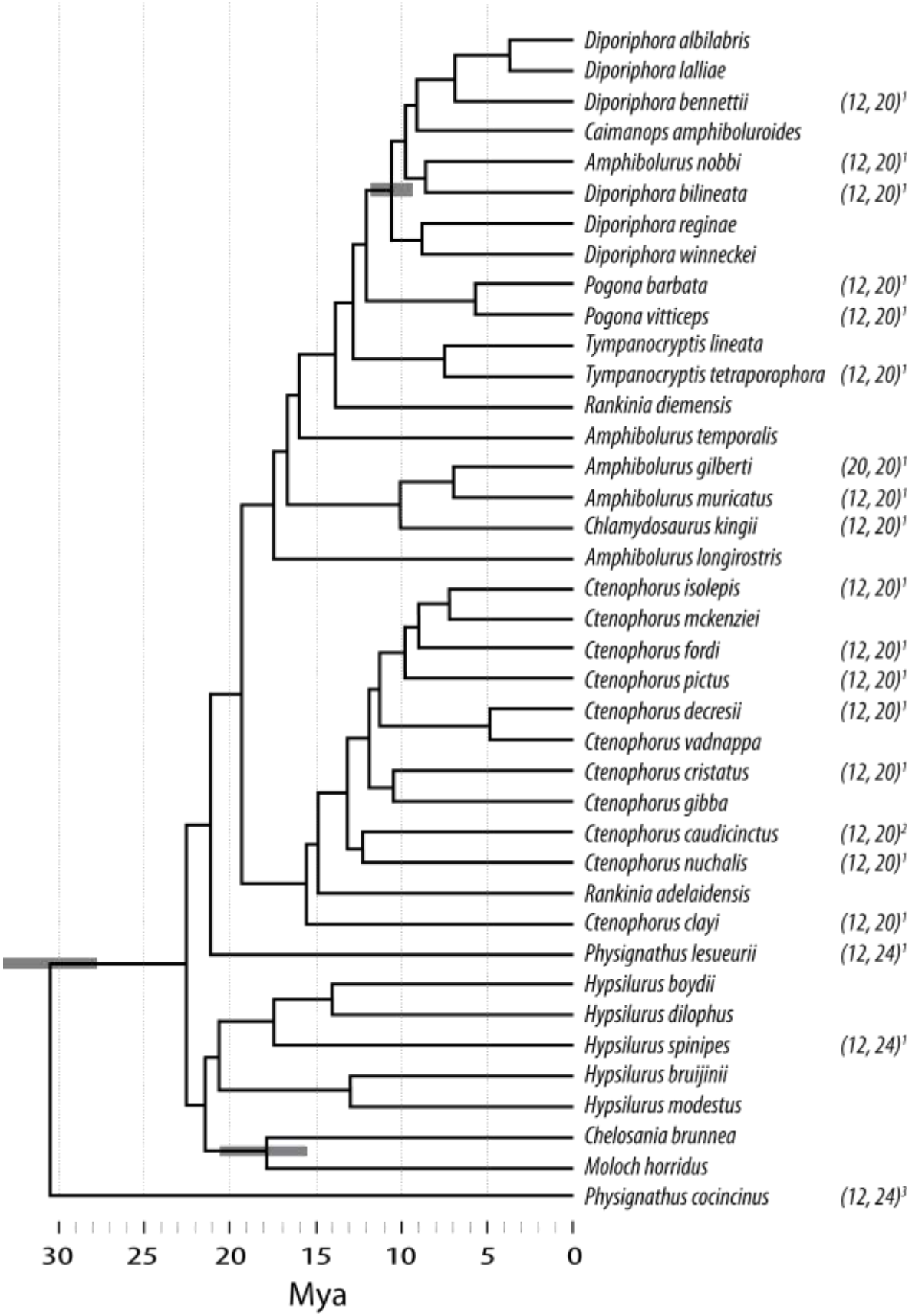
Diporiphora albilabris
Diporiphora lalliae
Diporiphora bennettii (12, 20)[1]
Caimanops amphiboluroides
Amphibolurus nobbi (12, 20)[1]
Diporiphora bilineata (12, 20)[1]
Diporiphora reginae
Diporiphora winneckei
Pogona barbata (12, 20)[1]
Pogona vitticeps (12, 20)[1]
Tympanocryptis lineata
Tympanocryptis tetraporophora (12, 20)[1]
Rankinia diemensis
Amphibolurus temporalis
Amphibolurus gilberti (20, 20)[1]
Amphibolurus muricatus (12, 20)[1]
Chlamydosaurus kingii (12, 20)[1]
Amphibolurus longirostris
Ctenophorus isolepis (12, 20)[1]
Ctenophorus mckenziei
Ctenophorus fordi (12, 20)[1]
Ctenophorus pictus (12, 20)[1]
Ctenophorus decresii (12, 20)[1]
Ctenophorus vadnappa
Ctenophorus cristatus (12, 20)[1]
Ctenophorus gibba
Ctenophorus caudicinctus (12, 20)[2]
Ctenophorus nuchalis (12, 20)[1]
Rankinia adelaidensis
Ctenophorus clayi (12, 20)[1]
Physignathus lesueurii (12, 24)[1]
Hypsilurus boydii
Hypsilurus dilophus
Hypsilurus spinipes (12, 24)[1]
Hypsilurus bruijinii
Hypsilurus modestus
Chelosania brunnea
Moloch horridus
Physignathus cocincinus (12, 24)[3]
30
25
20
15
10
5
0
Mya

Cytogenetic investigation of Australian agamid genomes has revealed variation in chromosome number such as 2n = 40 in *Amphibolurus gilberti* (formerly *Lophagnathus gilberti centralis*), 2n = 36 in the water dragon *P. lesueurii*, and 2n = 32 in many other dragon species including *P. vitticeps* (Witten, 1983). This suggests that during the adaptive radiation of these lizards throughout the Australian continent a number of changes in genome organisation have occurred (Witten, 1983). Cytogenetic characterisation of multiple Australian agamid genomes and comparative mapping of genetic markers could begin to illuminate some of the mechanisms of genome evolution that have occurred amongst these squamate reptiles. The recent development of genomic resources such as a 6.2x coverage *P. vitticeps* genomic BAC library (Ezaz *et al.*, 2009a), has provided the opportunity to develop a comprehensive physical map of this species and to use it in comparative mapping analysis between agamids and among amniotes.

1.5 Aims and Objectives

In this study I use molecular cytogenetic techniques and comparative mapping analyses to address the following aims and objectives. Broadly, the objectives of this study are to gain insight into:

1. The molecular organisation of a squamate genome.

2. Mechanisms of genome evolution between closely-related squamates.

3. Mechanisms of genome evolution among amniotes.

1.5.1 Specific research aims

The research aims of this study are to:

Aim 1: Develop a BAC-based physical map of the Australian central bearded dragon, *Pogona vitticeps*.

Aim 2: Construct a BAC-based comparative map between *Pogona vitticeps* and the eastern water dragon, *Physignathus lesueurii*.

Aim 3: Construct a comparative map between *Pogona vitticeps*, chicken and human.

Chapter 2: Materials and Methods

2.1 Animals and cell suspensions

All cell suspensions used in this study had been previously prepared by Ezaz *et al*. (2009a) and were available in the Wildlife Genetics Laboratory at the University of Canberra, Australia. These included *P. vitticeps* cell suspensions from two females and one male (preparation numbers PvFTH1, PvF56, and PvM78 respectively) and *P. lesueurii* cell suspensions from one female and one male (preparation numbers PlFYBYg-2+B and PlYYYg-1+B respectively). Ezaz *et al*. (2009a) prepared cell suspensions from short-term whole blood, peripheral blood leukocytes, or fibroblast cell cultures following procedures described in Ezaz *et al*. (2005). Specimens of *P. vitticeps* had been collected from wild populations in northwest New South Wales (NSW) and southwest Queensland (QLD), while *P. lesueurii* animals had been collected from wild populations in the Australian Capital Territory (ACT) (Figure 2.1.). All animals were collected under State permits and with University of Canberra Animal Experimentation Ethics Committee approval.

Cell suspensions from *P. vitticeps* and *P. lesueurii* were dropped onto 25×75×1 mm superfrost glass microscope slides (HD Scientific) and air dried. Slides were stored at -80°C. Immediately before use, slides were dehydrated in ethanol (100%) for 3 seconds (s) and air dried.

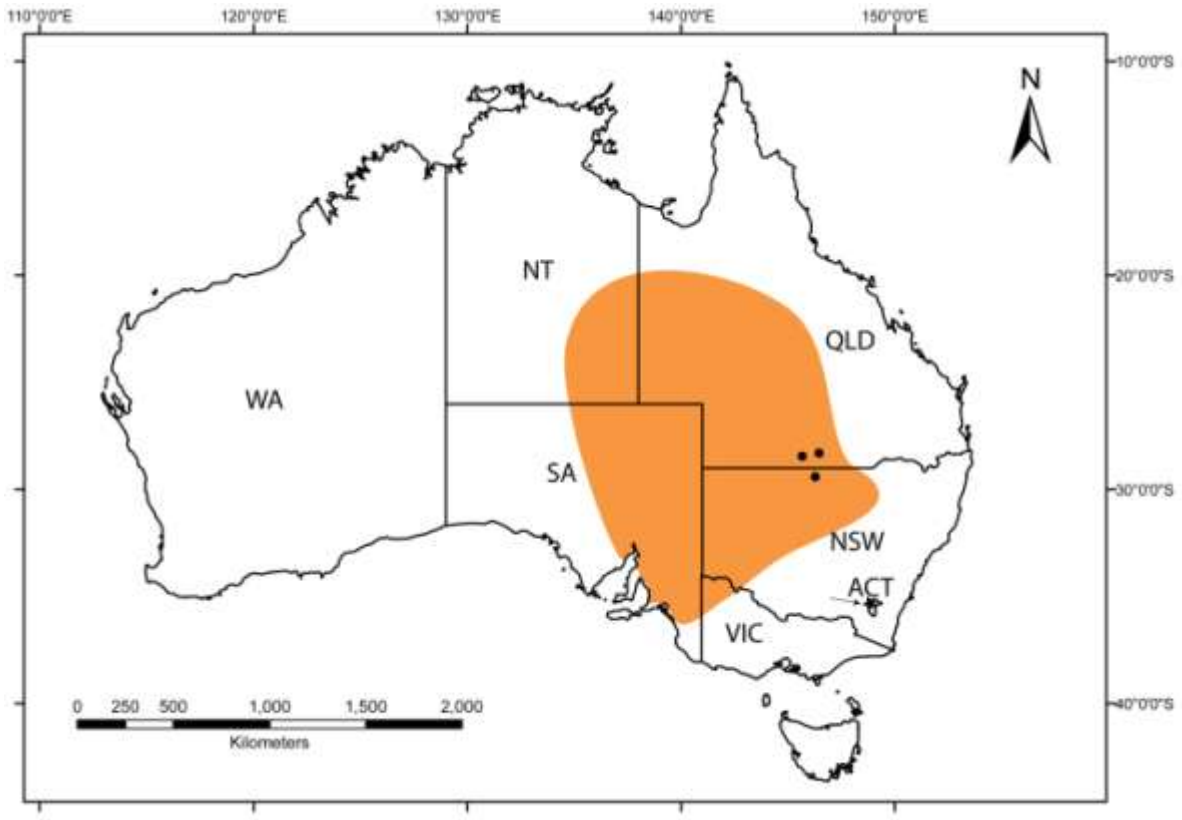

Figure 2.1. Map of Australia showing the approximate species distribution of *P. vitticeps* (orange shaded area) across parts of Queensland (QLD), New South Wales (NSW), Victoria (VIC), South Australia (SA), and Northern Territory (NT). Data sourced from Wilson & Swan (2008). Approximate sampling locations for *P. vitticeps* and *P. lesueurii* are indicated by black dots and a black star, respectively. Basal map generated using ArcGIS v9.3.1.

2.2 *Pogona vitticeps* BAC Library and Probe selection

Clones were selected from a female *P. vitticeps* 6.2x coverage genomic bacterial artificial chromosome (BAC) library, (Amplicon Express, Pullman WA, USA; http://www.genomex.com/) with an average insert size of ~120 kb (Ezaz *et al.*, 2009a). Of the 73 clones selected, 64 mapped uniquely as diagnostic molecular markers identifying a *P. vitticeps* chromosome pair. Twenty-two of the 64 *P. vitticeps* diagnostic clones were randomly selected from the BAC library, 42 of these clones had been previously extracted from a BAC library screening (but were not mapped) by Ezaz *et al*. (2009b). These clones were used to develop a *P. vitticeps* physical map. Thirteen clones were included in the development of the *P. vitticeps* physical map that had been previously mapped and end sequenced by either Ezaz *et al*. (2009b) or Patel *et al*. (2010). One tammar wallaby (*Macropus eugenii*) BAC clone was mapped from the AGI, *M. eugenii* genomic BAC

library that contains the 18S rDNA locus (Haines, 2005. as cited in O'Meally *et al*. 2009). Forty-one of the clones mapped to *P. vitticeps* were also mapped to *P. lesueurii* chromosomes to construct an agamid comparative map.

2.3 Laboratory methods

2.3.1 BAC DNA extraction

Clones were grown overnight at 37°C in 15 mL liquid cultures of Luria-Bertani (LB) medium (0.01 g/mL Tryptone and 0.01 g/mL Yeast Extract (Bacto laboratories); 85 mM NaCl) which was sterilised by autoclaving and supplemented with 12.5 mg/mL chloramphenicol (Sigma-Aldrich) before use. BAC DNA was extracted using the Promega Wizard Plus SV Minipreps DNA Purification System following the manufacturers protocols with volumes scaled up for 15 mL cultures. DNA concentration was quantitated using a BioPhotometer (Eppendorf).

2.3.2 Fluorescence in situ *hybridization (FISH), microscopy and image capture*

Fluorescence *in situ* hybridisation (FISH) was used to map BAC clones onto mitotic metaphase chromosomes of *P. vitticeps* and *P. lesueurii* following protocols described in Ezaz *et al*. (2009b). BAC clones were directly labeled by nick translation incorporating either Spectrum Orange-dUTP or Spectrum Green-dUTP (Abbott Molecular). Reactions were carried out in 25 µL volumes containing ~250-500 ng of BAC DNA, 1× nick translation buffer (0.5 mg/mL BSA Solution (Roche), 1 mM DTT (Sigma), 100 mM $MgSO_4$, 500 mM TrisHCL), 1.75 mM dNTPs mix (Roche) (0.5 mM of each; dATP, dCTP, dGTP, and 0.25 mM dTTP), 28 µM labeled dUTP, 0.01 units DNase I (Roche) and 5 units DNA polymerase I (Roche). Samples were incubated for two hours at 15°C, 300 rpm using a Thermomixer (Eppendorf).

For single-colour FISH, the 25 µL nick translation product was precipitated by adding glycogen (1 µL; 20 µg/µL) (Roche), and the volume made to 100 µL with double distilled (dd) H_2O to which 3 volumes of 100% ethanol was added and the solution incubated at -20°C overnight. For multi-colour FISH, the 25 µL nick translation product of one Spectrum Green-dUTP labeled and one Spectrum Orange-dUTP labeled BAC probes were combined, followed by precipitation as mentioned above. After incubation the precipitated

samples were centrifuged at ~13,200 rpm, the supernatant aspirated and the precipitated DNA pellet left to air dry. BAC DNA pellets were resuspended in hybridisation buffer (~25-30 µL; 50% (v/v) deionised (DI) formamide (Sigma-Aldrich), 10% (w/v) dextran sulfate (Sigma-Aldrich), 2×SSC, 40 mM Na_3PO_4, 1× Denhardt's solution (Sigma-Aldrich)) for 30 min at 37°C. Resuspended probe (~12-15 µL) was added to slides under cover slips and sealed with rubber cement (Weldtite). The probe and chromosomes were denatured by heating sealed slides at 68.5°C for 5 min on a dry block heater (Ratek) and hybridised overnight at 37°C in a humidified chamber.

Cover slips were removed and slides washed for 2 min in 0.4× SSC, 0.3% IGEPAL-CA630 (Sigma-Aldrich) at 60°C, and for 1 min in 2× SSC, 0.1% IGEPAL-CA630 at room temperature, dehydrated through an ethanol series (1 min each; 70%, 90% and 100% ethanol) and left to air dry. Metaphases were counterstained by incubating slides for ~30 s in DAPI (50 µg/mL in 2× SSC), followed by a 3 s rinse in ddH_2O and left to air dry. Cover slips were mounted with VectaShield (Vecta Laboratories). For each BAC probe, images of metaphases were captured from 10-20 cells and their Vernier coordinates recorded using a Zeiss Axio Scope.A1 epifluorescence microscope fitted with a high resolution microscopy camera (AxioCam MRm Rev. 3). Images were analysed using the applications AxioVision (v4.8.1) and Adobe Photoshop (v9 CS2).

Multi-colour FISH mapping of BAC probes onto the same metaphase was performed by successive rounds of two-colour FISH to the same slide (see Figure 3.5.). This was performed up to five times depending on the cell suspension used. After the first round of FISH and image capture, cover slips and VectaShield were removed by washing for 5 min in 2× SSC at room temperature followed by dehydration of the slides through an ethanol series (70%, 90% and 100% ethanol) and left to air dry. Slides were then aged overnight at -80°C before hybridisation with different probes. Multiple hybridisation images of the same metaphases were merged using Adobe Photoshop.

2.3.3 Hybridisation of telomeric probe

Telomeres were visualised by FISH of a $(TTAGGG)_5$ oligonucleotide probe labeled with Cy3 (GeneWorks). Twelve µL of probe solution (1 µL probe (1µg/µL), 11µL

hybridisation buffer) was added to slides under cover slips and FISH performed as described in section 2.3.2.

2.3.4 DAPI banding

Chromosomes were stained with DAPI (50 µL/mL in 2× SSC) for ~10 to 15 s and rinsed in ddH_2O for 3 s to remove excess DAPI. VectaShield was added under cover slips and images taken as described above. One cell from a female and one from a male *P. vitticeps* that had the most clearly visible chromosomes were used for analysis.

2.3.5 BAC end-sequencing

Both ends of 64 BAC clones were sequenced using three primers (GeneWorks): pCC1 / pEpiFOS-5 Forward Sequencing Primer and T7 Promoter that bind the vector 5' to the insert, and pCC1 / pEpiFOS-5 Reverse Sequencing Primer that binds the vector 3' to the insert. BAC end sequencing was undertaken commercially by Macrogen Inc. (Seoul, Korea). BAC clone agar stabs were prepared in 1.5 mL tubes containing 1 mL LB agar supplemented with chloramphenicol (12.5 mg/mL) and shipped at ambient temperature.

2.4 Measurements and data analysis

2.4.1. Chromosome nomenclature, sizes, banding, signal and centromere position

Arm length measurements were taken from each *P. vitticeps* macro- and microchromosome and from each *P. lesueurii* macrochromosome from five of the most well-spread metaphases from one male and one female. For *P. lesueurii* the total length of microchromosomes was measured as individual arms were frequently not discernable. All measurements were taken using the measure-line tool in the application AxioVision (v4.8.1) or ruler tool in Adobe Photoshop. All data were recorded and calculations made using Microsoft EXCEL.

The length of each chromosome was calculated as a proportion of the total haploid length and averaged over ten metaphases using the equation:

where *A* is either the *p* or *q* chromosome arm length from one homolog of one chromosome in a single metaphase and *THL* is the total haploid length from that same metaphase.

The centromeric index (CI) was calculated for each *P. vitticeps* chromosome and *P. lesueurii* macrochromosome using the equation:

$$\frac{\quad}{\quad}$$

where *p* is the length of the p arm and *q* is the length of the q arm of the one chromosome. Nomenclature was assigned following the arm relationship proposed by dos Santos, (1986).

Genome size in base pairs (bp) and individual chromosome size in base pairs was estimated using conversion formulas derived from Dolezel *et al*. (2003):

Where (0.978×10^9) is the number of base pairs in 1 pg of DNA and the diploid DNA content of one *P. vitticeps* cell is 3.62 pg (MacCulloch *et al.*, 1996). Individual chromosome sizes in bp were then estimated by first estimating the DNA content (pg) of each chromosome using the formula:

Where *%THL* is the percent of the total haploid length of a chromosome, (0.978×10^9) is the number of base pairs in 1 pg of DNA and 1.81 pg is the haploid DNA content of one *P. vitticeps* cell.

The percentage of the *P. vitticeps* genome mapped in this study was estimated by multiplying the total number of *P. vitticeps* mapped clones (77) by the average insert size (120 kb) and dividing by the genome size.

BAC clone localisations in *P. vitticeps* were estimated by measuring the distance from the centromere to the centre of the BAC signal and from the centromere to telomere using the measure-line tool in AxioVision (v4.8.1) from five well-spread metaphases. The centromere to signal length was divided by the total arm length, and the mean ratio calculated from the five metaphases. Localisations in *P. lesueurii* were estimated using the same measurements that were taken from only one metaphase.

Measurements were taken of the banding pattern shown in each chromosome from one female and one male *P. vitticeps* cell as described above, which were processed and adjusted for brightness and contrast using Adobe Photoshop. The position and length of visible DAPI bands were estimated by measuring the length from centromere to telomere for each chromosome arm, and the distance of each band from the telomere and from the centromere. Measurements were taken using the ruler tool in Adobe Photoshop. Chromosome banding nomenclature was assigned following the guidelines for banding of human chromosomes (ISCN 1995).

2.4.3 Sequence analysis, gene identification and comparative mapping

Initial analysis of BAC end sequences was undertaken using Geneious Pro v5.1.6 (Biomatters) by searching for and removing vector contamination using the Trim Ends function in Geneious. Sequence quality was analysed using the Chromatogram – Show Quality function in Geneious, failed or low quality sequences were not used for further analyses. The *P. vitticeps* GC composition was estimated from the T7 and R1 primer end sequence reads by averaging the GC percent estimate of each read supplied by Geneious. *P. vitticeps* BAC end sequences were analysed, annotated and mapped *in silico* as described in Chapus & Edwards (2009) with some modification (see sections 2.4.3.1 and 2.4.3.2)

2.4.3.1 BLAST (Basic Local Alignment Search Tool) analyses

A total of 185 *P. vitticeps* BAC end sequence reads from 64 BACs (average length 694 bp) were searched against the nucleotide nr database (http://blast.ncbi.nlm.nih.gov/Blast.cgi) using BLAST with the BLASTN algorithm in Geneious. Hits to the nr database that were

≥100 bp in length and had an E value ≤ 10^{-20} were recorded as significant. In contrast to the methods of Chapus & Edwards (2009), clones were not annotated with gene names when there were multiple ambiguous significant hits due to the uncertainty in results.

2.4.3.2 BLAT (BLAST-Like Alignment Tool) analyses

P. vitticeps BAC end sequence reads were also searched against the green anole (*Anolis carolinensis*; Squamata; Iguania) whole genome assembly database (anoCar1: Feb 2007; http://genome.ucsc.edu) using BLAT following the approach of Chapus & Edwards, (2009). Significant results were identified as those fulfilling one of three criteria that ranked the level of confidence in the hit, these were:

A. High quality; ≥100 bp homology of a forward and reverse sequence of a particular *P. vitticeps* BAC to the same region on an *A. carolinensis* scaffold between ~80-160 kb apart.

B. Medium quality; ≤100 bp homology of a *P. vitticeps* forward (either F1 or T7) and a reverse sequence to an *A. carolinensis* scaffold between ~80-160 kb apart

C. Low quality; ≥100 bp homology of either a forward (either F1 or T7 or F1+T7) or a reverse sequence to an *A. carolinensis* scaffold without homology of the opposite sequence within ~80-160 kb.

In categories A and B, a more stringent exclusion regime based upon a sequence length of ~80-160 kb was adopted instead of the ≤200 kb method of Chapus & Edwards (2009), because there were multiple ambiguous significant hits ≤200 kb to the same *A. carolinensis* scaffold. BACs were annotated with genes whose exons and introns spanned the homologous *P. vitticeps* sequence, or if they were within ~80-160 kb of the sequences on the *A. carolinensis* scaffold. For category C hits, BACs were annotated with a gene name if an exon was within the vicinity of 50 kb on the *A. carolinensis* scaffold. Recommended gene symbols were obtained from the HUGO Gene Nomenclature Committee (http://www.genenames.org/). Orthologues of the identified genes were located on the

chicken (*Gallus gallus*) and human (*Homo sapiens*) genomes using the Ensembl genome browser database (http://www.ensembl.org/).

Chapter 3: Results

3.1 Physical map of *Pogona vitticeps*

3.1.1 Karyotype of Pogona vitticeps

Cells from the two female and one male *P. vitticeps* examined possessed a consistent karyotype composed of macrochromosomes (M) and microchromosomes (m), with a diploid number of 32 chromosomes (2n = 12M + 20m) (Figure 3.1.). There are 15 pairs of autosomes and two sex microchromosomes ZW female: ZZ male (Ezaz *et al.*, 2005). The macrochromosomes consist of five metacentric pairs (1st, 3rd, 4th, 5th and 6th), and one submetacentric pair (2nd), the microchromosomes are all metacentric (Table 3.1.). Collectively, the macrochromosomes represent approximately 78% of the total haploid length and microchromosomes approximately 22% (Table 3.1.).

Chromosomes 1, 2, 5 and 6 can be distinguished morphologically based upon a combination of size and centromere position. Chromosomes 3 and 4 are relatively similar in morphology, and due to differential contraction in some metaphases unequivocal pairing of homologs is not always possible. Chromosome pair 7 can be commonly distinguished from other microchromosome pairs because of its larger size. Other microchromosome pairs cannot reliably be distinguished because of their similar size and centromere position. Throughout this thesis, unidentified microchromosomes are referred to using an alphabetical system that is assigned on a temporary basis. Distinguishing between the *p* and *q* arms of metacentric chromosomes 3, 4 and 5 and microchromosomes is not always possible due to similar arm ratios (Table 3.1.). Other distinguishing features of the karyotype include a prominent secondary constriction in the sub-telomeric region of chromosome 2q and a W chromosome that is frequently observed to be slightly extended and/or faintly counterstained with DAPI (Figure 3.1.).

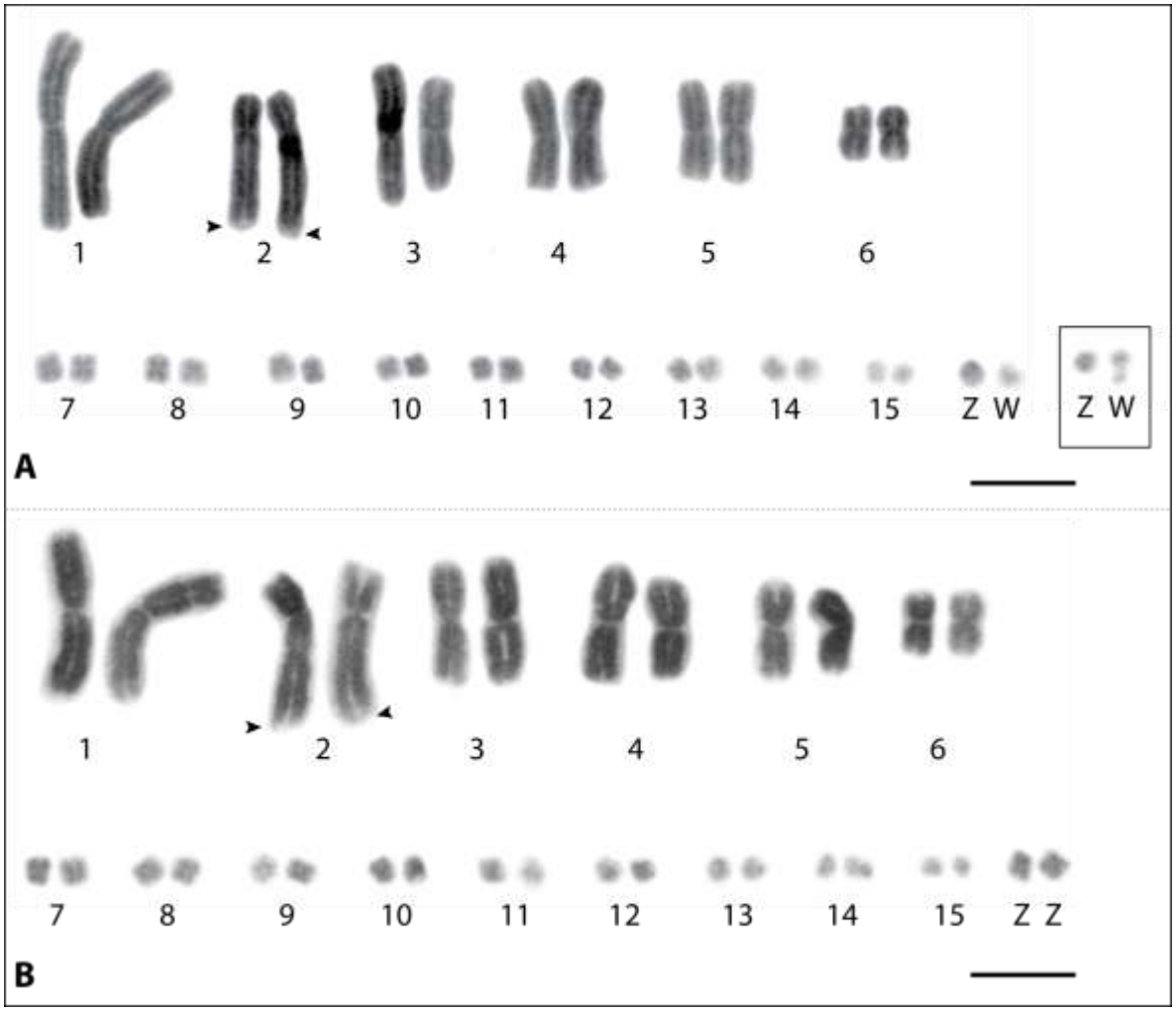

Figure 3.1. Karyotype of *P. vitticeps*. (A) DAPI stained karyotype from one female cell, combined with a ZW pair from another cell (inset box) showing an extended W chromosome. (B) Male karyotype from a single cell. The karyotype consists of 12 macrochromosomes and 20 microchromosomes (2n = 32), with 15 autosomal pairs (macrochromosomes 1-6, microchromosomes 7-15) and two slightly differentiated sex microchromosomes (ZW). Arrowheads indicate secondary constrictions on chromosome 2q. Sex chromosomes were identified in both karyotypes by FISH mapping of a diagnostic BAC that hybridises to both the Z and W microchromosomes (see Figure 3.6.). Scale bars represent 10 µm.

Table 3.1. Relative sizes, centromeric index, and proportional lengths of *P. vitticeps* chromosomes. Each arm (*p* and *q*) was measured of DAPI-stained chromosomes from five female and five male cells and the mean and standard error calculated; arm ratio was calculated as the centromeric index (CI: *p*/total), percent haploid length (%HAL) was calculated as a proportion of the total haploid length (*p* + *q*/total haploid length), and chromosome size (Chr size) was calculated by converting the haploid genome size 1.81 pg to base pairs (bp) then dividing by the percent haploid length of each chromosome.

Chromosome	*p* arm		*q* arm				
	(µm)	Range	(µm)	Range	CI	% HAL	CS (Mb)
Macrochromosomes							
1	9.08 ± 0.21	8.04-9.85	10.35 ± 0.23	9.34-11.36	0.47	19.44	344.07
2	4.81 ± 0.10	4.46-5.43	12.45 ± 0.23	11.16-13.64	0.28	17.26	305.48
3*	6.75 ± 0.16	5.57-7.32	7.17 ± 0.19	6.20-8.37	0.48	13.91	246.29
4*	6.13 ± 0.12	5.77-6.68	6.58 ± 0.16	5.99-7.69	0.48	12.71	225.01
5	4.77 ± 0.11	4.18-5.49	5.18 ± 0.12	4.73-5.89	0.48	9.95	176.16
6	2.67 ± 0.07	2.38-3.16	3.55 ± 0.14	2.83-4.52	0.43	6.22	110.10
Microchromosomes							
7	1.15 ± 0.06	0.96-1.62	1.52 ± 0.07	1.29-1.88	0.43	2.67	47.32
8	1.08 ± 0.03	0.95-1.29	1.23 ± 0.06	1-1.59	0.47	2.30	40.78
9	1.04 ± 0.03	0.90-1.21	1.17 ± 0.05	0.96-1.48	0.47	2.20	38.98
10	0.98 ± 0.04	0.84-1.19	1.09 ± 0.04	0.90-1.29	0.47	2.07	36.57
11	0.91 ± 0.04	0.78-1.14	1.11 ± 0.04	0.98-1.30	0.45	2.02	35.72
12	0.87 ± 0.04	0.75-1.16	1.05 ± 0.05	0.88-1.39	0.45	1.92	33.98
13	0.83 ± 0.05	0.59-1.11	1.03 ± 0.04	0.88-1.24	0.45	1.86	32.94
14	0.77 ± 0.03	0.64-0.96	0.93 ± 0.03	0.75-1.07	0.45	1.70	30.12
15	0.74 ± 0.03	0.61-0.89	0.82 ± 0.04	0.68-1.16	0.47	1.55	27.51
ZW; Sex chromosomes†	1.03 ± 0.05	0.87-1.29	1.27 ± 0.10	1.02-2.14	0.45	2.30	40.74

* Measurements were taken from five separate female metaphases in which homologs of chromosomes 3 or 4 were identified by mapping of a diagnostic BAC.

† Chromosome pair identified by size and DAPI staining properties.

3.1.2 DAPI banding Idiogram

A preliminary DAPI banded idiogram was developed from two *P. vitticeps* cells, one female and one male. Each macrochromosome except chromosome 5 had observable DAPI bands from the two cells examined. In both the male and female metaphases the secondary constriction in the sub-telomeric region of chromosome 2q stained faintly with DAPI. Most microchromosomes stained faintly with DAPI including the ZW pair, the exception being one pair (designated microchromosome pair 'E') that had a DAPI band on one arm in both the female and male metaphases (Figure 3.2.).

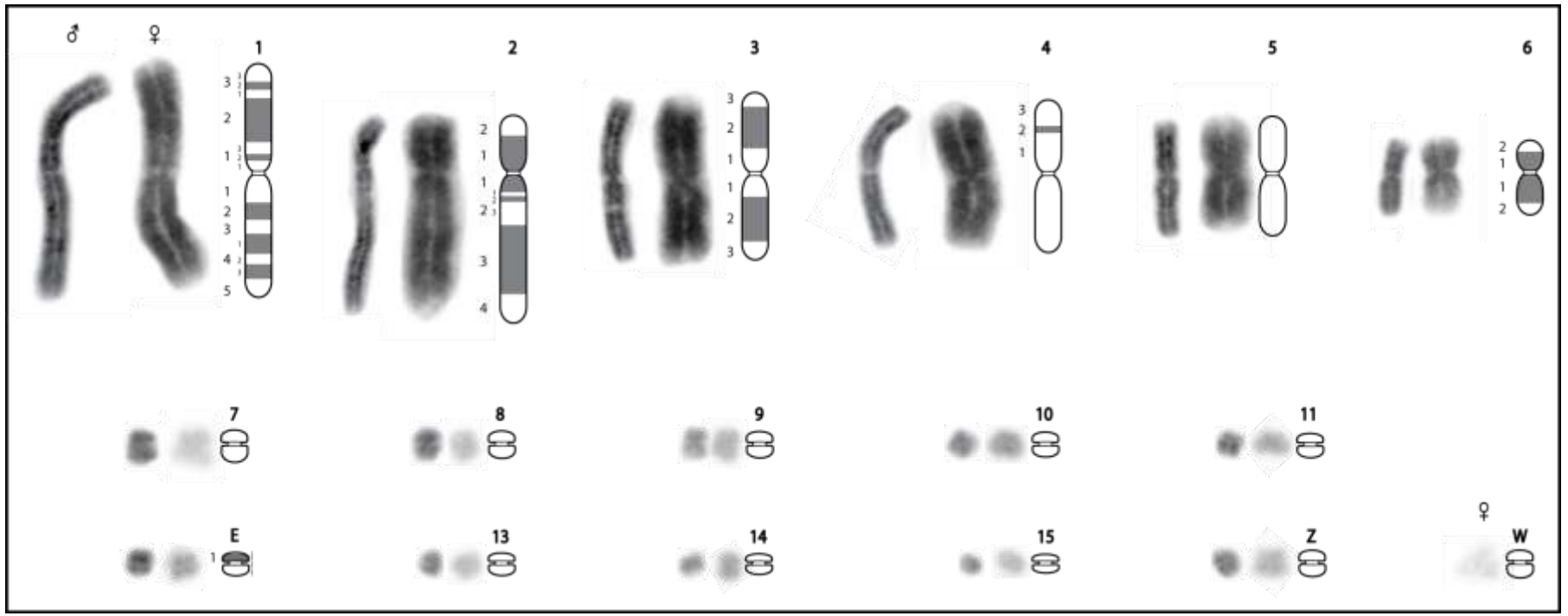

Figure 3.2. Ideogram of *P. vitticeps* DAPI bands. DAPI-stained haploid karyotypes are adjacent to their corresponding chromosome ideogram. Haploid karyotypes are from one female cell (immediate left) and one male cell (far left). DAPI bands are indicated in grey.

3.1.3 18S rDNA localisation

A single nucleolus organizer region (NOR) was identified in the sub-telomeric region of 2q by FISH mapping of a BAC probe containing the 18S rDNA locus. Of the 10 cells examined, signals on both homologs consistently mapped to the same location with similar intensity (Figure 3.3.).

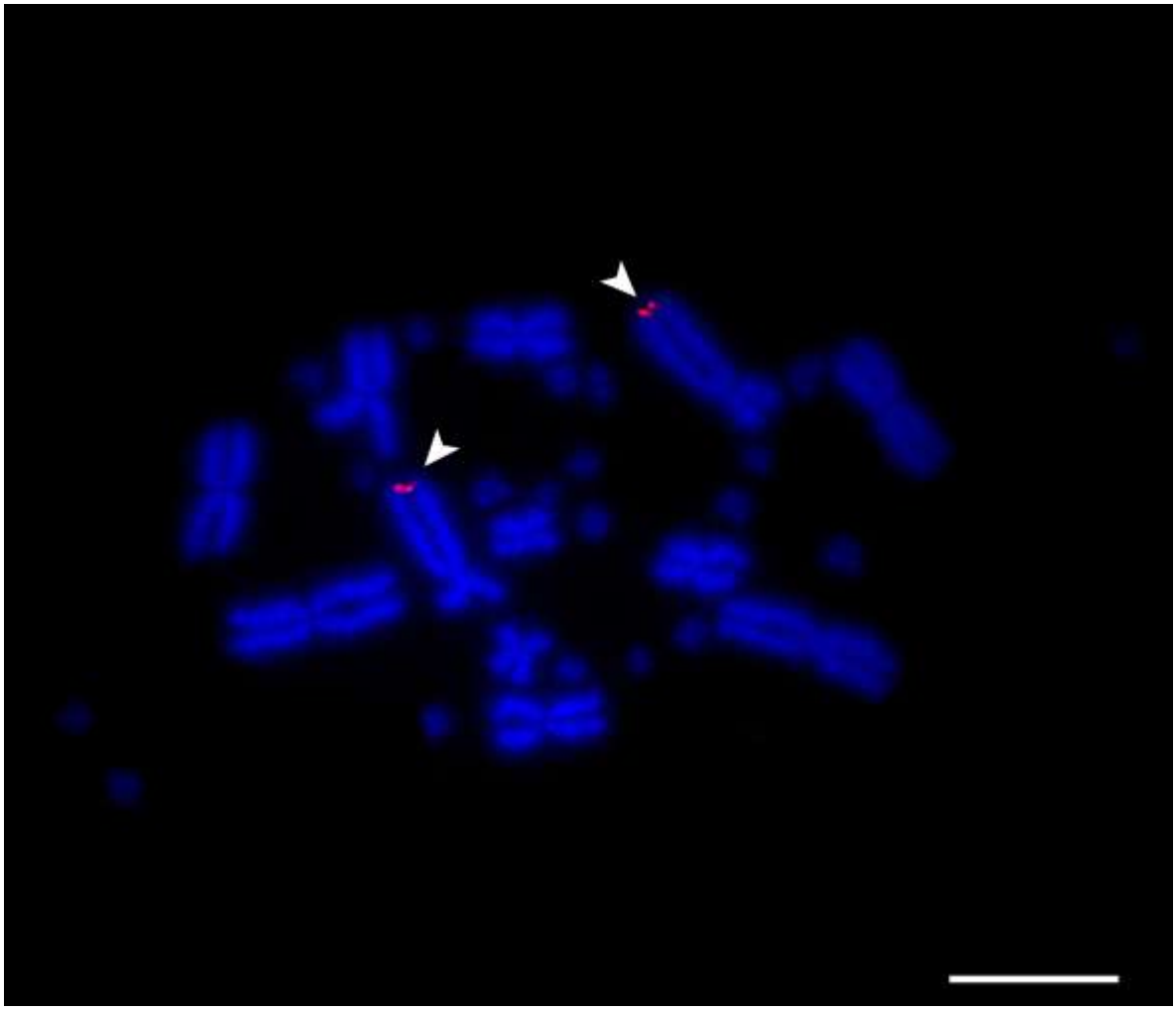

Figure 3.3. 18S rDNA FISH on *P. vitticeps* metaphase chromosomes. Arrowheads indicate the position of the NOR on the *q* arm of chromosome 2. Metaphase chromosomes are counter-stained with DAPI. The scale bar represents 10 µm.

3.1.4 Telomere localisation

Telomeres were identified at the ends of each chromosome by hybridising a $(TTAGGG)_5$ Cy3 labeled oligonucleotide probe to metaphase spreads. Within each metaphase, the telomeres of one or more chromosomes had very weak fluorescent hybridisation signals. Interstitial telomeric sequences were identified in three microchromosome pairs (Figure 3.4.).

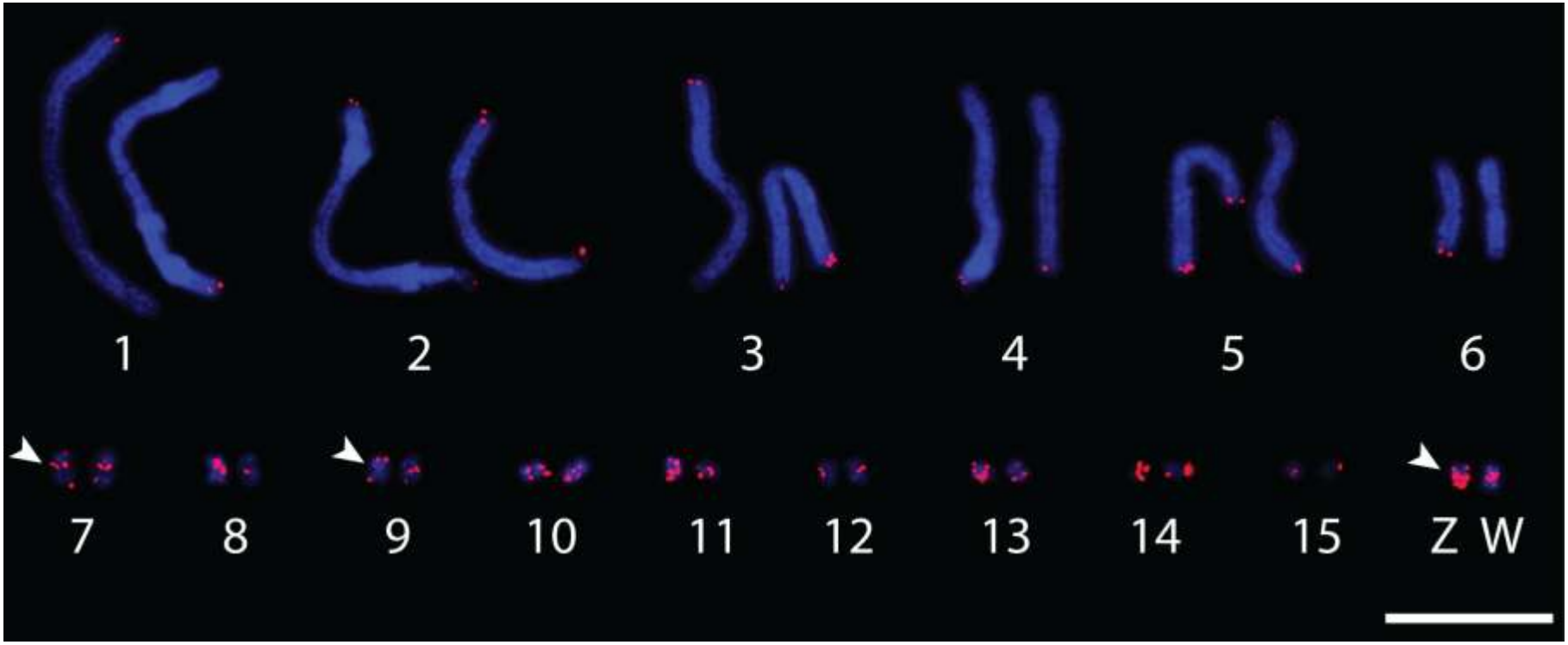

Figure 3.4. Karyotype of *P. vitticeps* chromosomes showing hybridisation signals of telomeric probe $(TTAGGG)_5$. Telomeres were identified at the ends of all chromosomes and interstitially in three microchromosome pairs (Arrowheads). Scale bar represent 10 µm.

3.1.5 BAC-based Physical map of Pogona vitticeps

Sixty-five BAC clones were mapped to *P. vitticeps* mitotic metaphase spreads using single-colour and two-colour FISH (Figure 3.5.). In conjunction with previous *P. vitticeps* mapping studies by Ezaz *et al*. (2009b) and Patel *et al*. (2010), 64 clones mapped to macrochromosomes and 13 clones mapped to microchromosomes. Each macrochromosome had two or more clones mapped to the *p* and *q* arms. Sixty-four clones were end sequenced and where possible, one or more loci were identified through a combination of BLASTN and BLAT (Appendix 1) (Table 3.2.). Of the 13 clones that mapped uniquely to one of the 10 microchromosome pairs, only those which mapped to identifiable microchromosomes (microchromosome pairs 7 and ZW) could be considered diagnostic (those that uniquely identify one chromosome pair).

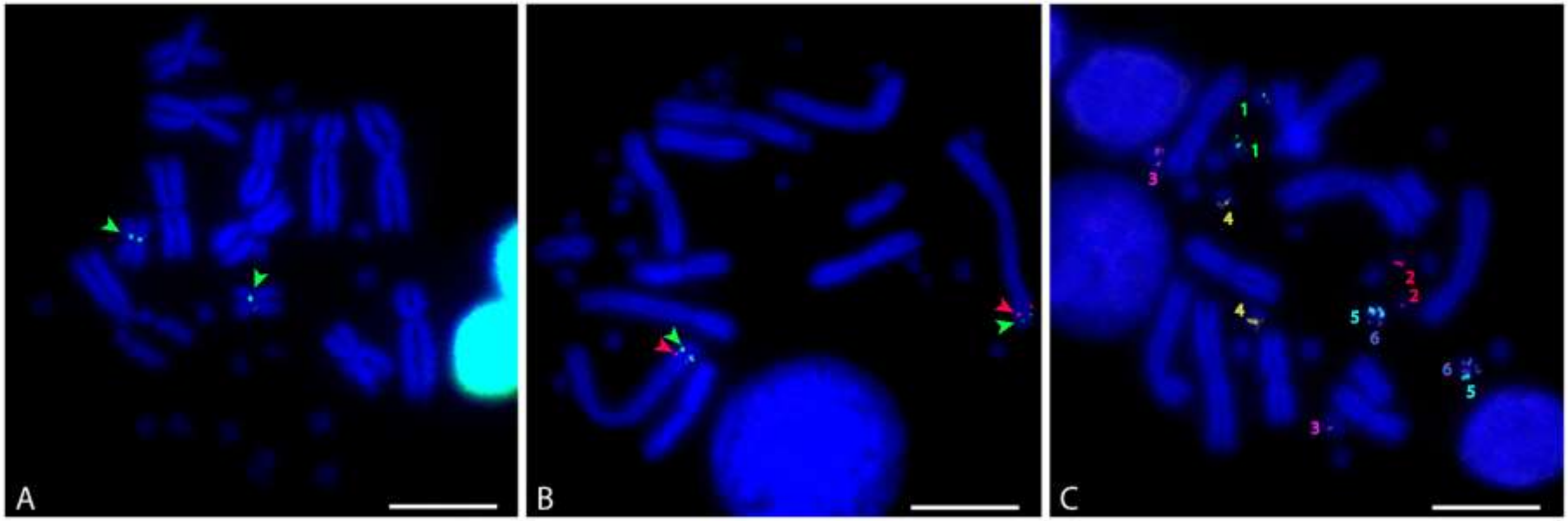

Figure 3.5. Example FISH experiments in *P. vitticeps*. (A) Single-colour FISH of clone 16A11 diagnostic for chromosome 6p (green). (B) Two-colour FISH of clones 229E3 (green) and 232K10 (red) diagnostic for chromosome 1q. (C) Multiple rounds of two-colour FISH of clones 1; 221B16 (green), 2; 16A10 (red), 3; 197P21 (magenta), 4; 230K11 (yellow), 5; 232P19 (aqua) and 6; 105P18 (purple) that uniquely identify microchromosomes, but remain inconclusive as they were unable to be assigned a specific pair in the karyotype. Multiple rounds of two-colour FISH were used to identify clones that uniquely mark a single microchromosome pair; or the relative positions of clones on the same chromosome arm. For example, clones 221B16, 16A10, 197P21 and 230K11 (1-4) all map to separate microchromosome pairs, while 232P19 (5) and 105P18 (6) map to the same pair. All scale bars represent 10 µm.

Table 3.2. Gene contents and mapped locations of BAC clones in *P. vitticeps* and locations of chicken and human orthologues. A total of 78 BAC clones were mapped to the chromosomes of *P. vitticeps*, in this study and by Ezaz *et al*. (2009b) and Patel *et al*. (2010). Forty-four of these clones were also mapped in *P. lesueurii*. Representative loci within end sequenced clones were identified by BLAST and BLAT. Gene symbols are those recommended by the HUGO Gene Nomenclature Committee (http://www.genenames.org/). The locations of chicken and human orthologues were downloaded from the Ensembl database (http://www.ensembl.org/index.html).

Library ID	Reference	Clone ID	Gene symbol	Chromosomal location			
				P. vitticeps	*P. lesueurii*	Chicken orthologue	Human orthologue
AGI, *Macropus eugenii* (tammar wallaby)	Haines, 2005	329J14	*18S rDNA*	2q	2q	16	22p12 + Yp11.2[±]
Pv, *Pogona vitticeps* (central bearded dragon)	*This study*	57H2		1p	1p		
		16A1	*HMGCLL1; FAM83B; HCRTR1*	1p		3	6p12.1
		219E3		1p			
		16A7		1q			
		220D7	*TTN*	1q		7	2q31.2
		16A12		1q			
		16A9		1q			
		215H24		1q			
		170F19	*ZNF143; IPO7; TMEM41B*	1q	1q	5	11p15.4
		184J20		1q	1q		
		220D11		1q	1q		
		232K10		1q	1q		
		222N5		1q	1q		
		229E3		1q	1q		
		206D14	*GMPPA*	1q		7	2q35
		16A4		2p	2p		
		176E5	*DDX58*	2q		Z	9p21.1

Library ID	Reference	Clone ID	Gene symbol	Chromosomal location			
				P. vitticeps	*P. lesueurii*	Chicken orthologue	Human orthologue
		195K1		2q			
Pv, *Pogona vitticeps* (central bearded dragon)	*This study*	200H9		2q			
		203J2		2q			
		189J12	*TNFRSF11B*	2q		2	8q24.12
		16A23		2q	2q		
		238E7		2q	2q		
		219G15		2q	2q		
		199D4		3p			
		185A1		3p			
		220D15	*NAV2*	3*	3*	5	11p15.1
		214J17		3q	3q		
		213B13		3q	3q		
		221A23	*CTBP2*	3q	3q	6	10q26.13
		233A1		3q	3q		
		219I19		4p	4p		
		230L10		4p	4p		
		219N21		4q	4q		
		16A5	*EIF3H*	4q	4q	2	8q23.3-q24.11
		240P5		4q	4q; µ		
		16A22		5p	5p		
		16A3		5p	5p		
		220D13		5*	5*		
		201K21	*BCL6*	5q	5q	9	3q27.3
		208G18		5q	5q		

Library ID	Reference	Clone ID	Gene symbol	Chromosomal location			
				P. vitticeps	*P. lesueurii*	Chicken orthologue	Human orthologue
		210E16		5q			
Pv, *Pogona vitticeps*	*This study*	233L23		5q			
(central bearded dragon)		198N24		6p	6p		
		211I19	*IBSP*	6p		4	4q22.1
		174P24	*KAT2B*	6p		2	3p24.3
		16A11	*SUB1*	6p		Z	5p13.3
		212P4		6q			
		200O10		6q	6q		
		225A2		6q			
		200H5	*CA10*	6q	6q	18	17q21.33
		197P21		7	µ		
		220D8		µ			
		230Kll		µ	µ		
		237P23		Z; W	2q		
		151D5		Z; W	2q		
		220D12		µ			
		188M22	*IQSEC3*	µ		1	12p13.33
		105P18	*PSMA2*	µ		2	7p14.1
		232P19		µ			
		214G3	*FBRSL1*	µ		15	12q24.33
		221B16		µ	µ		
		185N3		µ			
		16A10		µ	µ		
	Ezaz *et al*., 2009b	107D1	*GHR*	2p	2p	Z	5p12-p13.1

Library ID	Reference	Clone ID	Gene symbol	Chromosomal location			
				P. vitticeps	*P. lesueurii*	Chicken orthologue	Human orthologue
		126K15	*ATP5A1*	2p	2p	Z	18q21.1
Pv, *Pogona vitticeps*	Ezaz *et al*., 2009b	201M16	*CHD1*	2p		Z	5q15-q21.1
(central bearded dragon)		141L17	*DMRT1*	2p	2p	Z	9p24.3
		151O19	*APTX*	2q		Z	9p21.1
		129O15	*WAC*	6p	6p	2	10p12.1
		168D8	*KLF6*	6p	6p	2	10p15.1
		101M20	*RAB5A*	6p	6p	2	3p24.3
		22H1	*TAX1BP1*	6p		2	7p15.2
		9I16	*CTNNB1*	6p		2	3p22.1
		132P11	*MYST2*	6q		27	17q21.33
	Patel *et al*., 2010	61D8	*RRM1*	3q		1	11p15.4
		236C5	*NPRL3*	µ		14	16p13.3

*Clones that hybridise close to the centromeric region and were not able to be assigned a chromosome arm.
±: Pseudogene
µ: Microchromosome

The diagnostic BAC clones were used to develop a BAC-based physical map of each *P. vitticeps* macrochromosome and seven of the 10 microchromosomes, with 71 BAC molecular markers. Loci identified in non-diagnostic microchromosome clones are assigned to a microchromosome on a provisional basis using an alphabetical system (A-D) (Appendix 2). Twenty-one loci were identified on 9 chromosomes that in conjunction with published data brings the total number of loci on *P. vitticeps* chromosomes to 35 spanning 10 chromosomes (Figure 3.6.).

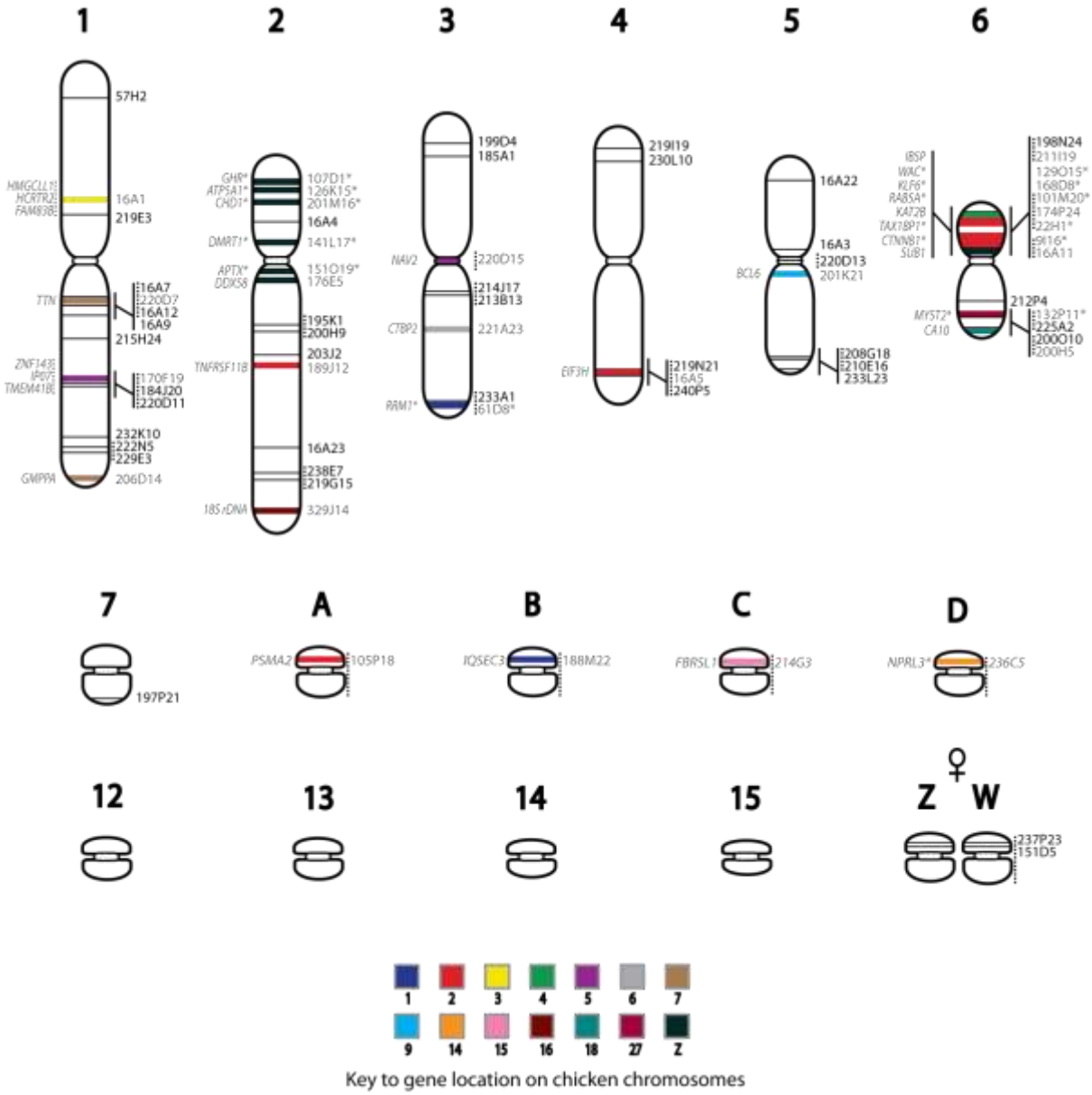

Figure 3.6. Physical map of *P. vitticeps* showing the location of diagnostic BAC clones mapped by FISH and orthology to chicken chromosomes. All chromosomes are drawn to scale based upon the mean percent total haploid length from five female cells (Appendix 3). Clone numbers are shown to the right of a horizontal line indicating the mapped location and colour indicates orthology to chicken chromosomes. Genes symbols are shown to the left of each chromosome and are shaded grey along with the clones in which they are contained. Clone numbers and gene symbols joined by a dotted line indicate that the order of these clones and/or the loci they contain is unknown. Dotted lines joining gene symbols indicate that loci found within the same BAC clone have an unknown order on the chromosome. Gene symbols are those listed by the HUGO Gene Nomenclature Committee (http://www.genenames.org/).

For each diagnostic BAC consistent fluorescent hybridisation signals were observed across all metaphases examined (Appendix 4 provides examples) except the two clones 237P23 and 151D5 which have a strong fluorescent hybridization signal to the ZW pair, but also have a weak diffuse signal on the subtelomeric region of 2q (see Appendix 4 Figure 7. A). Multiple fluorescent hybridisation signals were observed for 11 clones on chromosomes 1, 2, 5, 6, ZW and on unidentified microchromosomes (Table 3.3).

Table 3.3. BAC clones that hybridise to multiple *P. vitticeps* chromosomes.

Library ID	Clone ID	Chromosomal location
		P. vitticeps
Pv, *Pogona vitticeps* (central bearded dragon)	238C5	1p; 5q
	238M20	2q; 6p
	016A2	2q; 5q; µ
	016A6	2 Centromeric; 5 Centromeric
	188D4	6p; µ
	193O17	
	197L22	Multiple µ
	237P23	Z; W; 2q
	151D5	Z; W; 2q
	229A16	2q; 2q
	097B13	2p; 2p

µ: Microchromosome

3.2 Molecular characterisation of *Physignathus lesueurii* chromosomes

3.2.1 Karyotype of Physignathus lesueurii

The single female and single male *P. lesueurii* specimens examined each possessed a karyotype composed of macrochromosomes and microchromosomes, similar to *P. vitticeps*. However, the diploid number of *P. lesueurii* is 36 autosomes; 2n = 12M + 24m, possessing two more microchromosomes than *P. vitticeps*. The macrochromosomes consist of five metacentric pairs (1st, 3rd, 4th, 5th and 6th), and one submetacentric pair (2nd) (Figure 3.7.). The centromere positions on microchromosomes could not be identified in all *P. lesueurii* cells. Collectively, the macrochromosomes represent ~72% of the total haploid length and microchromosomes ~28% (Table 3.4.). No estimation of chromosome size in bp could be made, as the genome size for this species has not been determined.

Chromosomes 1, 2, 5 and 6 can be distinguished morphologically based upon a combination of size and centromere position. Chromosomes 3 and 4 are relatively similar in morphology and homologs cannot always reliably be distinguished. The microchromosome pairs are indistinguishable because of their similar sizes, and the centromere could not be identified in all cells. Distinguishing between the *p* and *q* arms of chromosomes 3, 4 and 5 is not always possible due to similar arm ratios (Table 3.3.), and chromosome 2q bears a prominent secondary constriction in the sub-telomeric region (Figure 3.7.).

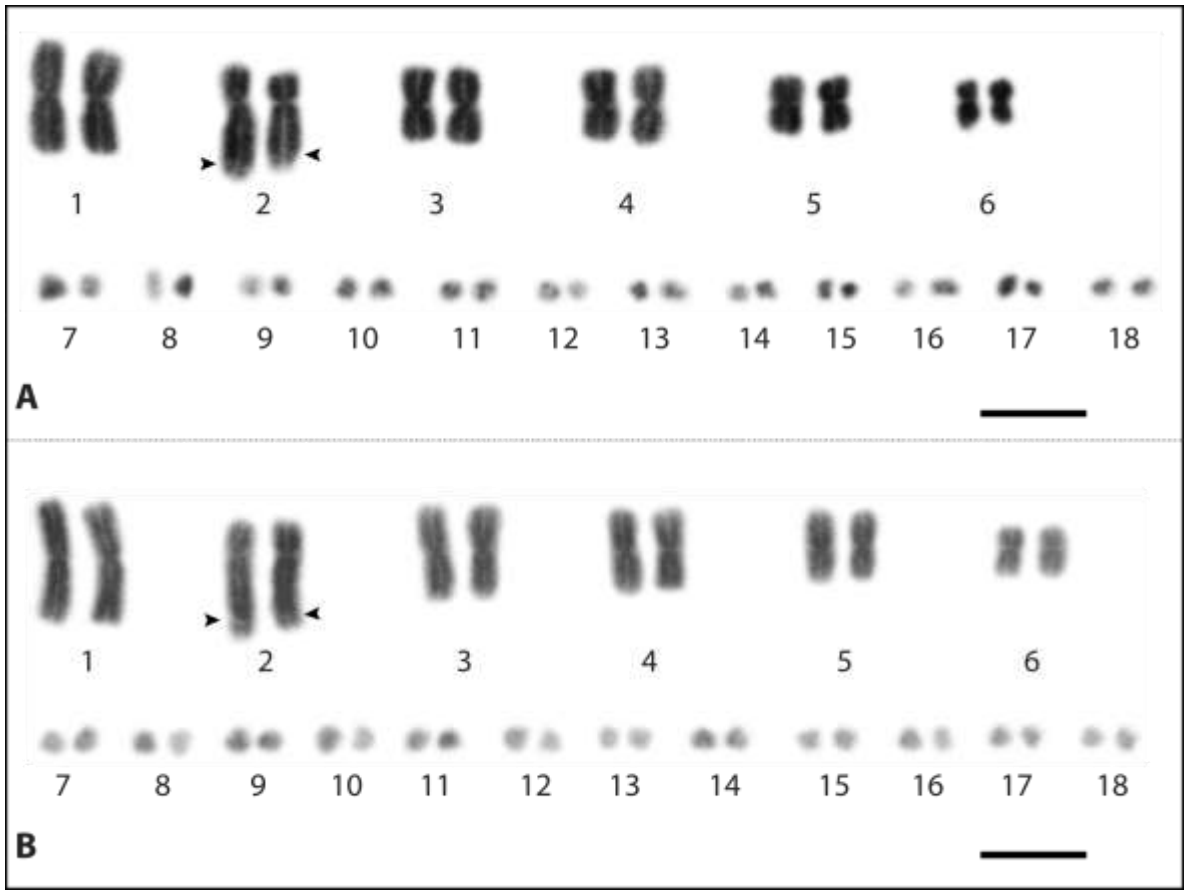

Figure 3.7. Karyotype of *P. lesueurii*. (A) DAPI stained karyotype from one female cell. (B) Male karyotype from a single cell. The karyotype consists of 12 macrochromosomes and 24 microchromosomes (2n = 36). Arrowheads indicate secondary constriction on chromosome 2q. Scale bars represent 10 µm.

Table 3.4. Relative sizes, centromeric index, and proportional lengths of *P. lesueurii* chromosomes. Each arm (*p* and *q*) was measured of DAPI-stained macrochromosomes from five female and five male cells and the mean and standard error calculated; arm ratio was calculated as the centromeric index (CI: *p*/total), total length was measured for microchromosomes, percent haploid length (% HAL)was calculated as a proportion of the total haploid length (*p* + *q*/total haploid length). .

Chromosome	*p* arm		*q* arm			
	(µm)	Range	(µm)	Range	CI	% HAL
Macrochromosomes						
1	7.92 ± 0.18	6.51-9.73	8.96 ± 0.24	7.07-10.96	0.48	16.88
2	4.62 ± 0.11	3.87-5.64	11.02 ± 0.30	9.13-14.01	0.30	15.64
3	6.11 ± 0.11	5.22-7.21	6.32 ± 0.10	5.36-7.08	0.50	12.42
4	5.47 ± 0.06	4.91-5.93	5.73 ± 0.06	5.22-6.25	0.50	11.20
5	4.30 ± 0.08	3.51-4.94	5.01 ± 0.09	4.39-6.03	0.47	9.31
6	2.92 ± 0.05	2.54-3.42	3.8 ± 0.07	3.15-4.25	0.45	6.72
Microchromosomes						
7			2.84 ± 0.09	2.15-3.51		2.84
8			2.69 ± 0.08	1.99-3.31		2.69
9			2.57 ± 0.08	1.92-3.09		2.57
10			2.48 ± 0.07	1.85-2.91		2.48
11			2.41 ± 0.07	1.85-2.78		2.41
12			2.34 ± 0.06	1.77-2.73		2.34
13			2.29 ± 0.06	1.74-2.69		2.29
14			2.21 ± 0.06	1.70-2.66		2.21
15			2.14 ± 0.05	1.63-2.58		2.14
16			2.07 ± 0.05	1.62-2.48		2.07
17			1.97 ± 0.04	1.59-2.20		1.97
18			1.80 ± 0.04	1.35-1.91		1.80

3.2.2 18S rDNA localization

A single NOR was identified in the sub-telomeric region of chromosome 2q by FISH mapping of a BAC probe containing the 18S rDNA locus. Of the 10 cells examined, signals on both homologs consistently mapped to the same location with similar intensity (Figure 3.8.).

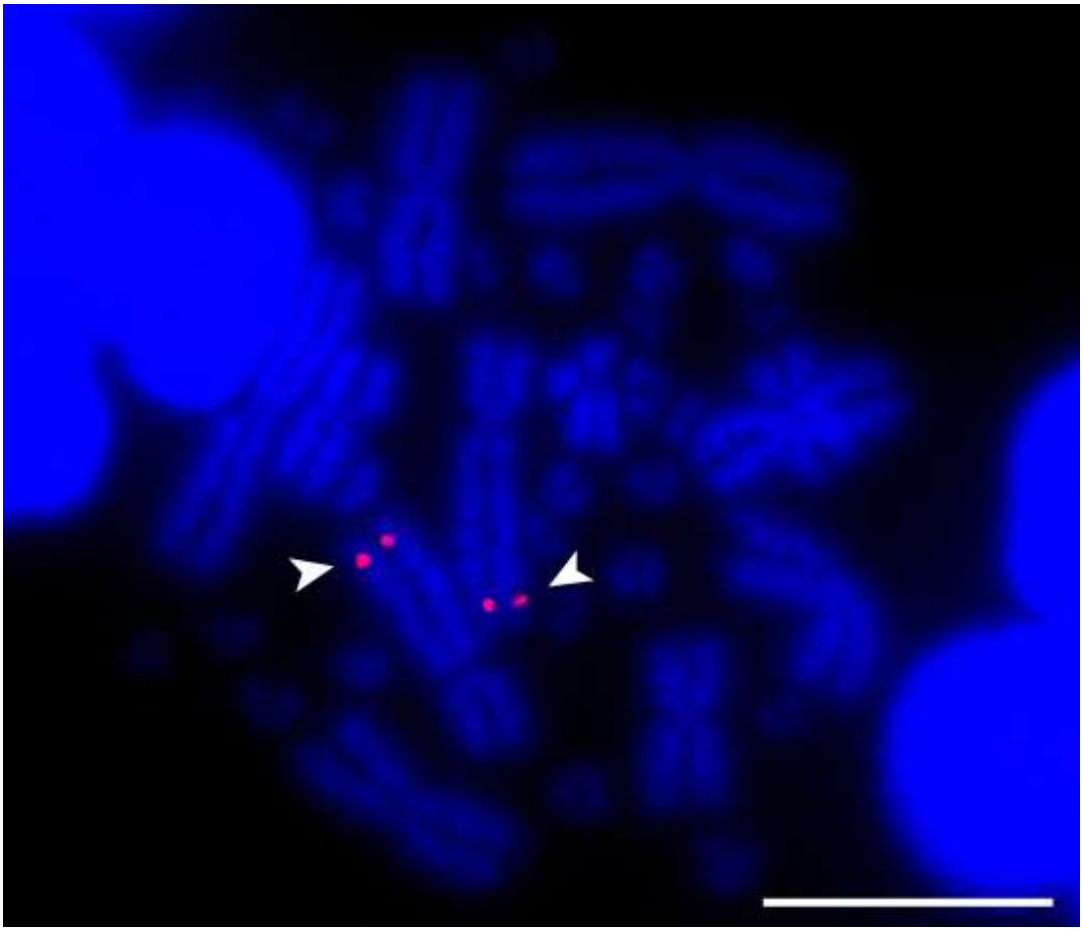

Figure 3.8. 18S rDNA FISH on *P. lesueurii* metaphase chromosomes. Arrowheads indicate the position of the NOR on 2q. Metaphase chromosomes are counter-stained with DAPI. Scale bar represents 10 µm.

3.2.3 Telomere localization

Telomeres were identified as for *P. vitticeps*. No interstitial telomeric sequences were identified (Figure 3.9.).

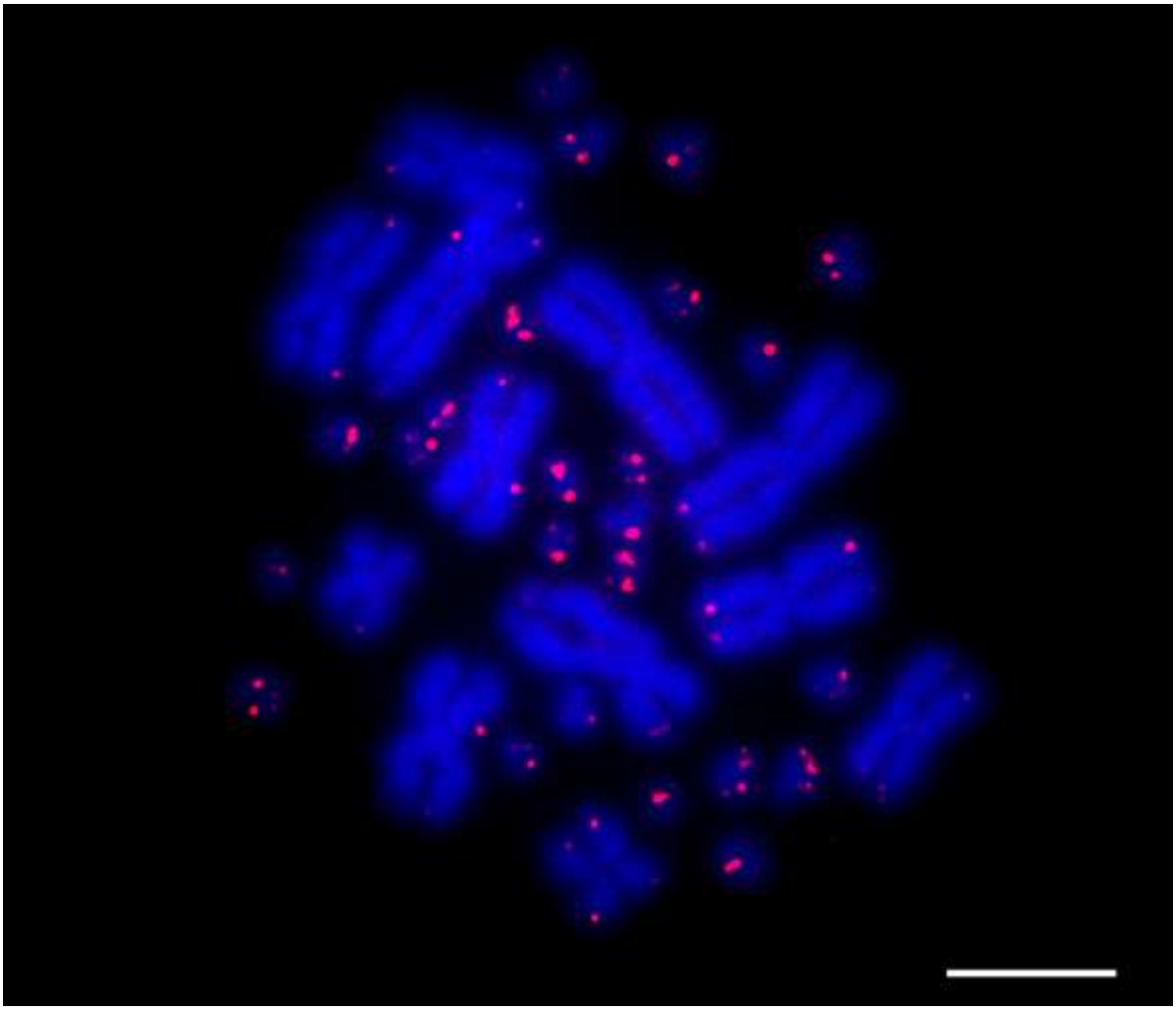

Figure 3.9. Hybridisation of telomeric sequences in *P. lesueurii* chromosomes. Telomeric sequences were identified by hybridising a $(TTAGGG)_5$ Cy3 labeled oligonucleotide probe to metaphase spreads. Telomeres were identified at the ends of all chromosomes and no interstitial signals were observed. Scale bar represent 10 µm.

Chapter 4: Discussion

The following discussion is in three parts, reflecting the three aims of my research and the phylogenetic depth of the comparative analysis undertaken. I first discuss the molecular characterisation of the *P. vitticeps* genome and integrate the insights gained with what is known about the structure and function of amniote genomes. I also discuss in this section the development of a *P. vitticeps* physical map and its value as a genomic resource for investigating genome evolution. Secondly, I compare the genomic organisation of the two agamids *P. lesueurii* and *P. vitticeps* by integrating findings from the molecular characterisation of both genomes. I also discuss findings from the construction of a BAC-based comparative map between *P. vitticeps* and *P. lesueurii*. Finally, I compare the genome organisation of the model squamate species *P. vitticeps* to that of chicken and human and discuss findings from comparative analyses among amniotes. This chapter finishes with discussion on future research directions and conclusions.

4.1. Molecular characterisation of *Pogona vitticeps* chromosomes

4.1.1 Karyotype of Pogona vitticeps

Karyotyping of *P. vitticeps* metaphases revealed a chromosomal complement composed of macrochromosomes and microchromosomes, with a diploid number of 2n = 12M + 20m, as first described by Witten, (1983) (Figure 3.1.). With the exception of the second largest sub-metacentric pair, the macrochromosomes are mostly metacentric, also confirming the findings of Witten, (1983) (Table 3.1.). There is a distinct break in size between the macro- and microchromosomes: between macrochromosome 6 (6.22 percent haploid length; 110 Mb) and microchromosome 7 (2.67 percent haploid length; 47 Mb) (Table 3.1). The microchromosome complement of *P. vitticeps* makes up a substantial proportion of the genome, approximately 22% of the total haploid length and 364.66 Mb (Table 3.1.). The microchromosomes of *P. vitticeps* were first described as mostly telocentric, except the two largest pairs described as metacentric (Witten, 1983). However, a recent study utilising fluorescent microscopy, which provides greater resolution than the photomicrograph methods employed by Witten (1983), proposed that most microchromosomes are metacentric (Ezaz *et al.*, 2005). This proposition is confirmed here, as close examination of the karyotype revealed all microchromosomes are metacentric (Figure 3.1.).Examination of

female *P. vitticeps* metaphases showed that the sex microchromosome pair is frequently heteromorphic, with a slightly extended region on the W not present on the Z (Figure. 3.1.). The extended region is indicative of degeneration of the W chromosome, which occurs by the accumulation of heterochromatin and repetitive or transposable elements at the site of non-recombination between the Z and W (Charlesworth, 1991; Steinmann & Steinmann, 2005). The W chromosome stains DAPI-faint, inferring that the W chromosome contains mostly GC rich sequences. These characteristics correspond with previous findings that the *P. vitticeps* W chromosome is highly heterochromatic and differentiated from the Z, with a large band of GC-rich, constitutive heterochromatin revealed through C-banding (Ezaz *et al.*, 2005).

4.1.2 DAPI ideograms and GC composition

The pattern of isochore structures revealed by DAPI staining of *P. vitticeps* chromosomes indicates compartmentalization of the genome into GC and AT rich sequences on chromosomes 1, 2, 3 and 6, with faint banding on both chromosome 4 and an anonymous microchromosome pair 'E', and a uniform GC distribution on chromosome 5 (Figure 3.2.). The secondary constriction in chromosome 2q stained DAPI-faint, and corresponded with the 18S rDNA probe signal, indicating a single NOR (Figure 3.3). The DAPI-faint staining of this region indirectly provides evidence that it is GC rich, a trait which is shared by all vertebrate NORs (Varriale *et al.*, 2008). The DAPI banded ideograms developed from the observed isochore structures reliably distinguish each macrochromosome (Figure 3.2.), including chromosomes 3 and 4 which are morphologically similar (Table 3.1.). These ideograms can therefore function as a low resolution map to enable consistent mapping of markers to macrochromosomes and also between the arms of most metacentric macrochromosomes, except chromosome 5.

Most microchromosomes lacked isochore structures and were DAPI-faint, giving indirect evidence that the microchromosomes have a higher content of GC rich sequences than the rest of the genome. This result is also supported by direct evidence, as *P. vitticeps* microchromosomes have been observed to stain brightly with CMA_3 methyl green (Ezaz *et al.*, 2005). The estimation of both micro- and macrochromosome GC content and 95% confidence intervals from the 64 BAC clone end sequence reads in this study (Table 3.2.)

did not showed a non-significant difference between microchromosomes (43.2% ± 2.25%), and macrochromosomes (42.1% ± 0.96%). However, so few end sequence reads from both microchromosome and macrochromosome clones do not give a reliable estimate, as it is far short of the bp coverage used in estimates from other studies (Shedlock *et al.*, 2007).

The isochore structure of the *P. vitticeps* genome shares similarities with the organisation of other sauropsid genomes. The isochore structure on most macrochromosomes indicates compartmentalization of the genome to a moderate degree, as has been observed in other agamids (Srikulnath *et al.*, 2009b), except chromosome 5 that shows a homogenous GC distribution similar to tuatara chromosomes (O'Meally *et al.*, 2009). *P. vitticeps* microchromosomes share similarity to the microchromosomes of chicken and *P. sinensis* as they contain mostly GC rich sequences. A high GC content correlates with a higher gene density, shorter intron size, increased CpG island density and increased recombination rate, features that might be expected of *P. vitticeps* microchromosomes (Auer *et al.*, 1987; Hillier *et al.*, 2004; Kuraku *et al.*, 2006; Freudenberg *et al.*, 2009). The hybridisation patterns of *P. vitticeps* BACs that contain repetitive sequences also suggests similarities with repeat distribution in chicken, where macrochromosomes have a higher repeat density than microchromosomes (Hillier *et al.*, 2004). In *P. vitticeps*, most of these repeat-rich BACs hybridised to chromosome 2 or other macrochromosomes (Table 3.3).

The genome-wide GC content of *P. vitticeps* is 42.3% (SD = 5.26), estimated from 64 *P. vitticeps* BAC end sequences (Table 3.2; ~0.005% genome coverage). *Pogona vitticeps* GC content is similar to that found in other reptiles, such as the Bahamian green anole *Anolis smaragdinus* (Squamata), the painted turtle *Chrysemys picta* (Testudines) and the American alligator *Alligator mississippiensis* (Crocodylia) (Table 4.1.). The ancestral amniote genome is estimated to have a GC content of approximately 41% (Shedlock *et al.*, 2007), suggesting that there has been an independent increase in the GC content of Testudines, Crocodylia and Squamata. The tuatara genome has also accumulated GC rich sequences, with the highest estimated GC content of any vertebrate so far (Table 4.1.), indicating an increase of approximately 6.8% in the 272 million years since it shared an ancestor with other amniotes (O'Meally *et al.*, 2009). In contrast, the chicken, human and opossum genomes show a reduction in GC content since they shared a common ancestor.

While the difference of 0.8% GC content between the two Iguanid lizards *P. vitticeps* and *A. smaragdinus* appears substantial with respect to other amniotes, it may be an overestimate due to the small proportion of the genome sampled (~0.005%).

Table 4.1. Genome-wide GC content of *P. vitticeps* and representative amniotes. Data are from this study, Mikkelsen *et al.* (2007), O'Meally *et al.* (2010), Shedlock *et al.* (2007) and Warren *et al.* (2008).

Amniote clade	Species	**%GC**
Eutheria	*Homo sapiens*	39.9
Metatheria	*Monodelphis domestica*	38.0
Prototheria	*Ornithorhynchus anatinus*	45.5
Aves	*Gallus gallus*	40.2
Crocodylia	*Alligator mississippiensis*	42.5
Testudines	*Chrysemys picta*	43.6
Squamata (Toxicofera)	*Anolis smaragdinus*	41.5
Squamata (Toxicofera)	*Pogona vitticeps*	42.3
Rhynchocephalia	*Sphenodon punctatus*	47.8

4.1.3 Telomeres

The presence of telomeric sequences is not only part of the normal structural organisation of eukaryotic genomes, but can also be indicative of genome evolution. For example, short interstitial telomeric sequences (ITS) are indicative of DNA repair at fragile sites within the genome, where double-stranded breaks have occurred (Ruiz-Herrera *et al.*, 2008). Also, interstitial telomeric sequences associated with constitutive heterochromatin may be indicative of ancestral chromosome rearrangements (Meyne *et al.*, 1990; Ruiz-Herrera *et al.*, 2008), and have been reported in many amniotes including members of Metatheria (Svartman & Vianna-Morgante, 1998; Metcalfe *et al.*, 2007), Squamata (Pellegrino *et al.*, 2009), and Aves (Nanda *et al.*, 2002). In *P. vitticeps*, telomeric sequences were found at the ends of each macrochromosome indicating that these chromosomes are evolutionarily stable (Figure 3.4.). However, telomeric sequences were also observed at the ends of each microchromosome and interstitially in three separate pairs, including the putative sex pair (Figure 3.4.). As constitutive heterochromatin has been identified in centromeric regions of most microchromosomes (Ezaz *et al.*, 2005), the *P. vitticeps* genome may have evolved

through fusion of a number of microchromosome pairs. These microchromosomes are therefore likely more recently derived than the macrochromosomes.

Compared to the macrochromosomes, microchromosomes generally have stronger fluorescent telomeric signals, which may indicate amplification of these repetitive sequences on microchromosomes (Figure 3.4.). This microchromosome-specific amplification has also been found in members of Aves (Nanda *et al.*, 2002) and in the tuatara (O'Meally *et al.*, 2009). It has been suggested that the higher number of telomeric repeats serve to protect the gene-dense microchromosomes from telomere erosion and degradation (Griffin *et al.*, 2007). If the microchromosomes of *P. vitticeps* prove to be gene-dense, a similar protective mechanism could be at play. Also, the weak pattern of hybridisation on some chromosomes may either be indicative of shorter telomeres on these chromosomes, or failure of the oligonucleotide probe to bind effectively to these repetitive sequences. The use of a peptide nucleic acid (PNA) oligonucleotide probe may prove better suited to establish differences in length and presence of telomeric sequences, as these types of probes are not only to be more stable but can also be used in quantitative measurement of repetitive sequences (Lansdorp *et al.*, 1996). Mapping telomeric sequences using a PNA telomeric probe in conjunction with a ZW marker will also confirm the presence of ITS on the ZW microchromosomes.

4.1.4 Pogona vitticeps physical map

The first physical map of *P. vitticeps* developed from FISH mapping of 64 BAC clones spans almost the entire genome, with diagnostic clones on all macrochromosomes and two of the 10 microchromosomes (Figure 3.6.). Chicken orthologs were identified in thirty clones, either in this study, Ezaz *et al*., (2009b) or Patel *et al*., (2010), bringing the total of Type I markers to 35 (Table 3.2.). Loci identified in non-diagnostic clones that map to microchromosomes are assigned a chromosomal location on a provisional basis using an alphabetical system (A-D), as further multi-colour FISH experiments are required to assign these clones diagnostically to a particular microchromosome (e.g. Figure 3.5. Appendix 2). Seven other non-diagnostic microchromosome clones mapped reliably to single microchromosome pairs that were not included in the physical map also require further multi-colour FISH experiments to assign them to a particular pair. Further multi-colour

FISH mapping of the set of clones mapped in this study (and others as required) will result in a physical map with markers diagnostic for each macro- and microchromosome spanning the entire *P. vitticeps* karyotype.

The diagnostic BACs mapped in this study provide a key resource for future characterisation of the *P. vitticeps* genome. Diagnostic clones were mapped to each arm of every macrochromosome and can therefore function as unambiguous molecular markers to distinguish between chromosomes, and between the arms of metacentric chromosomes in future mapping studies. In conjunction with the DAPI banded ideograms developed here, these clones can be used as reference points in future multi-colour FISH experiments to localise genes and other markers to *P. vitticeps* chromosomes. Another important resource obtained from the BAC clones is the end sequence data of use in anchoring to chromosomes contigs arising from whole-genome sequencing of the *P. vitticeps* genome currently underway (T. Ezaz, pers. comm.).

Characterisation of the *P. vitticeps* genome and development of a physical map has increased the utility of *P. vitticeps* as a model squamate species for investigation of genome evolution. The BAC-based approach used in developing the physical map has allowed comparative analyses at both close and distant phylogenetic distance. For example, the set of diagnostic clones developed in this study will be invaluable in cross-species mapping, enabling the development of low resolution maps in squamates that do not yet have physical maps. This comparative mapping will provide insight into the mechanisms of genome evolution within Squamata (e.g. section 4.2). The loci identified within clones are also useful in analysis over a much broader phylogenetic distance, by making comparisons with orthologues in the physical maps of other vertebrates (e.g. section 4.3)

4.2 Comparing genomes between Australian agamids

4.2.1 Molecular characterisation of Physignathus lesueurii chromosomes

The structure of the *P. lesueurii* genome shares many of the same characteristics with the other Australian agamid *P. vitticeps*. Similar to *P. vitticeps*, the karyotype of *P. lesueurii* is bimodal, containing both macrochromosomes and microchromosomes (Figure 3.7.), with a distinct break in size between macrochromosome 6 (6.72 percent haploid length) and microchromosome 7 (2.84 percent haploid length) (Table 3.4.). Similar to *P. vitticeps*, most macrochromosomes are metacentric, except macrochromosome pair 2, which is submetacentric (Figure 3.7.). As in *P. vitticeps*, there is a prominent secondary constriction on 2q which was identified as the NOR by mapping an 18S rDNA probe (Figure 3.8.), although the position of the NOR seems to be located slightly more medially than in *P. vitticeps*.

The diploid number of *P. lesueurii* is 2n = 12M + 24m, as first described by Witten, (1983). This number of chromosomes differs from that observed in *P. vitticeps* (2n = 12M + 20m) by an extra two pairs of microchromosomes. This difference, combined with the observed microchromosome ITS in *P. vitticeps* (Figure 3.4.), and lack of ITS on microchromosomes in *P. lesueurii* (Figure 3.9.), provides molecular cytogenetic evidence that since their divergence approximately 21 Mya (Hugall *et al.*, 2008), a reduction in chromosome number occurred through fusion of two microchromosome pairs in the lineage leading to *P. vitticeps*. Among other sauropsids (for example Aves and Crocodylia), reductions in chromosome number have commonly been associated with microchromosome fusions (de Oliveira *et al.*, 2005; Griffin *et al.*, 2007).

The hypothesis of microchromosome number reduction through fusion events in an ancestor leading to the *P. vitticeps* lineage is also supported by an outgroup comparison with the Asian Indo-Chinese water dragon *P. cocincinus*. *P. cocincinus* shared a common ancestor with the Australian agamids approximately 30 Mya (Hugall *et al.*, 2008), and has a chromosome number of 2n = 12M + 24m that is identical to *P. lesueurii* (Olmo & Signorino, 2005). Considering the distribution of karyotypes with both 20m and 24m across the Australian agamid phylogeny (Figure 1.2.), these fusion events must have occurred relatively early in the radiation of agamids throughout the Australian continent.

As the agamids *Ctenophorus clayi* and *Amphibolurus longirostris* also share the derived 2n = 12M + 20m karyotype, this indicates that the microchromosome fusion events occurred between 19 to 21 Mya (divergence dates after Hugall *et al.*, 2008).

4.2.2 Australian agamid BAC-based comparative map

The BAC-based physical map of *P. vitticeps* developed here (section 4.1) has allowed for the first molecular cytogenetic characterisation of the *P. lesueurii* genome and the first comparative mapping analysis between agamids. Using a cross-species comparative BAC mapping approach, 43 *P. vitticeps* clones and one *M. eugenii* clone were mapped by FISH to *P. lesueurii* chromosomes (Appendix 5), creating a low-resolution comparative map with 38 diagnostic molecular markers (Figure 4.1.). Microchromosome clones could not be used as diagnostic markers for particular pairs and were subsequently excluded from the construction of the comparative map. All clones that mapped to chromosomes 1, 3, 4, 5 and 6 demonstrated conserved synteny between the two agamids, indicating that these clones span conserved chromosome segments (Figure 4.1.). There are two rearrangements identified by diagnostic clones that map to the *P. vitticeps* ZW sex microchromosome pair and chromosome 4 (Figure 4.1.).

Figure 3.11. (following page) *P. vitticeps* and *P. lesueurii* comparative map. BAC clone numbers are to the right of each chromosome at the position of hybridization. BAC numbers joined by a dotted line indicate that the order of these clones is unknown. Chromosomes are drawn to scale intraspecifically using percent total haploid length. Chromosome proportions are based on measurements from five female *P. vitticeps* metaphases (Appendix 4) and five male *P. lesueurii* metaphases (Appendix 5). Branch lengths are proportional with divergence date from Hugall *et al.* (2008). Mya: millions of years ago.

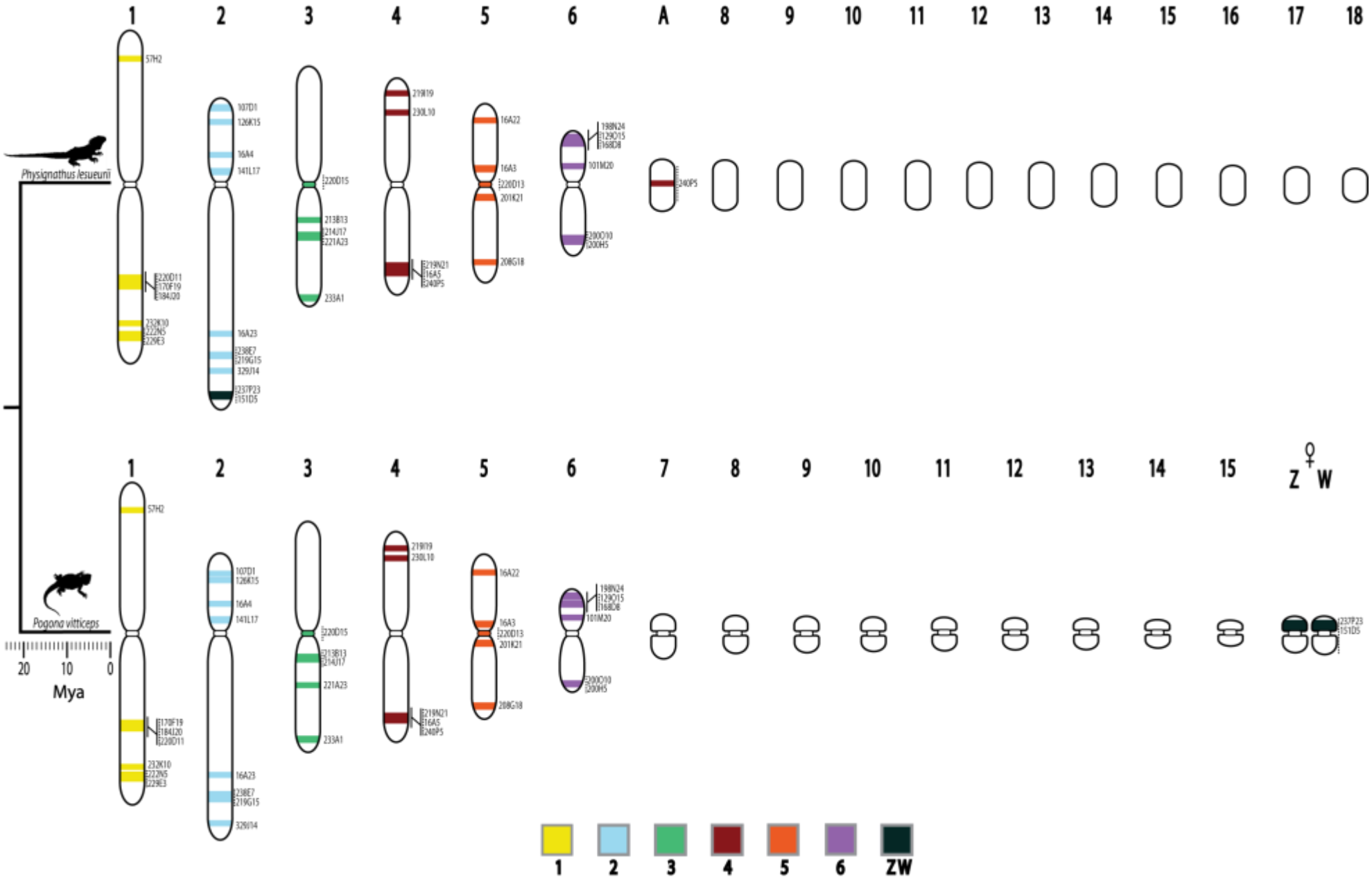
1
2
3
4
5
6
A
8
9
10
11
12
13
14
15
16
17
18
Physignathus lesueurii
57H2
220D11
170F19
184J20
232K10
222N5
229E3
107D1
126K15
16A4
141L17
16A23
238E7
219G15
329J14
237P23
151D5
220D15
213B13
214J17
221A23
233A1
219I19
230L10
219N21
16A5
240P5
16A22
16A3
220D13
201K21
208G18
198N24
129Q15
168D8
101M20
200Q10
200H5
240P5
7
Z
W
Pogona vitticeps
20
10
0
Mya
1
2
3
4
5
6
ZW
Key to BAC location on Pogona vitticeps chromosomes

Clones 237P23 and 151D5 were observed to have a strong fluorescent signal on the ZW sex microchromosome pair and a weakly diffuse signal on the sub-telomeric region of 2q in *P. vitticeps* (Appendix 4, Figure 7 A). In contrast, these clones were observed to hybridize uniquely with a strong fluorescent signal to the sub-telomeric region on 2q in *P. lesueurii* (Figure 4.1.) (Appendix 5, Figure 2 F). One hypothesis is that these two clones may span an evolutionary breakpoint. This is corroborated by the observed ITS on the putative *P. vitticeps* ZW (Figure 3.4.), and the absence of ITS in *P. lesueurii* chromosome 2q (Figure 3.9.). Under this scenario, a fission event led to the loss of the sub-telomeric region of chromosome 2q in the lineage leading to *P. vitticeps*, and this material subsequently fused with a microchromosome to form the ZW. This hypothesis goes against previous supposition based on morphology that the *P. vitticeps* ZW microchromosomes formed through fission of chromosomes 6, which is orthologous to the Snake Z chromosome (Ezaz *et al.*, 2009b; Quinn *et al.*, 2010).

Further evidence supporting this hypothesis is the position of the NOR in the two Australian agamids (BAC 329J14). In contrast to *P. vitticeps*, the NOR in *P. lesueurii* is located more medially, suggesting that there is a chromosome segment below the NOR that is not borne by *P. vitticeps* chromosome 2 (Figure 4.1.). Because the short arm and a portion of the long arm of *P. vitticeps* chromosome 2 are orthologous to the chicken Z (Ezaz *et al.*, 2009a), this would suggest that the ancestral autosomal segment fused with the ZW microchromosome pair sometime in the last 21 million years. An outgroup comparison is needed to confirm this hypothesised rearrangement, such as mapping *P. vitticeps* ZW clones in *P. cocincinus*.

An alternate hypothesis is that the clones 237P23 and 151D5 each contain a mobile element such as a retrotransposon and this retrotransposon has undergone independent amplification in both *P. vitticeps* and *P. lesueurii* lineages: in the Z and W microchromosome pair of *P. vitticeps* and in the sub-telomeric region of 2q in *P. lesueurii*. This would indicate that the weakly diffuse signal on chromosome 2q observed in *P. vitticeps* is also a retrotransposon which has not been active since the divergence of *P. vitticeps* from *P. lesueurii* 21 Mya (Hugall *et al.*, 2008). Evidence supporting this hypothesis comes from the finding that a *P. vitticeps* sex chromosome marker spanning both the Z and W

microchromosomes contains a CR1-like retrotransposon (Quinn *et al.*, 2010), which has been previously hybridised to the same region of chromosome 2q in *P. lesueurii* (Ezaz *et al.*, 2009b). However, this evidence is not incompatible with the first hypothesis of an ancestral autosomal origin of ZW-linked sequences on 2q followed by fission and fusion with a microchromosome pair.

The second rearrangement identified through cross-species BAC mapping involves the clone 240P5, which maps to 4q in *P. vitticeps*. This clone maps to both 4q and a microchromosome in *P. lesueurii* (Figure 4.1.). The microchromosome, (arbitrarily assigned pair 'A') showed a strong fluorescent signal as on the *q* arm of chromosome 4 (Appendix 5, Figure 4 A), suggesting hybridisation to homologous regions of approximately the same size. The clones 16A5 and 219N21 map to chromosome 4q in *P. vitticeps* but do not map to this microchromosome in *P. lesueurii*, making it unlikely that this chromosome segment has arisen in *P. lesueurii* by duplication (that is, the two segments are not paralogous). Also, as neither of these clones hybridised to the microchromosome, it is unlikely that the clone 240P5 spans an evolutionary breakpoint. This could indicate that this BAC contains a retrotransposon that has been active in the *P. lesueurii* lineage since the divergence of *P. lesueurii* and *P. vitticeps* 21 Mya (Hugall *et al.*, 2008). This observation provides more evidence that synapsid and sauropsid genomes have recent retrotransposon activity, while avian species have the derived condition of retroelement loss, without recent activity (Hillier *et al.*, 2004; Shedlock *et al.*, 2007).

4.3 Amniote comparative map

Through identifying representative loci contained within *P. vitticeps* BAC clones and mapping the locations of human and chicken orthologues, a comparative map was constructed between the major amniote groups (Figure 4.2.).

Pogona vitticeps chromosome 1 shares homology with regions on chicken chromosomes 3, 5 and 7, and human chromosomes 2, 6, and 11 (Figure 4.2.). The genes *HMGCLL1*, *HCRTR2* and *FAM83B* (contained within the same BAC clone) map to *P. vitticeps* chromosome 1 and are syntenic and have the same gene order in human chromosome 6 and chicken chromosome 3. This indicates that synteny has been conserved between sauropsids and synapsids since their divergence from a common ancestor approximately 324 Mya (Hedges *et al.*, 2006). The genes *TTN* and *GMPPA* are syntenic in the chicken, human and *P. vitticeps* since their divergence from an common ancestor 324 Mya. However, gene order has not been maintained in the *P. vitticeps* lineage, as genes *ZNF143*, *IPO7* and *TMEM41B* (contained within the same BAC clone) are located between *TTN* and *GMPPA*. This indicates that a rearrangement occurred in the lineage leading to *P. vitticeps* after the chicken and *P. vitticeps* common ancestor diverged approximately 277 Mya (Hedges *et al.*, 2006). Further evidence for the rearrangement occurring in the squamate lineage is that the genes *ZNF143*, *IPO7*, *TMEM41B* and *NAV2* are syntenic in both the chicken and human but not in *P. vitticeps*.

Figure 4.2. (following page) Chromosomal homologies among representative amniotes. Human and chicken orthologues were mapped using data from http://ensembl.org. Branch lengths are proportional to divergence dates from http://timetree.org (Hedges *et al.*, 2006; Hedges & Kumar *et al*., 2009). Mya: millions of years ago; XY: male heterogamety; ZW: female heterogamety. Dotted lines joining gene symbols indicate loci found within the same *P. vitticeps* BAC clone and have an unknown order on the chromosome. Gene symbols are those listed by the HUGO Gene Nomenclature Committee (http://www.genenames.org/). * indicates data are from either Ezaz *et al.* (2009b) or Patel *et al.* (2010).

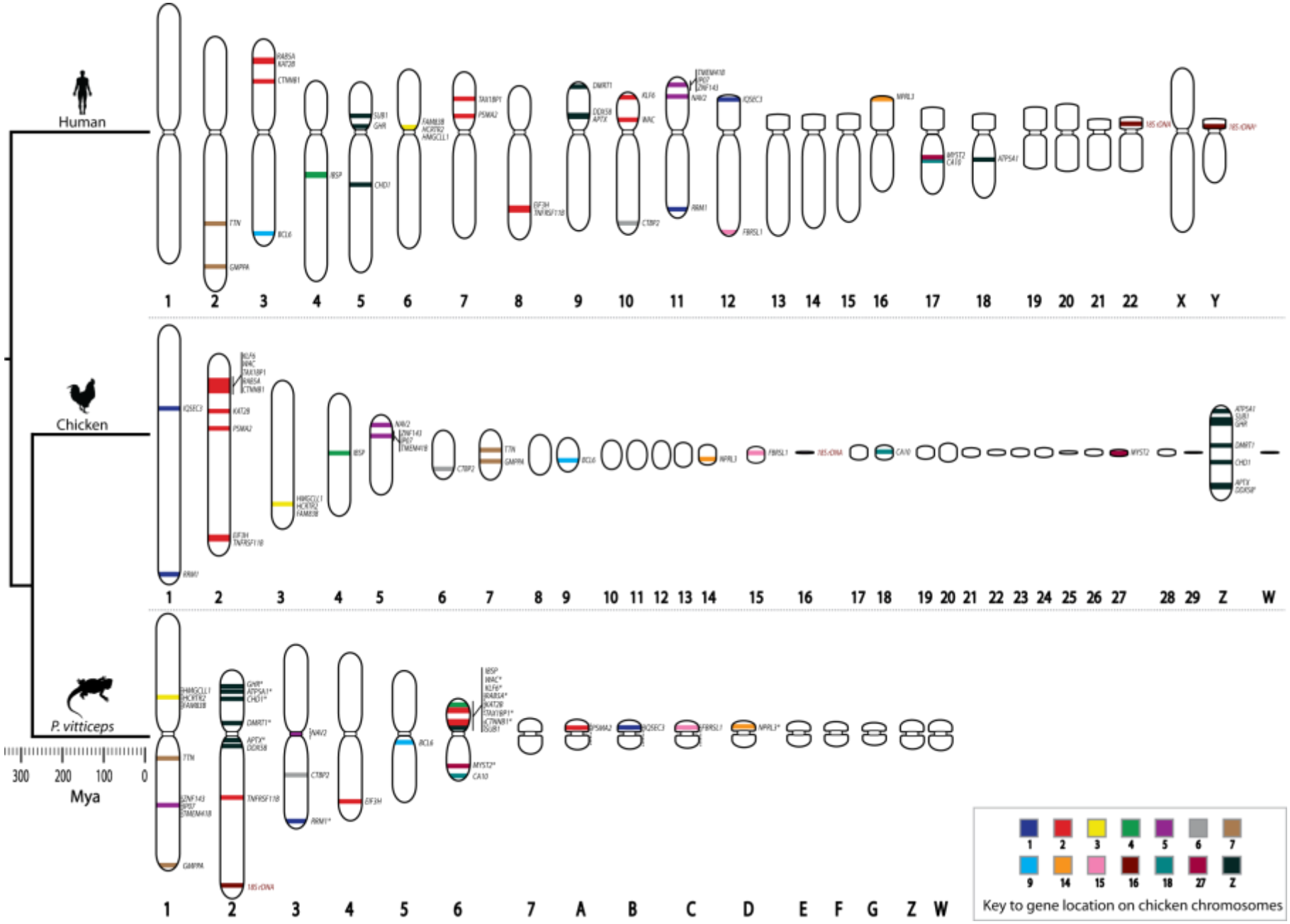
Human
Chicken
P. vitticeps
300
200
100
0
Mya
1 2 3 4 5 6 7 8 9 10 11 12 13 14 15 16 17 18 19 20 21 22 X Y
1 2 3 4 5 6 7 8 9 10 11 12 13 14 15 16 17 18 19 20 21 22 23 24 25 26 27 28 29 Z W
1 2 3 4 5 6 7 A B C D E F G Z W
Key to gene location on chicken chromosomes

Regions on *P. vitticeps* chromosome 2 share homology with chicken chromosomes 2, 16, and Z, and human chromosomes 5, 8, 9 and 18 (Figure 4.2.). The genes *SUB1*, *GHR*, *ATP5A1*, *CHD1*, *DMRT1* and *APTX* are all Z-borne in the chicken and have been previously mapped to a contiguous block of chromosome 2 in *P. vitticeps* (Ezaz *et al.*, 2009a). Mapping of the gene *DDX58* has extended the region on *P. vitticeps* 2q orthologous to chicken Z, while mapping of the chicken Z-borne gene *SUB1* to *P. vitticeps* chromosome 6p, has identified a break in synteny between chicken Z-linked genes on *P. vitticeps* chromosomes. As *P. vitticeps* chromosome 6p is homologous to the snake Z chromosome (Ezaz *et al.*, 2009a), the chicken Z-borne gene *SUB1* mapped to this chromosome gives indirect evidence of a common origin between chicken and snake sex chromosomes.

In contrast, previous comparative gene mapping studies have found no homology between the snake and chicken Z chromosomes, which has led to the supposition that these sex chromosomes evolved from different autosomes of an amniote common ancestor (Matsuda *et al.*, 2005; Matsubara *et al.*, 2006). Recently, mapping repetitive sequences common to bird and snake W chromosomes suggested either ancestral synteny or functional homology of snake and chicken sex chromosomes (O'Meally *et al.*, 2010). The mapping of *SUB1* to the orthologous region of the snake Z in *P. vitticeps* supports this proposed ancestral synteny. Recent comparative mapping has also identified regions on the multiple XY sex chromosome system of monotremes that share homology to the chicken Z chromosome (El-Mogharbel *et al.*, 2007; Veyrunes *et al.*, 2008). In conjunction with the aforementioned hypothesis of ancestral synteny between the chicken Z and *P. vitticeps* ZW (section 4.1), this may indicate ancestral synteny of the sex chromosomes of squamates, birds and monotremes.

Comparing the synteny and gene order of chicken Z-linked genes *GHR*, *ATP5A1*, *SUB1*, *CHD1*, *DMRT1*, *APTX* and *DDX58* reveals four rearrangements between chicken and *P. vitticeps*. The gene *GHR* is located distally and *ATP5A1* medially relative to *CHD1* in *P. vitticeps*, indicating an inversion with respect to chicken (Ezaz *et al.*, 2009a), while the human orthologs are not syntenic. The order of genes *ATP5A1-CHD1-DMRT1-APTX* in *P. vitticeps* is different from that of the chicken (*ATP5A1-DMRT1-CHD1-APTX*),

indicating an inversion involving *DMRT1* and *CHD1* in either lineage (Ezaz *et al.*, 2009a). The genes *APTX*, *DDX58* and *DMRT1* share synteny and the same gene order in both *P. vitticeps* and the chicken, while in human, the gene order of *APTX* and *DDX58* is reversed relative to *DMRT1* indicating an inversion in the eutherian lineage. Another rearrangement involves the genes *TNFRSF11B* and *EIF3H*, which are syntenic in both the human and chicken, but map to chromosomes 2 and 4 in *P. vitticeps*. This indicates that synteny has been conserved in the chicken and human lineages since their divergence from a common ancestor, while a rearrangement has occurred in the lineage leading to *P. vitticeps* since the chicken and *P. vitticeps* lineages diverged from a common ancestor approximately 277 Mya.

Pogona vitticeps chromosome 3 shares homology with chicken chromosomes 1, 5, and 6, and human chromosomes 10 and 11 (Figure 4.2.). In both *P. vitticeps* and human, the genes *NAV2* and *RRM1* are syntenic, while the chicken orthologs are on chromosomes 5 and 1, respectively. This indicates conserved synteny in the eutherian and squamate lineages since they diverged 324 Mya, while rearrangements occurred in the lineage leading to the chicken since archosaurs diverged from other sauropsids approximately 277 Mya. In *P. vitticeps*, *CTBP2* is found between *NAV2* and *RRM1*, a gene order not shared by the eutherian lineage, indicating an unknown rearrangement since sauropsids and synapsids diverged approximately 324 Mya.

No major inferences on ancestral syntenies can be made from the paucity of loci identified within BACs on *P. vitticeps* chromosomes 4 or 5. However, the location of *IBSP* on chicken and human chromosome 4 indicates that this gene is part of the syntenic region that is conserved in the avian and eutherian mammal lineages since they shared an ancestor 324 Mya (Chowdhary & Raudsepp, 2000). The location of *IBSP* on chromosome 6 in *P. vitticeps* indicates that the avian and eutherian arrangement of this contiguous block may not have been maintained in squamates. However, genes spanning the conserved region in human and chicken chromosome 4 have recently been mapped in the Asian agamid *L. r. rubritaeniata* to a contiguous block on chromosome 5 (Srikulnath *et al.*, 2009b). It is therefore likely that synteny of this contiguous block has also been conserved in *P. vitticeps* and will be identified as more markers are developed for these chromosomes.

Pogona vitticeps chromosome 6 shares homology with regions on chicken chromosomes 2, 4, 18, 27 and Z, and human chromosomes 3, 4, 5, and 17 (Figure 4.2.). The genes *WAC* and *KLF6* are syntenic in *P. vitticeps*, chicken and human but have a reversed gene order in *P. vitticeps* compared to that found in chicken relative to *TAX1BP1*, indicating an inversion. This gene order is conserved between *P. vitticeps* chromosome 6 and the snake Z (Ezaz *et al.*, 2009a), suggesting that this rearrangement occurred before Iguanid lizards and snakes diverged approximately 166 Mya (Hedges *et al.*, 2006). Also, in both *P. vitticeps* and chicken the synteny of genes *WAC, KLF6, RAB5A, KAT2B, TAX1BP1*, and *CTNNB1* is conserved, while in the eutherian lineage synteny is conserved only between some of these genes across multiple chromosomes. This indicates that either the chicken and *P. vitticeps* lineages share the ancestral gene arrangement and rearrangements have occurred in the eutherian lineage, or that this gene arrangement has arisen in sauropsids since their divergence from synapsids approximately 324 Mya.

The genes *MYST2* and *CA10* are syntenic in both *P. vitticeps* and human, but separated on different microchromosomes in the chicken. This indicates that the squamate and eutherian lineages have retained the ancestral synteny since their divergence from a common ancestor 324 Mya, while the chicken microchromosomes most likely arose through fission after the divergence of Archosauria and Lepidosauria 277 Mya. The conserved synteny of *MYST2* and *CA10* genes in squamates and eutherians also gives indirect evidence that the synteny of genes on snake sex chromosome may have arisen before the divergence of Aves and Squamata 277 Mya, an older estimate than the 166 Mya previously proposed (O'Meally *et al.*, 2010).

Regions on *P. vitticeps* microchromosomes A, B, C and D share homology with chicken chromosomes 1, 2, 14 and 15, and human chromosomes 7, 12, and 16 (Figure 4.2.). The genes *PSMA2* and *TAX1BP1* are syntenic in both the avian and eutherian lineages, while in *P. vitticeps PSMA2* is located on a microchromosome and *TAX1BP1* on chromosome 6. This indicates that the avian and eutherian synteny is conserved since the divergence of sauropsids and synapsids from a common ancestor, while the microchromosome in *P. vitticeps* must have arisen by fission since the divergence of Aves and Squamata 277

Mya. The gene *IQSEC3* is located on a microchromosome in *P. vitticeps*, but is located on a macrochromosome in the chicken, suggesting that this microchromosome has not been conserved amongst sauropsids, either fusing to chicken chromosome 1 or arising as a microchromosome through fission in *P. vitticeps*. The genes *FBRSL1* and *NPRL3* also map to microchromosomes pairs 14 and 15 in the chicken, suggesting that these microchromosomes have been conserved in both avian and squamate lineages since their divergence from an amniote common ancestor 277 Mya. The gene *FBRSL1* maps to *P. vitticeps* microchromosome 'C' and chicken chromosome 15, indicating homology with the ZW sex microchromosome pair of the turtle *P. sinensis* (Kawagoshi *et al.*, 2009). Further multi-colour FISH experiments mapping *FBRSL1* and *P. vitticeps* sex chromosome clones are required to determine if there is homology between *P. sinensis* sex microchromosomes and *P. vitticeps* sex microchromosomes. Collectively, these results indicate that while some microchromosomes have been retained since Archosauria and Lepidosauria diverged 277 Mya, it is also apparent that microchromosomes have arisen independently in both lineages since then.

4.4 Future research directions

As the *P. vitticeps* physical map developed in this study forms the basis for the squamate genome characterisation and all comparative mapping analysis undertaken in this study, further development of this genomic resource is the main priority for future research. This can be achieved through simultaneous mapping and end sequencing of *P. vitticeps* BACs to increase the number of markers on each chromosome. This would provide greater detail to the characterisation of this squamate's genome, giving greater insight into structural and functional organisation. A greater number of Type 1 markers would give a higher resolution to comparative analysis by which ancestral syntenies and genome rearrangements could be identified. Multi-colour FISH on interphase chromosomes may also provide a greater mapping resolution for clones that mapped within 1 Mb of each other and whose positions could not be identified relative to each other on chromosomes. Furthermore, multi-colour FISH experiments of identified microchromosome clones will make the *P. vitticeps* physical map the first to have markers across the entire karyotype of a non-avian sauropsid. These diagnostic clones will also function as chromosomal anchors for sequence contigs from current and future genome sequencing projects.

From the research undertaken in this study a number of key insights were gained which require further investigation. The ITS observed in the three microchromosome pairs requires further investigation. The use of a PNA telomeric probe will give a greater confidence in the observed result. Used simultaneously with diagnostic microchromosome BAC clones, the microchromosome pairs formed from fusion events could be identified. This approach could also be used with a ZW clone to confirm the location of the ITS on the ZW microchromosomes which would provide evidence for one or other of the hypotheses on the evolution of *P. vitticeps* sex microchromosomes.

The diagnostic *P. vitticeps* clones are also a valuable resource in cross-species comparative mapping analysis. For example, *P. vitticeps* autosomal and ZW BAC clones could be mapped in other Australian agamid species which have sex microchromosomes that are not homologous to those of *P. vitticeps*. This would provide further evidence for independent origins of sex chromosomes within agamids. Through identification of these sex chromosomes and future genome sequencing in *P. vitticeps,* sex-linked genes could be identified in other species. Also, as a clone identified in this study is orthologous to a region on chicken chromosome 15 that in turn is orthologous to the *P. sinensis* ZW microchromosomes, mapping of this clone with the *P. vitticeps* ZW microchromosome clones could determine homology between these two sex chromosome systems. Furthermore, cross-species mapping of this microchromosome clone in other species of turtle that have sex microchromosomes, like the Australian Eastern long-neck turtle *Chelodina longicollis,* could provide evidence for either independent or shared origins of sex chromosomes in Testudines.

The indirect evidence of ancestral synteny of snake and chicken sex chromosomes suggested by mapping of a BAC containing the gene *SUB1* should be further investigated. Full-sequencing of this close will increase the resolution of BLAST and BLAT analysis in identifying the loci contained within this clone. Once this has been done, further mapping of additional loci across species could directly identify homology of the chicken Z and the snake Z chromosome.

4.5 Conclusion

This study characterised the chromosomes of *P. vitticeps* at the cytogenetic level and developed a set of molecular markers spanning almost the entire karyotype to allow reproducible physical mapping and further map development. The comparative analyses undertaken in this study has demonstrated the utility of the first BAC-based squamate physical map and contributed substantial insights into the mechanisms of genome evolution among amniotes. This study represents the first attempt to characterise the microchromosomes of a squamate species in providing a comprehensive map of the entire genome. Comparative analysis was undertaken for the first time between agamid lizards and between an Australian reptile and other amniotes.

The comparative analysis undertaken at a narrow phylogenetic distance between Australian agamid species identified rearrangements that could have led to the formation of the *P. vitticeps* ZW sex chromosomes, suggested ancestral synteny between the chicken Z and *P. vitticeps* ZW sex chromosomes, and indicated independent activity of retrotransposons in both the *P. vitticeps* and *P. lesueurii* lineages. The comparative analysis also identified the mechanism of chromosome number reduction in Australian agamids as microchromosome fusions. Cross-species BAC mapping was shown to be a useful method for developing low-resolution comparative maps in a squamate, as has been found in mammals and birds.

Comparative analysis undertaken at a wider phylogenetic distance between *P. vitticeps*, chicken and human highlighted the value of using a squamate species in mammalian and avian comparative analysis. Ancestral syntenies and rearrangements were identified in each of the major amniote lineages, and also suggested a shared origin of snake and chicken sex chromosomes. Continuing development of the *P. vitticeps* physical map will provide a valuable genomic resource for future genome characterisation, underpin genome sequencing for this model squamate species and enable comparative analyses at a higher resolution. Furthermore, targeted comparative mapping analysis among representative amniotes that span the phylogenetic depth of this important group will give substantial insight into the mechanisms of genome evolution in all species.

References

Alsop, A.E., Miethke, P., Rofe, R., Koina, E., Sankovic, N., Deakin, J.E., Haines, H., Rapkins, R.W. and Graves, J.A.M. (2005) Characterizing the chromosomes of the Australian model marsupial *Macropus eugenii* (tammar wallaby). *Chromosome Research* **13**:627-636.

Andersson, L., Ashburner, M., Audun, S., Barendse, W., Bitgood, J., Bottema, C., Broad, T., Brown, S., Burt, D.W., Copeland, N.G., *et al.* (1996) The first international workshop on comparative genome organization. *Mammalian Genome* **7**:717-734.

Auer, H., Mayr, B., Lambrou, M and Schleger, W. (1987) An extended chicken karyotype, including the NOR chromosome. *Cytogenetics and Cell Genetics* **45**:218-221.

Becak, W. (1964) Close karyological kinship between the reptilian suborder Serpentes and the class Aves. *Chromosoma* **15**:606-617.

Bernardi, G. (2000) Isochores and the evolutionary genomics of vertebrates. *Gene* **241**:3-17.

Bertolotto, C.E.V., Pellegrino, K.C.M. and Yonenaga-Yassuda, Y. (2004) Occurrence of B chromosomes in lizards: a review. *Cytogenetic and Genome Research* **106**:243-246.

Blackburn, E.H. (1994) Telomeres: No end in sight. *Cell* **77**:621-623.

Bull, J.J. (1983) Evolution of sex determining mechanisms. Benjamin/Cummings, Menlo Park, CA.

Burt, D.W. (2002) Origin and evolution of avian microchromosomes. *Cytogenetic and Genome Research* **96**:97-112.

Capy, P. (2005) Classification and nomenclature of retrotransposable elements. *Cytogenetic and Genome Research* **110**:457-461.

Chapus, C. and Edwards, S.V. (2009) Genome evolution in Reptilia: in silico chicken mapping of 12,000 BAC-end sequences from two reptiles and a basal bird. *BMC Genomics* **10**:S8.

Charlesworth, B. (1991) The evolution of sex chromosomes. *Science* **251**:1030-1033.

Chowdhary, B.P and Raudsepp, T. (2000) HSA4 and GGA4: conservation despite 300-Myr divergence. *Genomics* **64**:102-105.

Cree, A., Thompson, M.B. and Daugherty, C.H. (1995) Tuatara sex determination. *Nature* **375**:543.

de Oliveira, E., Habermann, F., Lacerda, O., Sbalqueiro, I., Wienberg, J. and Muller, S. (2005) Chromosome reshuffling in birds of prey: the karyotype of the world's largest eagle (Harpy eagle, Harpia harpyja) compared to that of the chicken (Gallus gallus). *Chromosoma* **114**:338-343.

Deakin, J.E., Koina, E., Waters, P.D., Doherty, R., Patel, V.S., Delbridge, M.L., Dobson, B., Fong, J., Hu, Y., van dan Hurk, C., *et al.* (2008) Physical map of two tammar wallaby chromosomes: A strategy for mapping in non-model mammals. *Chromosome Research* **16**:1159-1175.

Deeming, D.C. (2004) Prevalence of TSD in crocodilians. in: *Temperature-Dependent Sex Determination in Vertebrates* (Eds N. Valenzuela and V. Lance), pp. 33-41 (Smithsonian Institute Press, Washington, DC).

Dolezel, J., Bartos, J., Voglmayr, H. and Greilhuber, J. (2003) Nuclear DNA content and genome size of trout and human. *Cytometry* **51A**:127-128.

Doody, S.J., Guarino, E., Georges, A., Corey, B., Murray, G. and Ewert, M. (2006) Nest site choice compensates for climatic effects on sex ratios in a lizard with environmental sex determination. *Evolutionary Ecology* **20**:307-330.

dos Santos, G.M. (1986) Reviewing the chromosome nomenclature of Levan et al. *Revista brasileira de genética* **9**:741-743.

El-Mogharbel, N., Wakefield, M., Deakin, J.E., Tsend-Ayush, E., Grutzner, F., Alsop, A.E., Ezaz, T. and Graves, J.A.M. (2007) DMRT1 gene cluster analysis in the platypus: New insights into genomic organization and regulatory regions. *Genomics* **89**:10-21.

Ellegren, H. (2000) Evolution of the avian sex chromosomes and their role in sex determination. *Trends in ecology and evolution* **15**:188-192.

Ewert, M.A., Etchberger, C.R. and Nelson, C.E. (2004) Turtle sex-determining modes and TSD patterns, and some TSD correlates. in: *Temperature-Dependent Sex Determination in Vertebrates* (Eds N. Valenzuela and V. Lance), pp. 21-32 (Smithsonian Institute Press, Washington, DC).

Ezaz, T., Moritz, B., Waters, P., Graves, J.A.M., Georges, A. and Sarre, S.D. (2009a) The ZW sex microchromosomes of an Australian dragon lizard share no homology with those of other reptiles or birds. *Chromosome Research* **17**:965-973.

Ezaz, T., Quinn, A.E., Miura, I., Sarre, S.D., Georges, A. and Graves, J.A.M. (2005) The dragon lizard *Pogona vitticeps* has ZZ/ZW micro-sex chromosomes. *Chromosome Research* **13**:763-776.

Ezaz, T., Quinn, A.E., Sarre, S.D., O'Meally, D., Georges, A. and Graves, J.A.M. (2009b) Molecular marker suggests rapid changes of sex-determining mechanisms in Australian dragon lizards. *Chromosome Research* **17**:91-98.

Ezaz, T., Sarre, S.D., O'Meally, D., Graves, J.A.M. and Georges, A. (2009c) Sex chromosome evolution in lizards: Independent origins and rapid transitions. *Cytogenetic and Genome Research* **127**:249-260.

Ezaz, T., Valenzuela, N., Grutzner, F., Miura, I., Burke, R. and Georges, A. (2006) An XX/XY sex microchromosome system in a freshwater turtle, Chelodina longicollis (Testudines: Chelidae) with genetic sex determination. *Chromosome Research* **14**:139-150.

Freudenberg, J., Wang, M., Yang, Y. and Li, W. (2009) Partial correlation analysis indicates causal relationships between GC-content, exon density and recombination rate in the human genome. *BMC Bioinformatics* **10**:S66.

Fujita, M.K. and Moritz, C. (2009) Origin and evolution of parthenogenetic genomes in lizards: current state and future directions. *Cytogenetic and Genome Research* **127**:261-272.

Gamble, T. (2010) A Review of Sex Determining Mechanisms in Geckos (Gekkota: Squamata). *Sexual Development* **4**:88-103.

Graves, J.A.M. (2008) Weird animal genomes and the evolution of vertebrate sex and sex chromosomes. *Annual Review of Genetics* **42**:565-586.

Griffin, D.K., Robertson, L.B.W., Tempest, H.G. and Skinner, B.M. (2007) The evolution of the avian genome as revealed by comparative molecular cytogenetics. *Cytogenetic and Genome Research* **117**:64-77.

Haines, H. How do male kangaroos cope with only half as many ribosomal RNA genes as female kangaroos? Honours Thesis. Australian National University, Canberra (2005).

Harlow, P.S. (2004) Temperature-dependent sex determination in lizards. in: *Temperature-Dependent Sex Determination in Vertebrates* (Eds N. Valenzuela and V. Lance), pp. 42-52 (Smithsonian Institute Press, Washington, DC).

Haussler, D., O'Brien, S.J., Ryder, O.A., Keith, B., Clamp, M., Crawford, A.J., Hanner, R., Hanotte, O., Johnson, W.E., McGuire, J.A., *et al.* (2009) Genome 10K: A proposal to obtain whole-genome sequence for 10 000 vertebrate species. *Journal of Heredity* **6**:659-674.

Hedges, S.B. (2009) Vertebrates (Vertebrata). in: *The timetree of life* (Eds S.B. Hedges and S. Kumar), pp. 309-314 (Oxford University Press.

Hedges, S.B., Dudley, J. and Kumar, S. (2006) Timetree: a public knowledge-base of divergence times among organisms. *Bioinformatics* **22**:2971-2972.

Hillier, L.W., Miller, W., Birney, E., Warren, W., Hardison, R.C., Ponting, C.P., Bork, P., Burt, D.W., Groenen, M.A.M., Delaney, M.E., *et al.* (2004) Sequence and comparative analysis of the chicken genome provide unique perspectives on vertebrate evolution. *Nature* **432**:695-716.

Hugall, A.F., Foster, R., Hutchinson, M. and Lee, M.S.Y. (2008) Phylogeny of australasian agamid lizards based on nuclear and mitochondrial genes: implications for morphological evolution and biogeography. *Biological Journal of the Linnean Society* **93**:343-358.

Hughes, A.L. and Hughes, M.K. (1995) Small genomes for better flyers. *Nature* **377**:391.

Hughes, A.L. and Piontkivska, H. (2005) DNA repeat arrays in chicken and human genomes and the adaptive evolution of avian genome size. *BMC Evolutionary Biology* **5**:12.

ISCN (1995) An international system for human cytogenetic nomenclature. S. Karger AG., Basel.

Janes, D.E., Organ, C.L., Fujita, M.K., Shedlock, A.M. and Edwards, S.V. (2010) Genome evolution in reptilia, the sister group of mammals. *Annual Review of Genomics and Human Genetics* **11**:239-264.

Janes, D.E., Valenzuela, N., Ezaz, T., Amemiya, C. and Edwards, S.V. (2011) Sex chromosome evolution in amniotes: applications for bacterial artificial chromosome libraries. *Journal of Biomedicine and Biotechnology* **2011**:6.

John, H., Birnstiel, M. and Jones, K. (1969) RNA-DNA hybrids at the cytological level. *Nature* **223**:582-587.

Kasai, F., Garcia, C., Arruga, M.V. and Ferguson-Smith, M.A. (2003) Chromosome homology between chicken (*Gallus gallus domesticus*) and the red-legged partridge (*Alectoris rufa*); evidence of the occurrence of a neocentromere during evolution. *Cytogenetic and Genome Research* **102**:326-330.

Kawagoshi, T., Uno, Y., Matsubara, K., Matsuda, Y. and Nishida, C. (2009) The ZW micro-sex chromosomes of the chinese soft-shelled turtle (*Pelodiscus sinensis*, Trionychidae, Testudines) have the same origin as chicken chromosome 15. *Cytogenetic and Genome Research* **125**:125-131.

Kawai, A., Ishijima, J., Nishida, C., Kosaka, A., Ota, H., Kohno, S. and Matsuda, Y. (2009) The ZW sex chromosomes of *Gekko hokouensis* (Gekkonidae, Squamata) represent highly conserved homology with those of avian species. *Chromosoma* **118**:43-51.

Kazazian, H.H.J. (2004) Mobile elements: drivers of genome evolution. *Science* **303**:1626-1632.

Koonin, E.V. (2005) Orthologs, paralogs, and evolutionary genomics. *Annual Review of Genetics* **39**:309-338.

Kordis, D. (2009) Transposable elements in reptilian and avian (Sauropsida) genomes. *Cytogenetic and Genome Research* **127**:94-111.

Kuraku, S., Ishijima, J., Nishida-Umehara, C., Agata, K., Kuratani, S. and Matsuda, Y. (2006) cDNA-based gene mapping and GC_3 profiling in the soft-shelled turtle suggest a chromosomal size-dependent GC bias shared by sauropsids. *Chromosome Research* **14**:187-202.

Lander, E.S., Linton, M., Birren, B., Nusbaum, C., Zody, M.C., Baldwin, J., Devon, K., Dewar, K., Doyle, M., FitzHugh, W., *et al.* (2001) Initial sequencing and analysis of the human genome. *Nature* **409**:860-921.

Lansdorp, P.M., Verwoerd, N.P., van de Rijke, F.M., Dragowska, V., Little, M., Dirks, R.W., Raap, A.K. and Tanke, H.J. (1996) Heterogeneity in telomere length of human chromosomes. *Human Molecular Genetics* **5**:685-691.

MacCulloch, R. D., Upton, D. E. and Murphy, R. W. (1996) Trends in Nuclear DNA content among Amphibians and Reptiles. *Comparative Biochemistry and Physiology* **113B**:601-605.

Masabanda, J., Burt, D.W., O'Brien, P.C.M., Vignal, A., Fillon, V., Walsh, P.S., Cox, H., Tempest, H.G., Smith, J., Habermann, F., *et al.* (2004) Molecular cytogenetic definition of the chicken genome: the first complete avian karyotype. *Genetics* **166**:1367-1373.

Matsubara, K., Tarui, H., Toriba, M., Yamada, K., Nishida-Umehara, C., Agata, K. and Matsuda, Y. (2006) Evidence for different origin of sex chromosomes in snakes, birds, and mammals and step-wise differentiation of snake sex chromosomes. *Proceedings of the National Academy of Sciences of the United States of America* **103**:18190-18195.

Matsuda, Y., Nishida-Umehara, C., Tarui, H., Kuroiwa, A., Yamada, K., Isobe, T., Ando, J., Fujiwara, A., Hirao, Y., Nishimura, O., *et al.* (2005) Highly conserved linkage homology between birds and turtles: Bird and turtle chromosomes are precise counterparts of each other. *Chromosome Research* **13**:601-615.

McGowran, B., Holdgate, G.R., Li, Q. and Gallagher, S.J. (2004) Cenozoic stratigraphic succession in southeastern Australia. *Australian Journal of Earch Sciences* **51**:459-496.

Metcalfe, C.J., Eldridge, M.D.B. and Johnston, P.G. (2007) Mapping the distribution of the telomeric sequence $(T_2AG_3)_n$ in the Macropodoidea (Marsupialia) by fluorescence in sity hybridization.II.The ancestral 2n = 22 macropodid karyotype. *Cytogenetic and Genome Research* **116**:212-217.

Meyne, J., Baker, R.J., Hobart, H.H., Hsu, T.C., Ryder, O.A., Ward, O.G., Wiley, J.E., Wurster-Hill, D.H., Yates, T.L. and Moyzis, R.K. (1990) Distribution of non-telomeric sites of the $(TTAGGG)_n$ telomeric sequence in vertebrate chromosomes. *Chromosoma* **99**:3-10.

Miller, O.J. and Therman, E. (2000) Mapping human chromosomes. in: *Human chromosomes*, pp. 431-446 (Springer-Verlag, New York).

Miller, W., Makova, K.D., Nekrutenko, A. and Hardison, R.C. (2004) Comparative Genomics. *Annual Review of Genomics and Human Genetics* **5**:15-56.

Nakatani, Y., Takeda, H., Kohara, Y and Morishita, S. (2007) Reconstruction of the vertebrate ancestral genome reveals dynamic reorganization in early vertebrates. *Genome Research* **17**:1254-1265.

Nanda, I., Schrama, D., Feichtinger, W., Haaf, T., Schartl, M. and Schmid, M. (2002) Distribution of telomeric (TTAGGG)(n) sequences in avian chromosomes. *Chromosoma* **111**:215-227.

Nanda, I., Shan, Z., Schartl, M., Burt, D.W., Koehler, M., Nothwang, G., Grutzner, F., Paton, I.R., Windsor, D., Dunn, I., *et al.* (1999) 300 million years of conserved synteny between chicken Z and human chromosome 9. *Nature Genetics* **21**:258-259.

NCBI (2011) National Center for Biotechnology Information. Internet references. Retrieved from: http://www.ncbi.nlm.nih.gov/genomes/leuks.cgi

Novick, P., Smith, J., Ray, D. and Boissinot, S. (2010) Independent and parallel lateral transfer of DNA transposons in tetrapod genomes. *Gene* **449**:85-94.

O'Brien, S.J., Menotti-Raymond, M., Murphy, W.J., Nash, W.G., Wienberg, J., Stanyon, R., Copeland, N.G., Jenkins, N.A., Womack, J.A. and Graves, J.A.M. (1999) The promise of comparative genomics in mammals. *Science* **286**:458-481.

O'Brien, S.J., Womack, J.E., Lyons, L.A., Moore, K.J., Jenkins, N.A. and Copeland, N.G. (1993) Anchored reference loci for comparative genome mapping in mammals. *Nature Genetics* **3**:103-112.

O'Meally, D., Miller, H., Patel, H.R., Graves, J.A.M and Ezaz, T. (2009) The first cytogenetic map of the tuatara *Sphenodon punctatus*. *Cytogenetic and Genome Research* **127**:213-223.

O'Meally, D., Patel, H.R., Stiglec, R., Sarre, S.D., Georges, A., Graves, J.A.M and Ezaz, T. (2010) Non-homologous sex chromosomes of birds and snakes share repetitive sequences. *Chromosome Research* **18**:787-800.

Ohno, S. (1967) Sex Chromosomes and Sex-Linked Genes. Springer-Verlag, Heidelberg.

Olmo, E. and Signorino, G. (2005) Chromorep: a reptile chromosomes database. Internet references. Retrieved from: http://ginux.univpm.it/scienze/chromorep/

Organ, C.L., Shedlock, A.M., Pagel, M. and Edwards, S.V. (2007) Origin of avian genome size and structure in nonavian dinosaurs. *Nature* **446**:180-184.

Pardue, M.L. and Gall, J.G. (1969) Molecular hybridization of radioactive DNA to the DNA of cytological preparation. *Proceedings of the National Academy of Sciences of the United States of America* **64**:600-604.

Patel, V.S., Ezaz, T., Deakin, J.E. and Graves, J.A.M. (2010) Globin gene structure in a reptile supports the transpositional model for amniote α- and β-globin gene evolution. *Chromosome Research* **18**:897-907.

Pellegrino, K.C.M., dos Santos, R.M.L., Rodrigues, M.T., Laguna, M.M., Amaro, R.C. and Yonenaga-Yassuda, Y. (2009) Chromosome evolution in the Brazilian geckos of the genus *Gymnodactylus* (Squamata, Phyllodactylidae) from the biomes of Cerrado, Caatinga and atlantic rain forest: Evidence of robertsonian fusion events and supernumerary chromosomes. *Cytogenetic and Genome Research* **127**:191-203.

Portugal, J. and Waring, M.J. (1988) Assignment of DNA binding sites for 4′,6-diamidino-2-phenylindole and bisbenzimide (Hoechst 33258). A comparative footprinting study. . *Biochimica et Biophysica Acta (BBA)* **949**:158-168.

Quinn, A.E., Ezaz, T., Sarre, S.D., Graves, J.A.M and Georges, A. (2010) Extension, single-locus conversion and physical mapping of sex chromosome sequences identify the Z microchromosome and pseudo-autosomal region in a dragon lizard, *Pogona vitticeps*. *Heredity* **104**:410-417.

Quinn, A.E., Georges, A., Sarre, S.D., Guarino, F., Ezaz, T. and Graves, J.A.M. (2007) Temperature sex reversal implies sex gene dosage in a reptile. *Science* **316**:411.

Radder, R.S., Quinn, A.E., Georges, A., Sarre, S.D. and Shine, R. (2008) Genetic evidence for co-occurrence of chromosomal and thermal sex-determining systems in a lizard. *Biology Letters* **4**:176-178.

Raudsepp, T., Kijas, J., Godard, S., Guerin, G., Andersson, L. and Chowdhary, B.P. (1999) Comparison of horse chromosome 3 with donkey and human chromosomes by cross-species painting and heterologous FISH mapping. *Mammalian Genome* **10**:277-282.

Reisz, R.R. (1997) The origin and early evolutionary history of amniotes. *Trends in ecology and evolution* **12**:218-222.

Rigby, P.W.J., Dieckmann, M., Rhodes, C. and Berg, P. (1977) Labelling deoxyribonucleic acid to high specific activity in vitro by nick translation with DNA polymerase. *Journal of Molecular Biology* **113**:237-251.

Ruiz-Herrera, A., Nergadze, S.G., Santagostino, M. and Giulotto, E. (2008) Telomeric repeats far from the ends: mechanisms of origin and role in evolution. *Cytogenetic and Genome Research* **122**:219-228.

Sandell, L.L. and Zakian, V.A. (1993) Loss of a yeast telomere: Arrest, recovery and chromosome loss. *Cell* **75**:729-739.

Sankovic, N., Delbridge, M.L., Grutzner, F., Ferguson-Smith, M.A., O'Brien, P.C.M. and Graves, J.A.M. (2006) Construction of a highly enriched marsupial Y chromosome-specific BAC sub-library using isolated Y chromosomes. *Chromosome Research* **14**:657-664.

Sarre, S.D., Georges, A. and Quinn, A.E. (2004) The ends of a continuum: genetic and temperature-dependent sex determination in reptiles. *BioEssays* **26**:639-645.

Schmid, M., Nanda, I., Guttenbach, M., Steinlein, C., Hoehn, H., Schartl, M., Haaf, T., Weigend, S., Fries, R., Buerstedde, J.M., *et al.* (2000) First report on chicken genes and chromosomes 2000. *Cytogenetics and Cell Genetics* **94**:169-218.

Shaw, P.J. and Jordan, E.G. (1995) The nucleolus. *Annual Review of Cell and Developmental Biology* **11**:93-121.

Shedlock, A.M., Botka, C.W., Zhao, S., Shetty, J., Zhang, T., Liu, J.S., Deschavanne, P. and Edwards, S.V. (2007) Phylogenomics of nonavian reptiles and structure of the ancestral amniote genome. *Proceedings of the National Academy of Sciences of the United States of America* **104**:2767-2772.

Shedlock, A.M. and Edwards, S.V. (2009) Amniotes (Amniota). in: *The timetree of life* (Eds S.B. Hedges and S. Kumar), pp. 375-379 (Oxford University Press.

Shetty, S., Griffin, D.K. and Graves, J.A.M. (1999) Comparative painting reveals strong chromosome homology over 80 million years of bird evolution. *Chromosome Research* **7**:289-295.

Sinclair, A.H., Berta, P., Palmer, M.S., Hawkins, J.R., Griffiths, B.L., Smith, M.J., Foster, J.W., Frischauf, A.M., Badge, R.L. and Goodfellow, P.N. (1990) A gene from the human sex-determining region encodes a protein with homology to a conserved DNA-binding motif. *Nature* **346**:240-244.

Smith, C.A., Roeszler, K.N., Ohnesorg, T., Cummins, D.M., Farlie, P.G., Doran, T.J. and Sinclair, A.H. (2009) The avian Z-linked gene DMRT1 is required for male sex determination in the chicken. *Nature* **461**:267-271.

Srikulnath, K., Matsubara, K., Uno, Y., Thongpan, A., Suputtitada, S., Apisitwanich, S., Matsuda, Y. and Nishida, C. (2009a) Karyological characterization of the butterfly lizard (*Leiolepis reevesii rubritaeniata*, Agamidae, Squamata) by molecular cytogenetic approach. *Cytogenetic and Genome Research* **125**:213-223.

Srikulnath, K., Nishida, C., Matsubara, K., Uno, Y., Thongpan, A., Suputtitada, S., Apisitwanich, S. and Matsuda, Y. (2009b) Karyotypic evolution in squamate reptiles: comparative gene mapping revealed highly conserved linkage homology between the butterfly lizard (*Leiolepis reevesii rubritaeniata*, Agamidae, Lacertilia) and the Japanese four-striped rat snake (*Elaphe quadrivirgata*, Colubridae, Serpentes). *Chromosome Research* **17**:975-986.

Steinmann, S. and Steinmann, M. (2005) Retroelements: tools for sex chromosome evolution. *Cytogenetic and Genome Research* **110**:134-143.

Sumner, A.T. (2003) Chromosomes: organization and function. Blackwell Science Ltd, Oxford.

Svartman, M. and Vianna-Morgante, A.M. (1998) Karyotype evolution of marsupials: From higher to lower diploid numbers. *Cytogenetics and Cell Genetics* **82**:263-266.

Trask, B.J. (1991) Fluorescence *in situ* hybridization: applications in cytogenetics and gene mapping. *Trends in Genetics* **7**:149-154.

Uetz, P. (2011) The EMBL reptile database. Internet references. Retrieved from: http://www.reptile-database.org

Varriale, A., Torelli, G. and Bernardi, G. (2008) Compositional properties and thermal adaptation of 18S rRNA in vertebrates. *RNA* **14**:1492-1500.

Veyrunes, F., Waters, P.D., Miethke, P., Rens, W., McMillan, D., Alsop, A.E., Grutzner, F., Deakin, J.E., Whittington, C.M., Schatzkamer, K., *et al.* (2008) Bird-like sex chromosomes of platypus imply recent origin of mammal sex chromosomes. *Genome Research* **18**:965-973.

Waltari, E. and Edwards, S.V. (2002) Evolutionary dynamics of intron size, genome size, and physiological correlates in archosaurs. *American Naturalist* **160**:539-552.

Waterston, R.H., Lindblad-Toh, K., Birney, E., Rogers, J., Abril, J.F., Agarwal, P., Agarwala, R., Ainscough, R., Alexandersson, M., An, P., *et al.* (2002) Initial sequencing and comparative analysis of the mouse genome. *Nature* **420**:520-562.

Wilson, S. and Swan, G. (2008) A complete guide to reptiles of Australia, 2nd. New Holland Publishers (Australia) Pty Ltd, Sydney.

Witten, G.J. (1983) Some karyotypes of Australian agamids (Reptilia: Lacertilia). *Australian Journal of Zoology* **31**:533-540.

Zhang, H-B. and Wu, C. (2001) BAC as tools for genome sequencing. *Plant Physiology and Biochemistry* **39**:195-209.

Appendices

Appendix 1: Confidence levels in BLAST and BLAT analysis of *P. vitticeps* orthologues identified from end sequenced BAC clones.

Library ID	Clone ID	Gene symbol	Confidence category*
Pv, *Pogona vitticeps* (central bearded dragon)	16A1	*HMGCLL1; FAM83B; HCRTR1*	A
	220D7	*TTN*	C
	170F19	*ZNF143; IPO7; TMEM41B*	A
	206D14	*GMPPA*	B
	176E5	*DDX58*	C
	189J12	*TNFRSF11B*	C
	220D15	*NAV2*	C
	221A23	*CTBP2*	C
	16A5	*EIF3H*	C
	201K21	*BCL6*	C
	211I19	*IBSP*	C
	174P24	*KAT2B*	C
	16A11	*SUB1*	C
	200H5	*CA10*	A
	188M22	*IQSEC3*	B
	105P18	*PSMA2*	B
	214G3	*FBRSL1*	C

* Refer to section 2. 4.3.2 for category descriptions

Appendix 2: *P. vitticeps* microchromosome BAC two-colour FISH experiments.

Chromosome	BAC ID	197P21	16A10	221B16	105P18	232P19	220D12	230K11	220D8	214G3	185N3	188M22	236C5	237P23	151D5
7	197P21														
Unknown	16A10	≠													
Unknown	221B16	≠	≠												
Unknown (A)	105P18	≠	≠	≠											
Unknown	232P19	≠	≠	≠	✓										
Unknown	220D12	≠	≠	.	.	.									
Unknown	230K11	≠	≠	≠	.	.	.								
Unknown	220D8	≠	≠	.	.	.	.	.							
Unknown (C)	214G3	.	.	.	.	.	≠	.	.						
Unknown	185N3	.	.	.	.	.	≠	.	.	≠					
Unknown (B)	188M22	.	.	.	.	.	≠	.	.	≠	≠				
Unknown (D)	236C5	.	.	.	.	.	.	.	.	.	.	.			
ZW	237P23	≠	.	.	.	≠	.	.	.	.	.	≠	.		
ZW	151D5	≠	.	.	.	≠	.	.	.	.	.	≠	.	✓	

✓ BAC clones map to the same microchromosome pair
≠ BAC clones map to separate microchromosome pairs
. BACs not yet mapped together in two-colour FISH experiment

Appendix 3: *P. vitticeps* physical map data (refer to section 3.1.5). Female *P. vitticeps* proportional chromosome lengths and relative chromosome sizes. DAPI-stained chromosomes from five female *P. vitticeps* were measured and averaged; chromosome length was calculated as a proportion of the total haploid length, and arm ratio was calculated as the centromeric index (p/total).

Chromosome	*Female*					
	p	Range	*q*	Range	Centromeric index	% Haploid length
Macrochromosomes						
1	9.08 ± 0.21	8.04-9.85	10.35 ± 0.23	9.34-11.36	0.47	19.44
2	4.81 ± 0.10	4.46-5.43	12.45 ± 0.23	11.16-13.64	0.28	17.26
3*	6.75 ± 0.16	5.57-7.32	7.17 ± 0.19	6.20-8.37	0.48	13.91
4*	6.13 ± 0.12	5.77-6.68	6.58 ± 0.16	5.99-7.69	0.48	12.71
5	4.77 ± 0.11	4.18-5.49	5.18 ± 0.12	4.73-5.89	0.48	9.95
6	2.67 ± 0.07	2.38-3.16	3.55 ± 0.14	2.83-4.52	0.43	6.22
Microchromosomes						
7	1.15 ± 0.06	0.96-1.62	1.52 ± 0.07	1.29-1.88	0.43	2.67
8	1.08 ± 0.03	0.95-1.29	1.23 ± 0.06	1-1.59	0.47	2.30
9	1.04 ± 0.03	0.90-1.21	1.17 ± 0.05	0.96-1.48	0.47	2.20
11	0.98 ± 0.04	0.84-1.19	1.09 ± 0.04	0.90-1.29	0.47	2.07
12	0.91 ± 0.04	0.78-1.14	1.11 ± 0.04	0.98-1.30	0.45	2.02
13	0.87 ± 0.04	0.75-1.16	1.05 ± 0.05	0.88-1.39	0.45	1.92
14	0.83 ± 0.05	0.59-1.11	1.03 ± 0.04	0.88-1.24	0.45	1.86
15	0.77 ± 0.03	0.64-0.96	0.93 ± 0.03	0.75-1.07	0.45	1.70
16	0.74 ± 0.03	0.61-0.89	0.82 ± 0.04	0.68-1.16	0.47	1.55
ZW; Sex chromosomes†	1.03 ± 0.05	0.87-1.29	1.27 ± 0.10	1.02-2.14	0.45	2.30

± Following value indicates standard error of the mean.

* Measurements were taken from five separate female metaphases which identified homologs of either chromosome 3 or 4 by mapping of a diagnostic BAC.

† Measurements assigned to chromosome pair based upon putative identification from intrinsic size and DAPI staining properties.

Appendix 4: FISH images of BACs mapped to *P. vitticeps* mitotic metaphase spreads, data were used in the development of the *P. vitticeps* cytogenetic map (section 3.1.5). All scale bars are 10 µm.

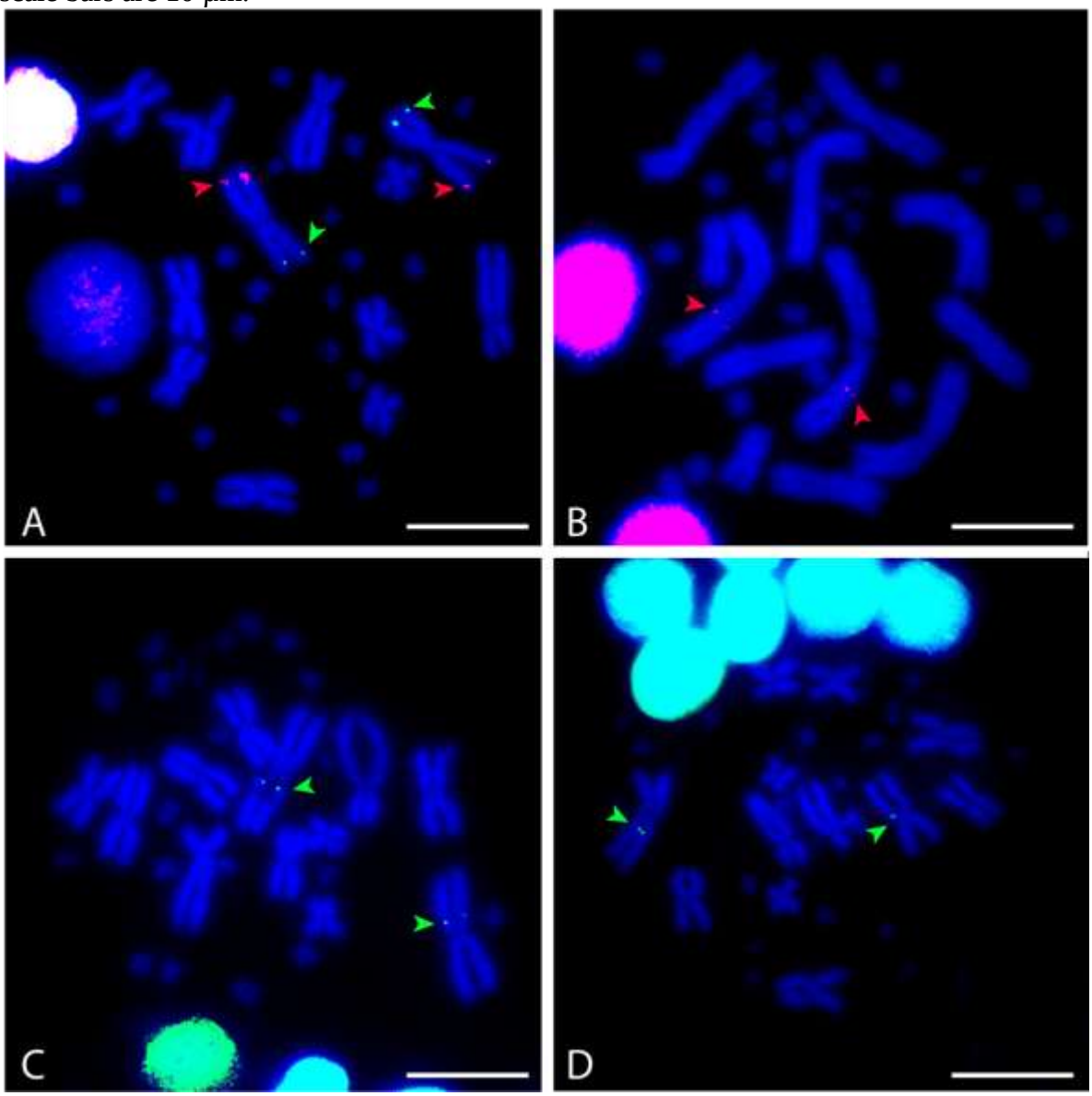

Figure 1. FISH images of chromosome 1 BACs. (A) 57H2 (green) and 222N5 (red); (B) 16A1 (red); (C) 219E3 (green); (D) 16A7 (green).

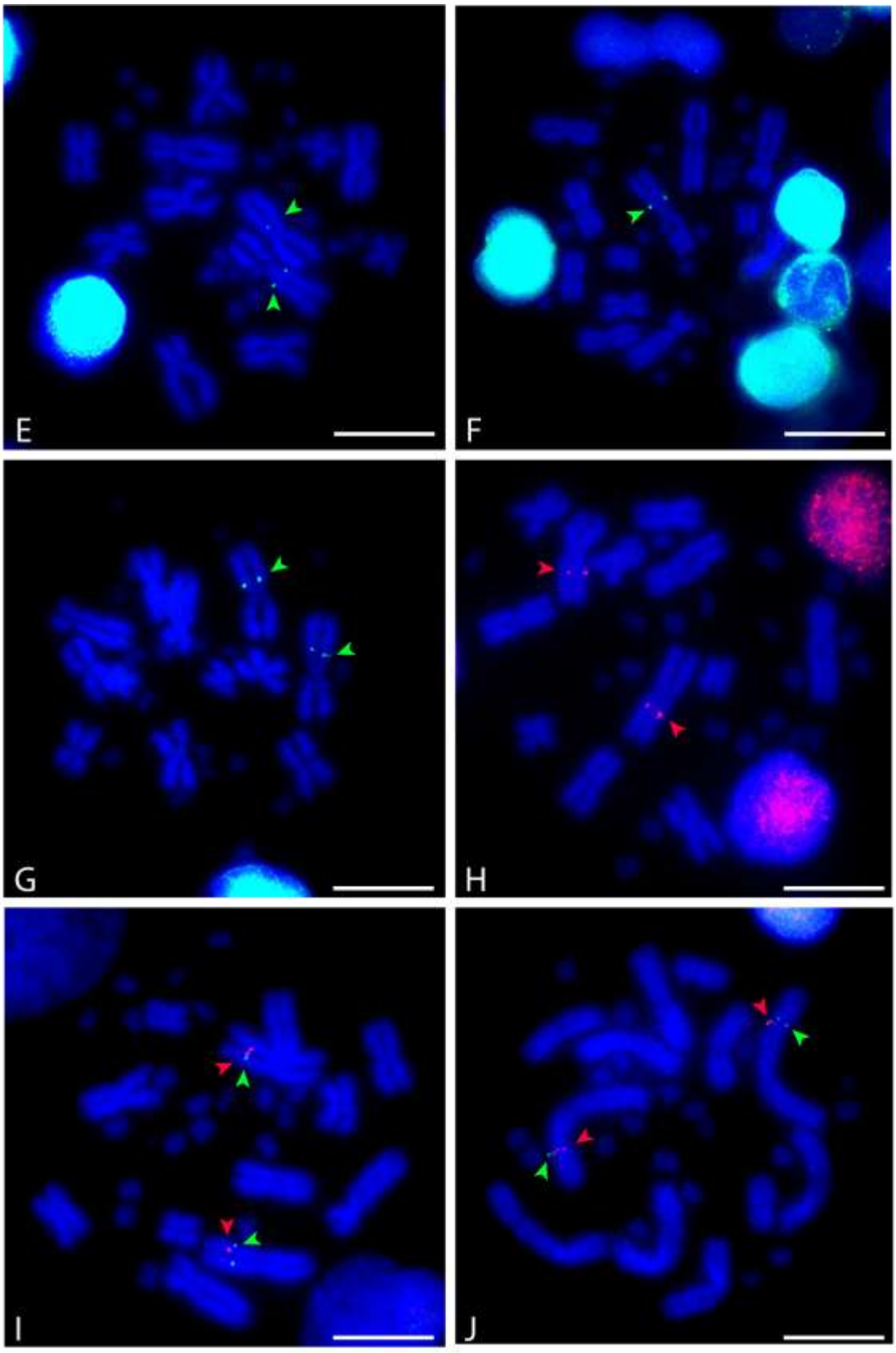

Figure 1 (continued). (E) 220D7 (green); (F) 16A12 (green); (G) 16A9 (green); (H) 215H24 (red); (I) 170F19 (green) and 220D11 (red); (J) 184J20 (green) and 220D11 (red).

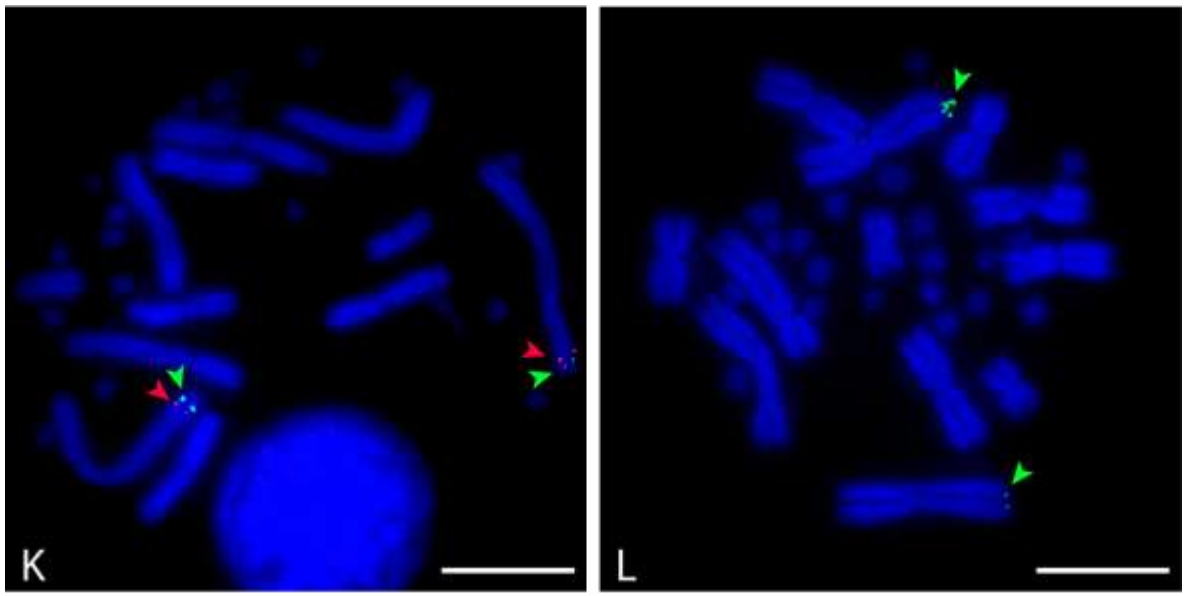

Figure 1 (continued). (K) 232K10 (red) and 229E3 (green); (L) 206D14 (green).

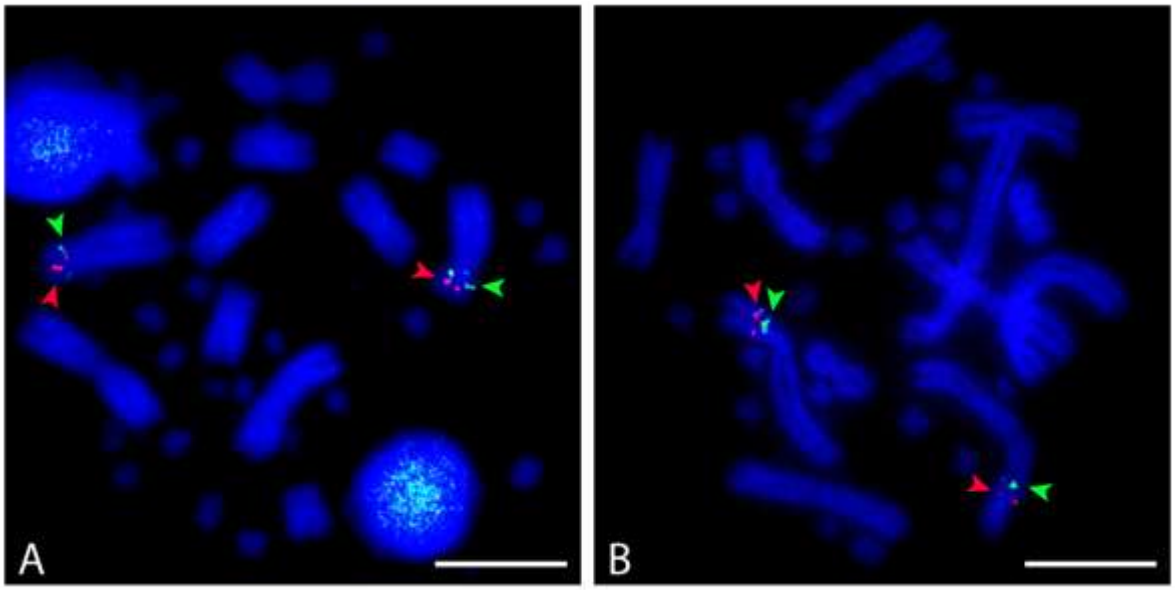

Figure 2. FISH images of chromosome 2 BACs. (A) 201M16 (red) and 16A4 (green); (B) 16A4 (red) and 141L17 (green).

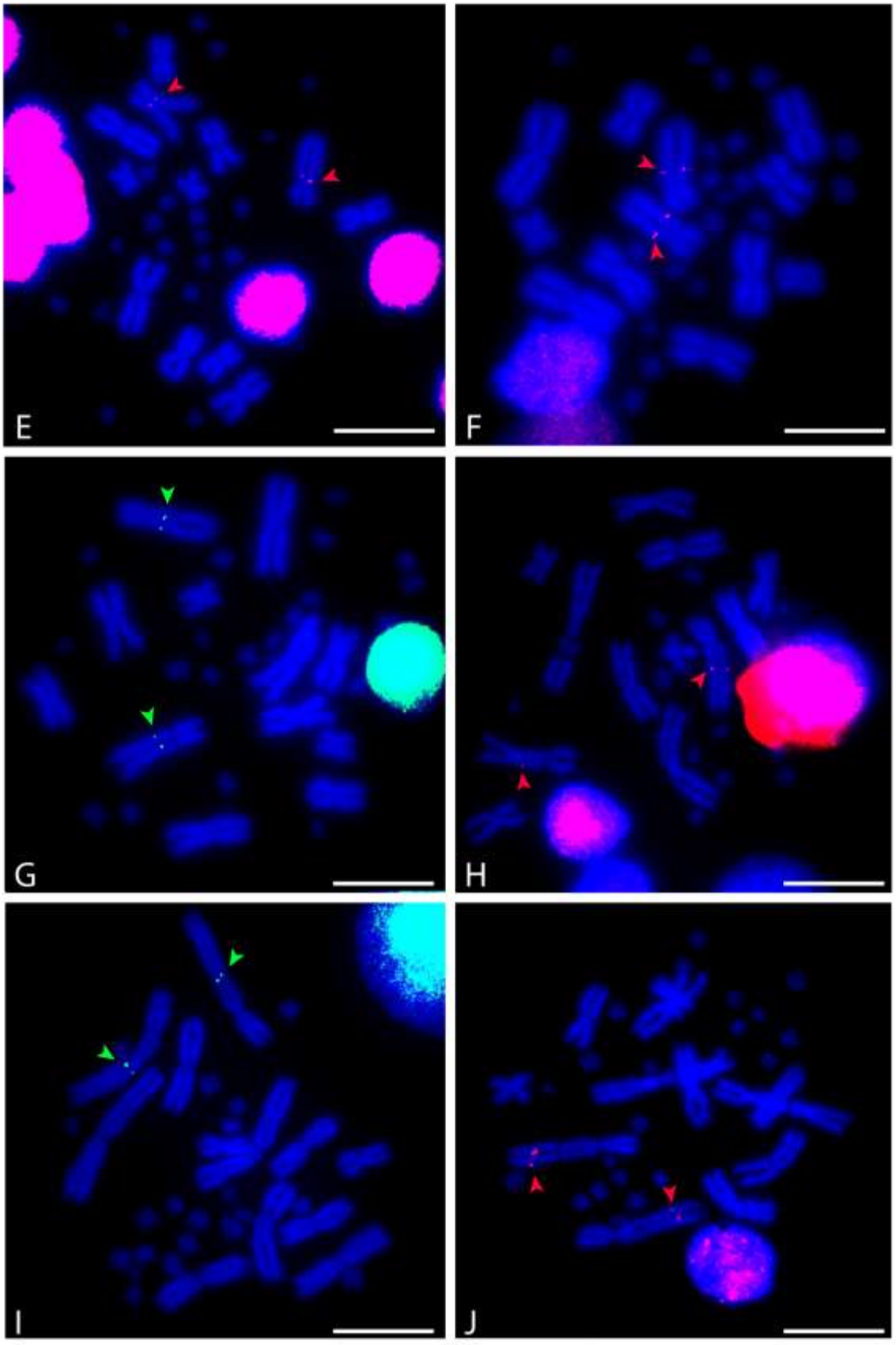
E
F
G
H
I
J

Figure 2 (continued). (C) 176E5 (red); (D) 195K1 (red); (E) 200H9 (green); (F) 203J2 (red); (G) 189J12 (green); (H) 16A23 (red).

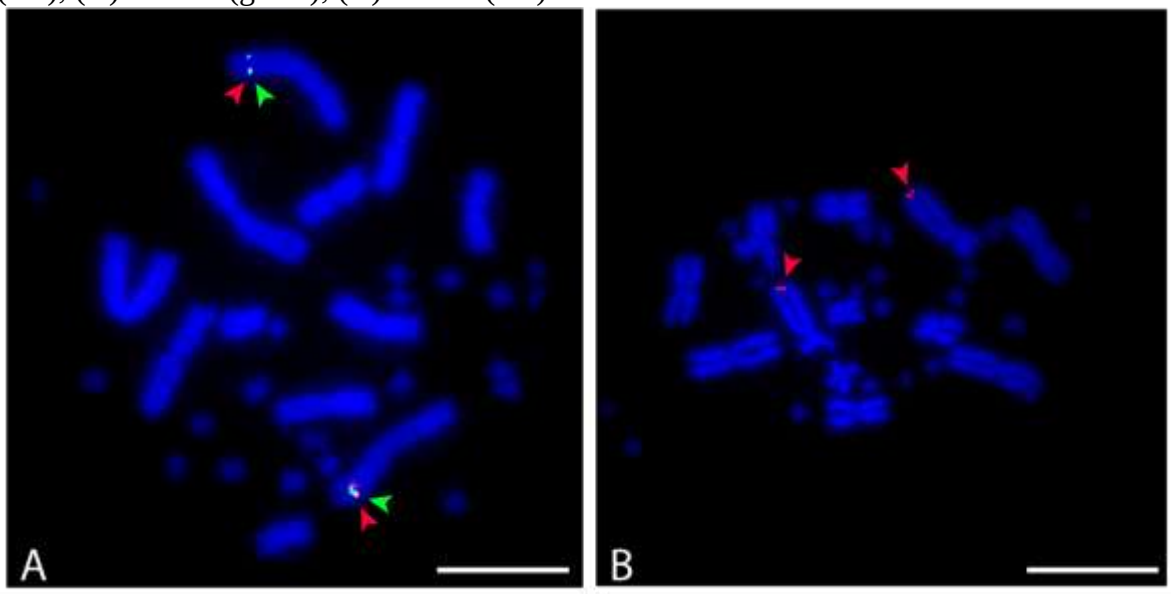

Figure 2 (continued). (I) 238E7 (green) and 219G15 (red); (J) 329J14 (red).

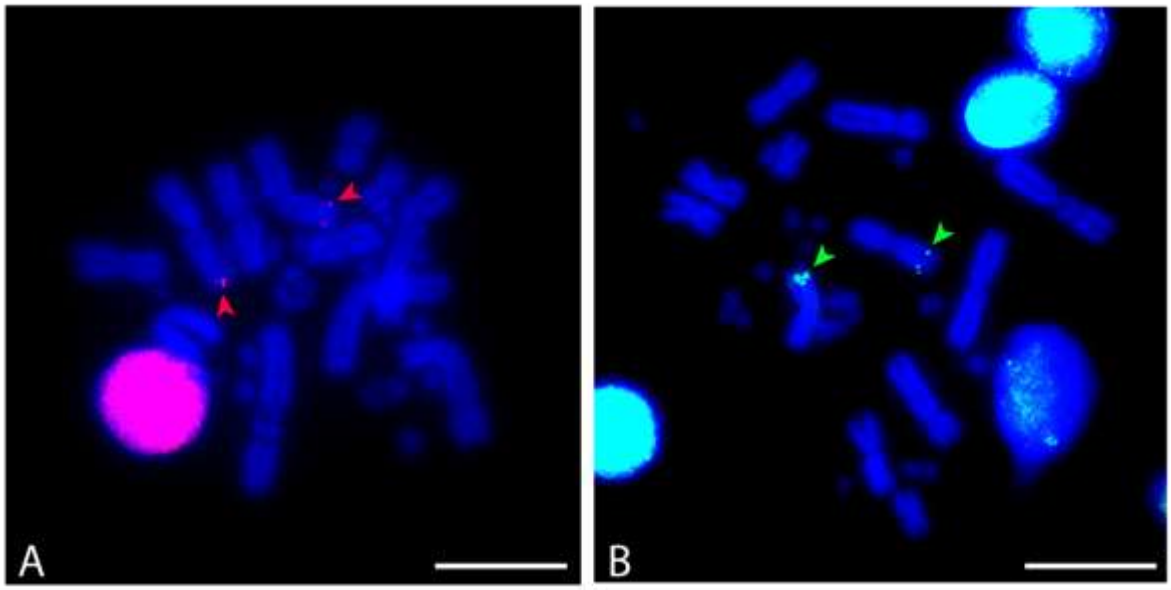

Figure 3. FISH images of chromosome 3 BACs. (A) 199D4 (red); (B) 185A1 (green).

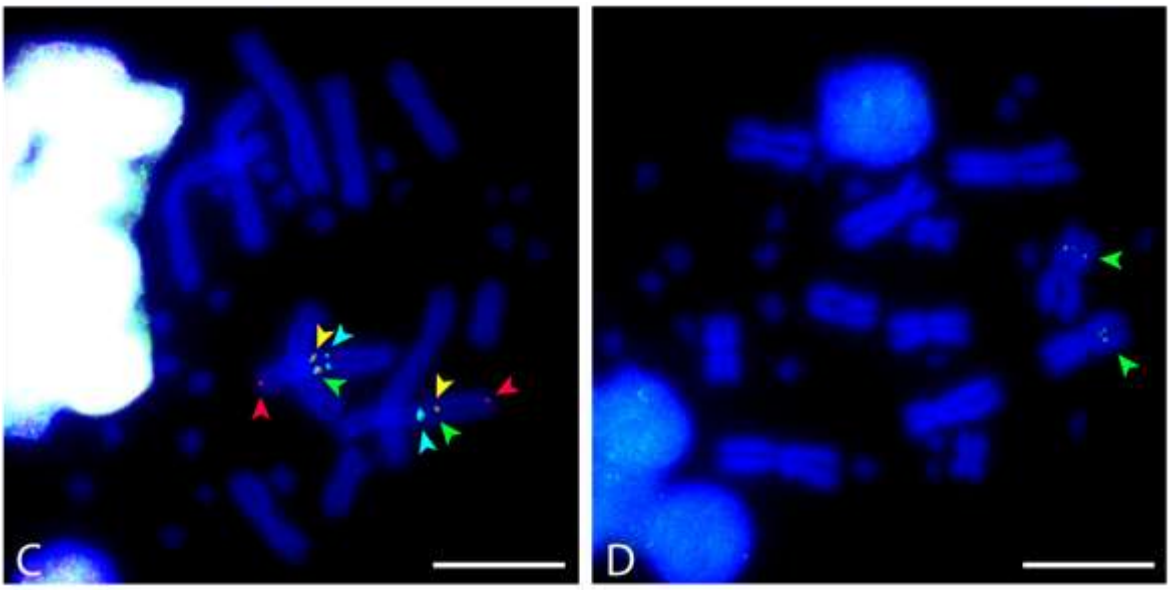

Figure 3 (continued). (C) 220D15 (aqua), 214J17 (yellow), 213B13 (green) and 233A1 (red); (D) 221A23 (green).

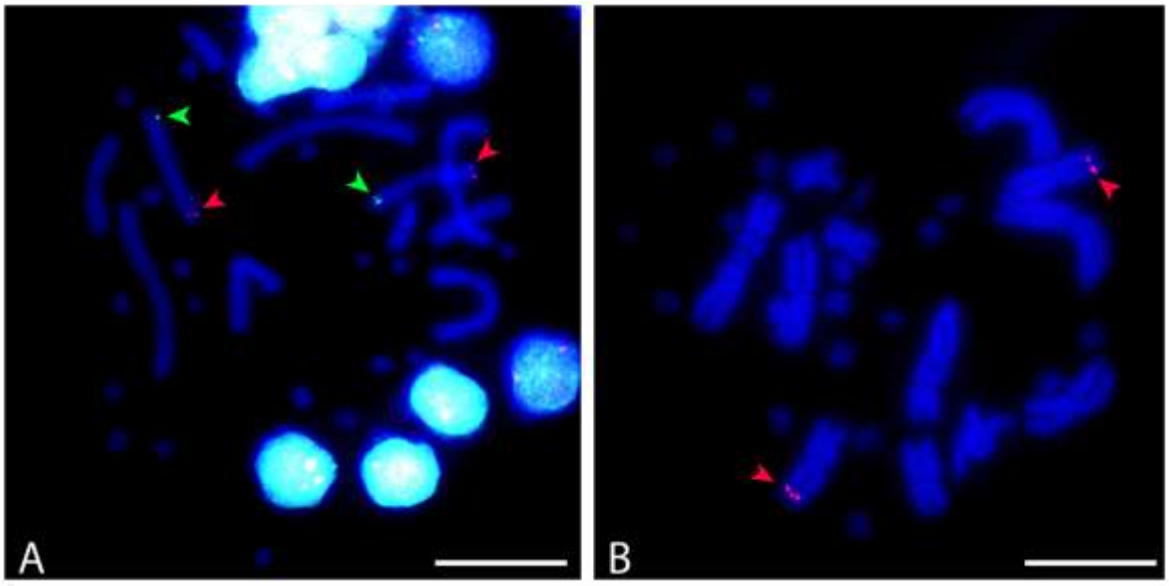

Figure 4. FISH images of chromosome 4 BACs. (A) 219I19 (red) and 240P5 (green); (B) 230L10 (red).

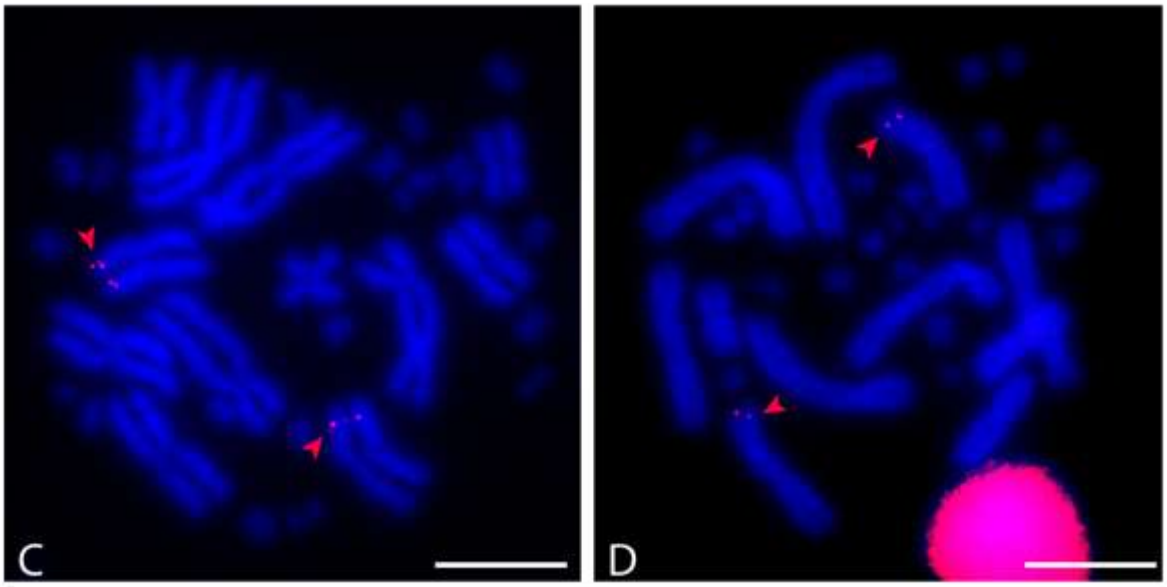

Figure 4 (continued). (C) 219N21 (red); (D) 240P5 (red).

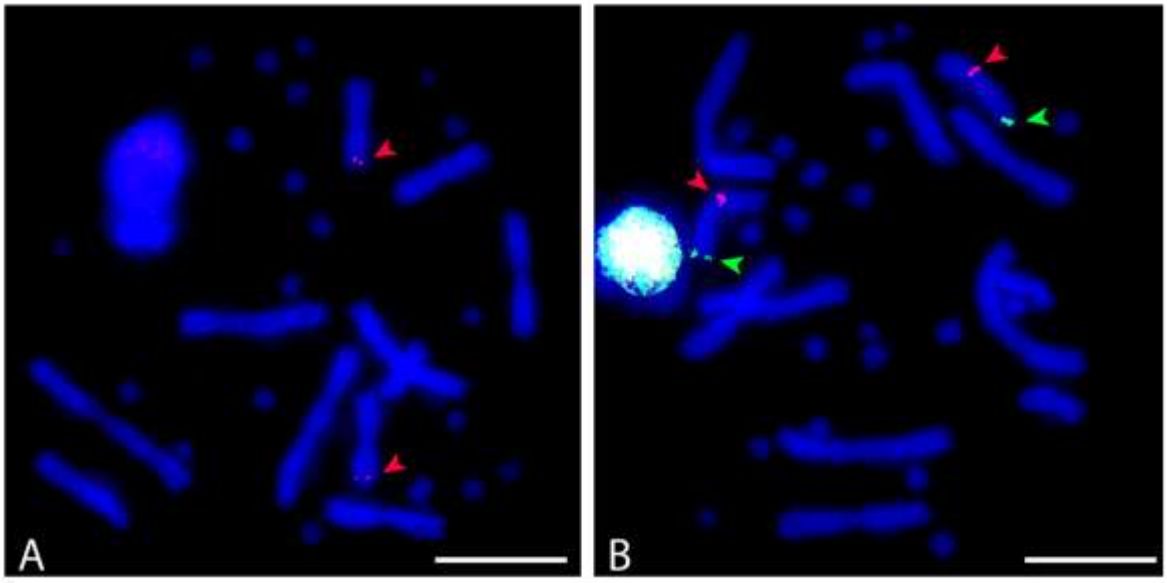

Figure 5. FISH images of chromosome 5 BACs. (A) 16A22 (red); (B) 16A3 (red) and 208G18 (green).

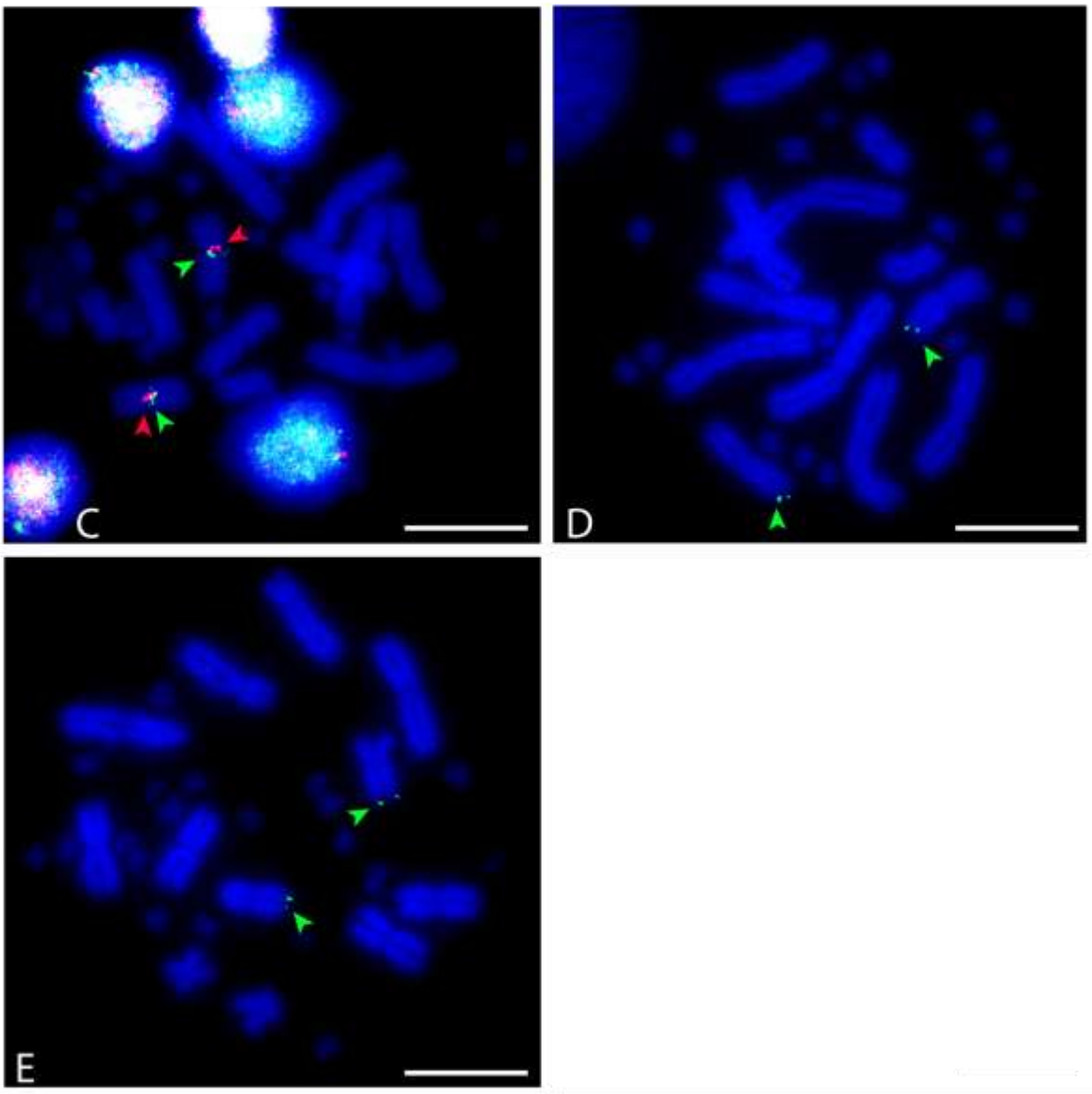

Figure 5 (continued). (C) 220D13 (red) and 201K21 (green); (D) 16A5 (green); (E) 233L23 (green).

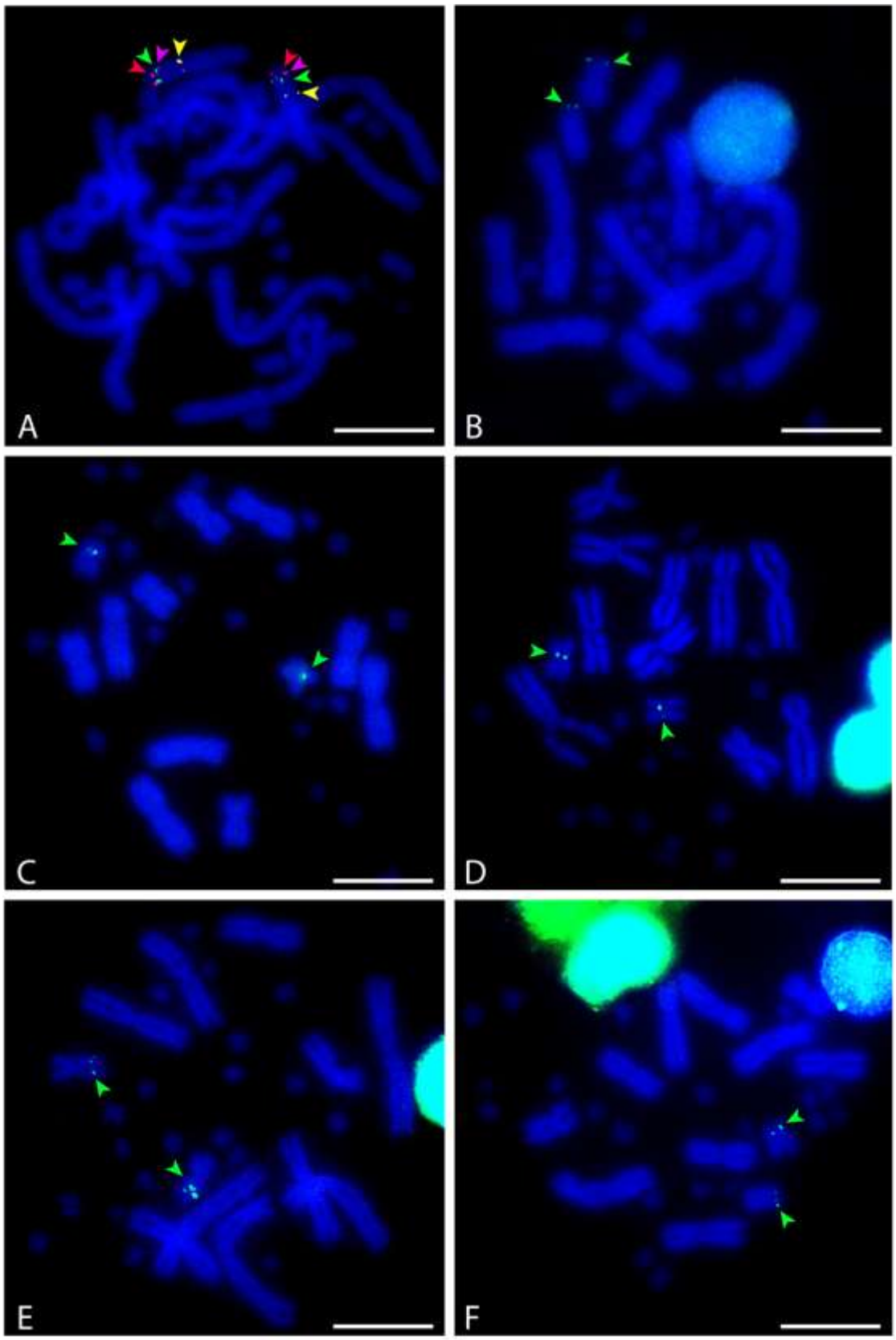
A
B
C
D
E
F

Figure 6. FISH images of chromosome 6 BACs. (A) 198N24 (red), 129O15 (green), 168D8 (magenta), 101M20 (yellow); (B) 211I19 (green); (C) 174P24 (green); (D) 16A11 (green); (E) 212P4 (green); (F) 132P11 (green).

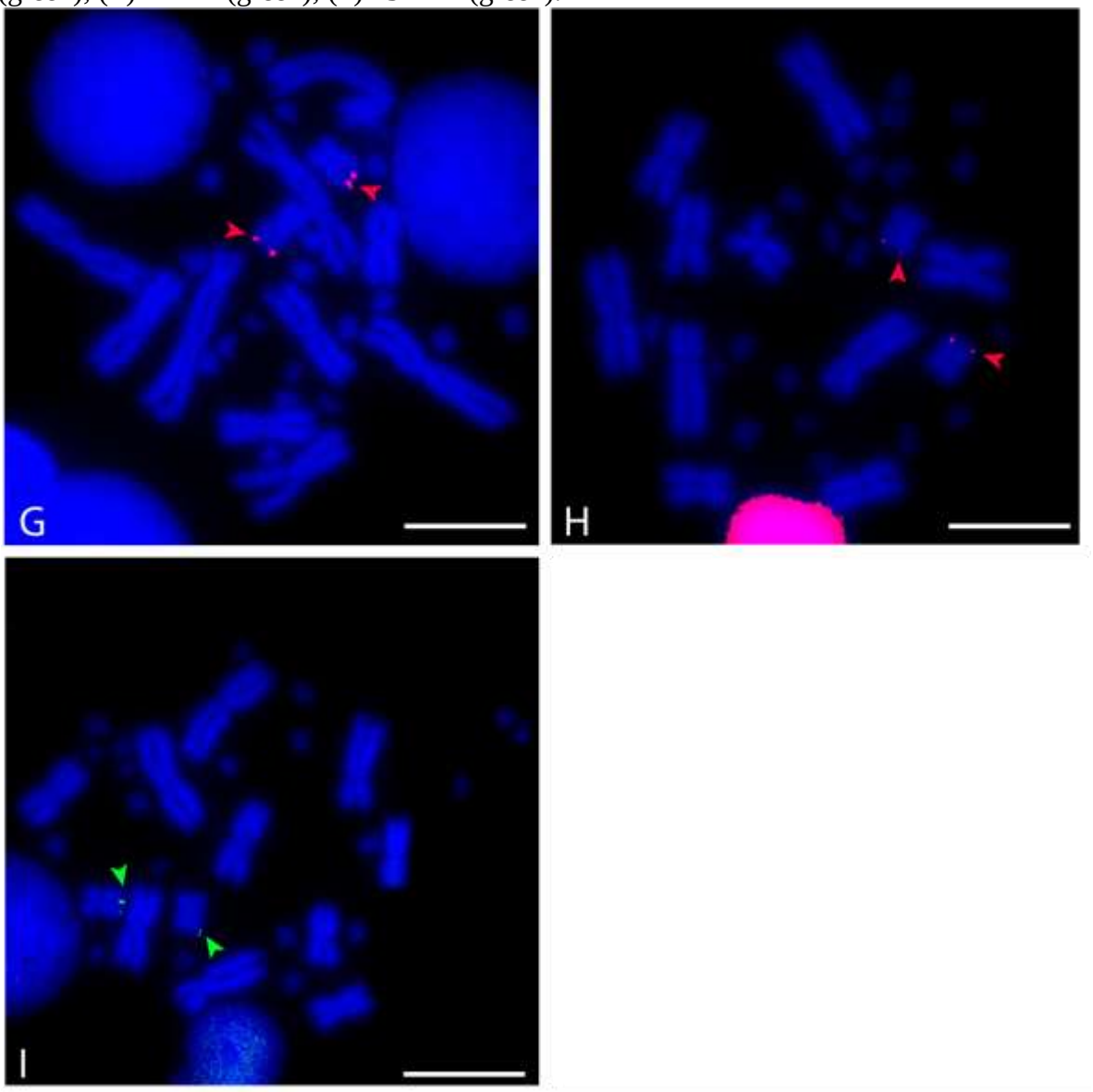

Figure 6 (continued). (G) 225A2 (red); (H) 200O10 (red); (I) 200H5 (green).

Figure 7. (Following page). FISH images of microchromosome BACs. Small arrowheads indicate weak diffuse signal of clones 151D5 and 237P23 on chromosome 2q. (A) 151D5 (green) and 237P23 (red); (B) 221B16 (green), 16A10 (red), 197P21 (magenta), 230K11 (yellow), 232P19 (aqua) and 105P18 (purple); (C) 197P21 (red) and 220D12 (green); (D) 197P21 (red) and 237P23 (green); (E) 185N3 (green), 214G3 (red), 188M22 (purple) and 220D12 (magenta).

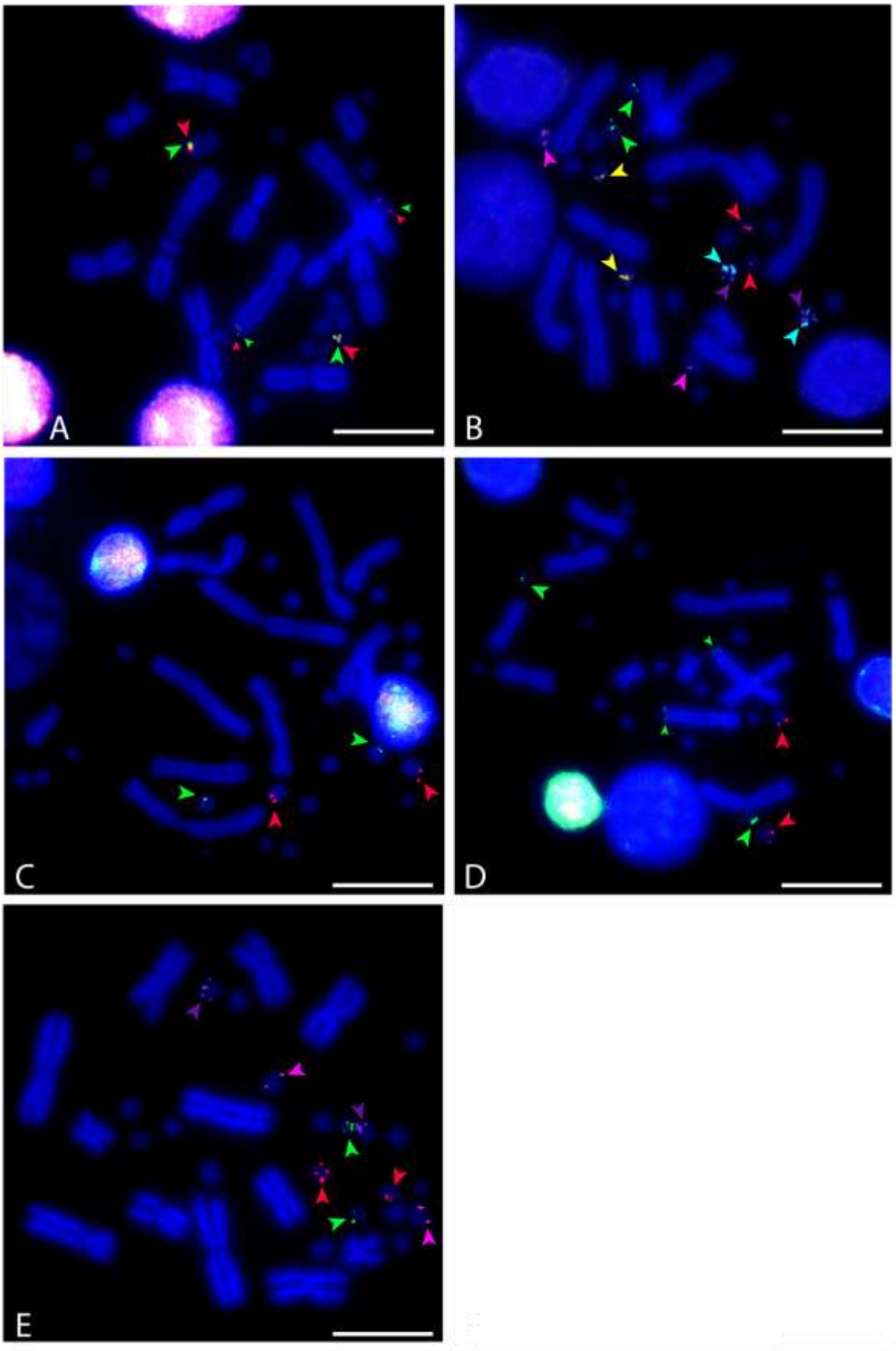
A
B
C
D
E

Appendix 5: FISH images of each BAC mapped to *P. lesueurii* mitotic metaphase spreads. Data were used in the construction of an agamid comparative map (section 3.2.4). All scale bars are 10 µm.

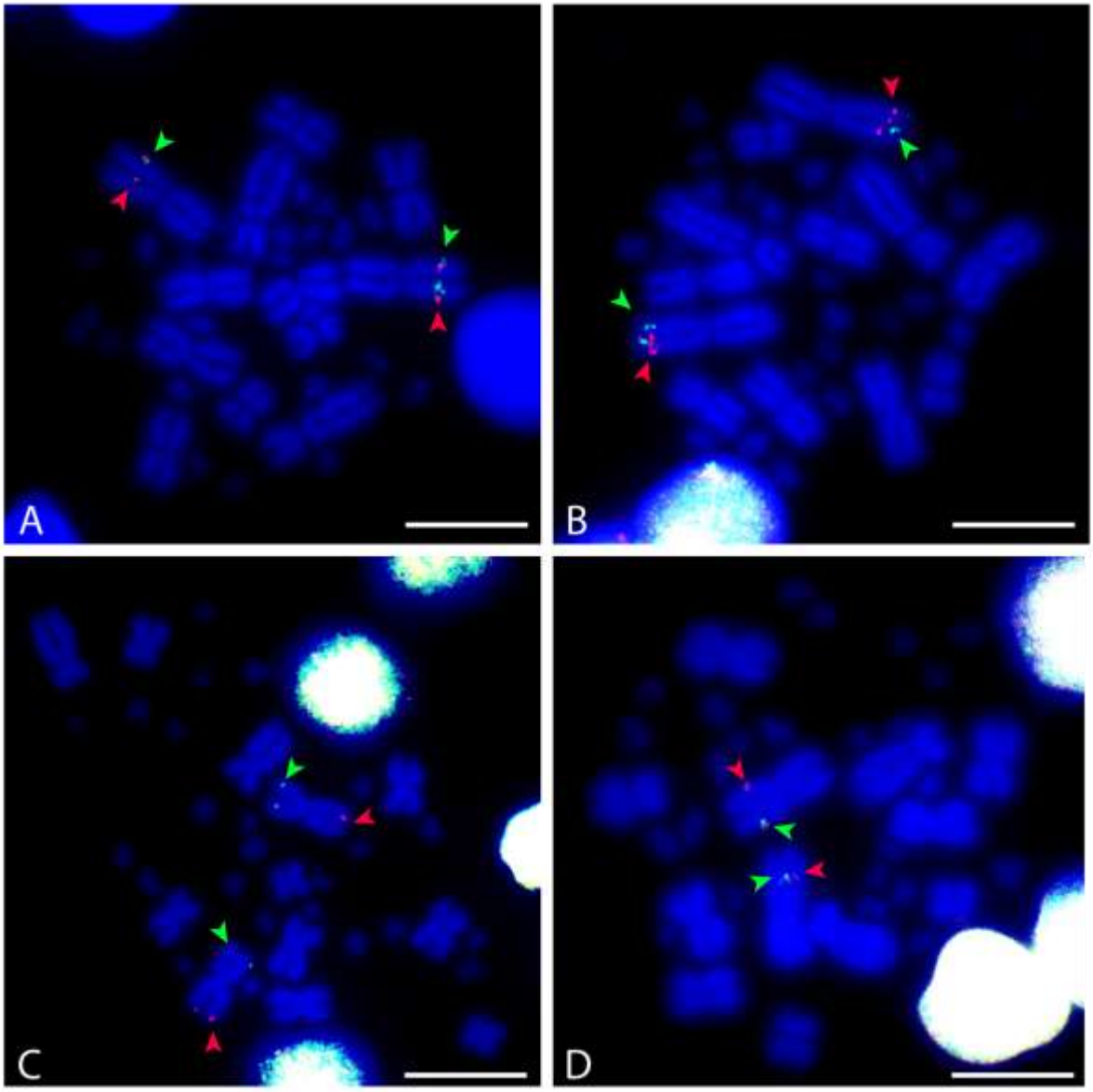

Figure 1. FISH images of chromosome 1 BACs. (A) 220D11 (red), 170F19 (green); (B) 229E3 (red), 232K10 (green); (C) 057H2 (green) and 222N5 (red); (D) 184J20 (green) and 220D11 (red).

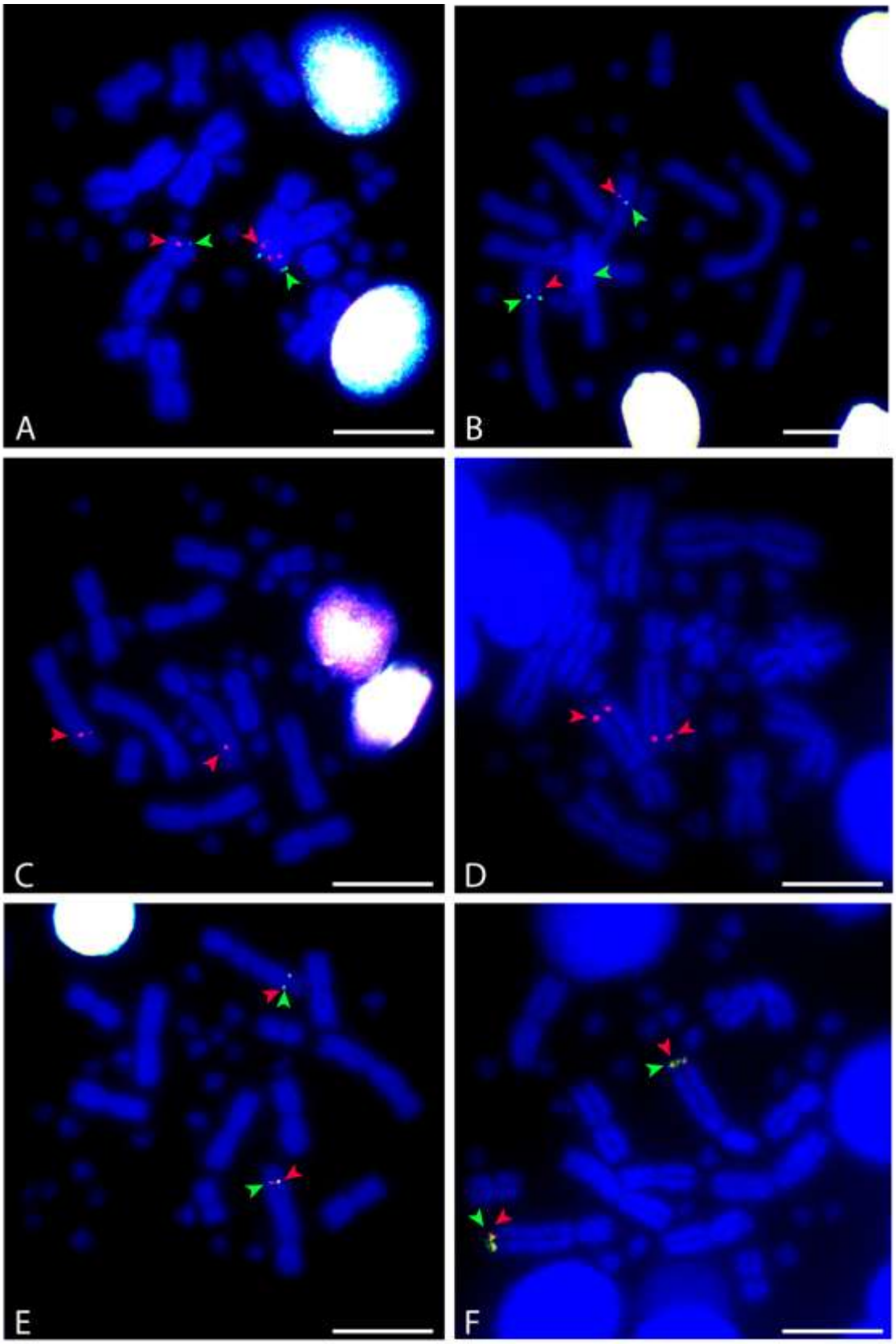
A
B
C
D
E
F

Figure 2. FISH images of chromosome 2 BACs. (A) 107D1 (green) and 126K15 (red); (B) 16A4 (red) and 141L17 (green); (C) 16A23 (red); (D) 329J14 (red); (E) 238E7 (green) and 219G15 (red); (F) 237P23 (green) and 151D5 (red).

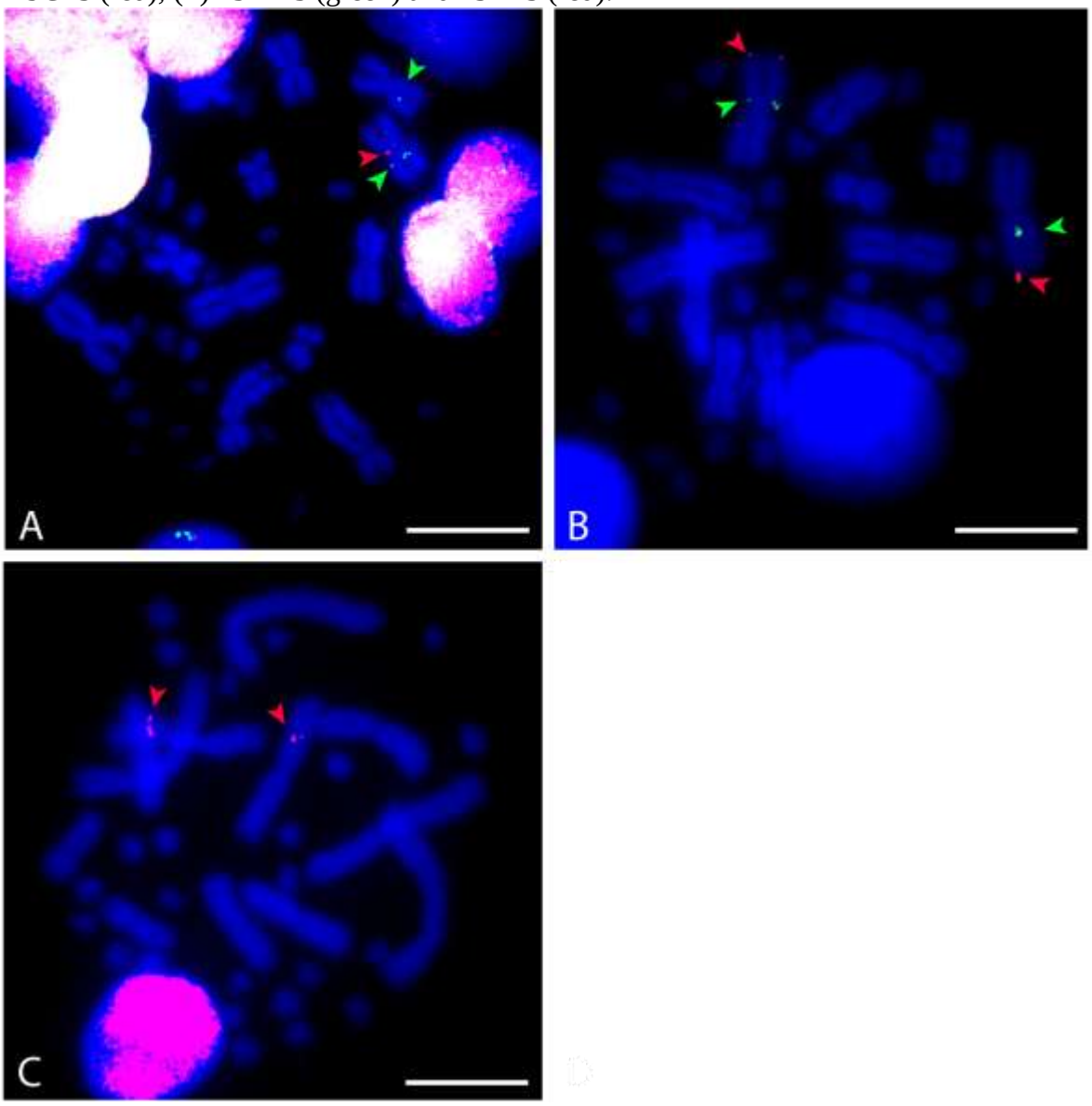

Figure 3. FISH images of chromosome 3 BACs. (A) 220D15 (red) and 214J17 (green); (B) 213B13 (green) and 233A1 (red); (C) 221A23 (red).

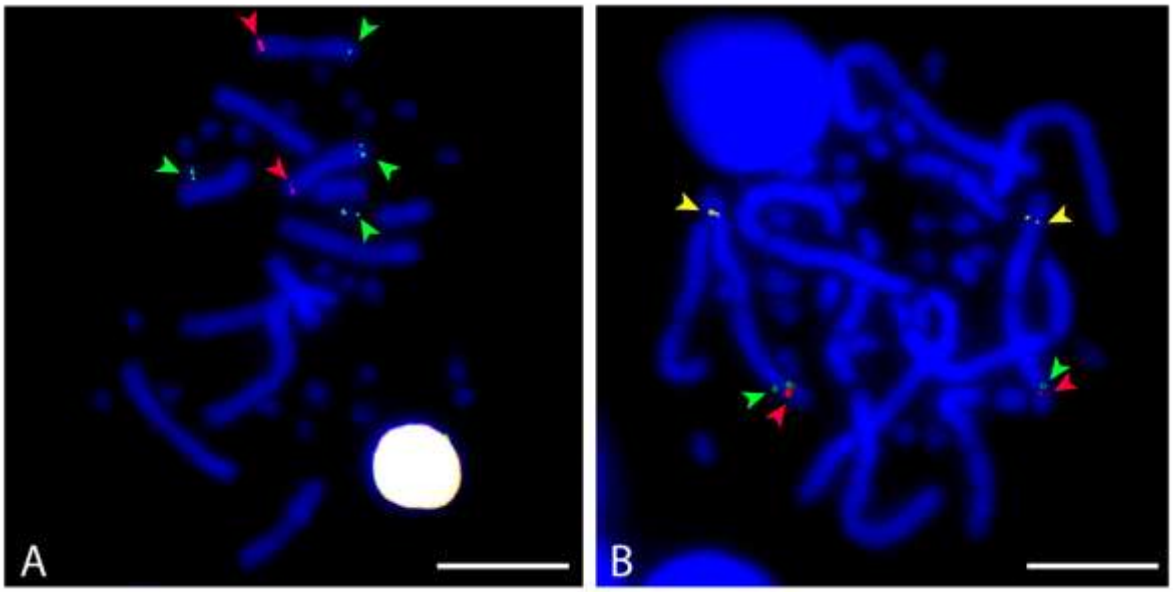

Figure 4. FISH images of chromosome 4 BACs. (A) 240P5 (green) and 219I19 (red); (B) 219N21 (green), 16A5 (red) and 230L10 (yellow).

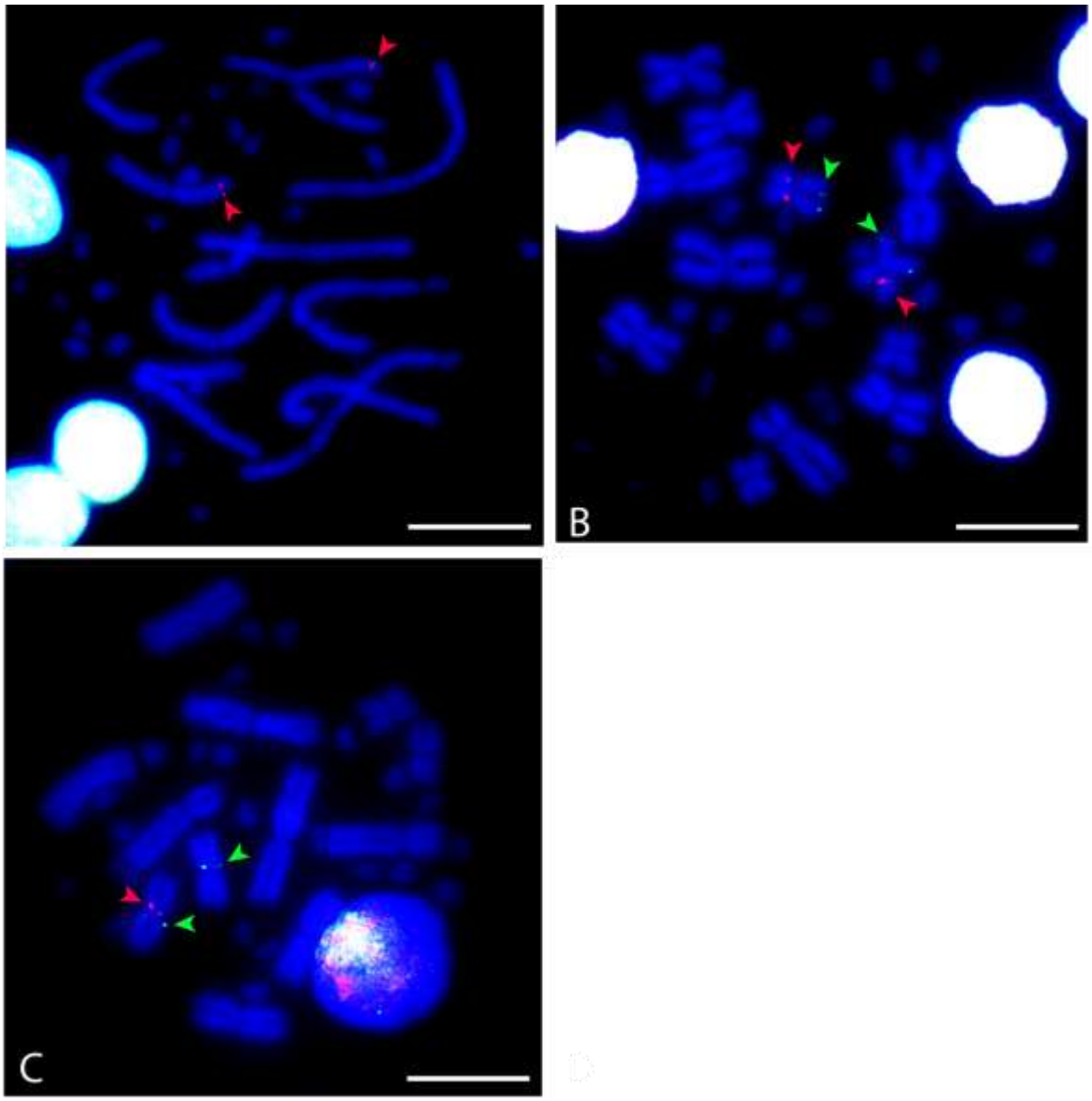

Figure 5. FISH images of chromosome 5 BACs. (A) 16A22 (red); (B) 16A3 (red) and 208G18 (green); (C) 220D13 (red) and 201K21 (green).

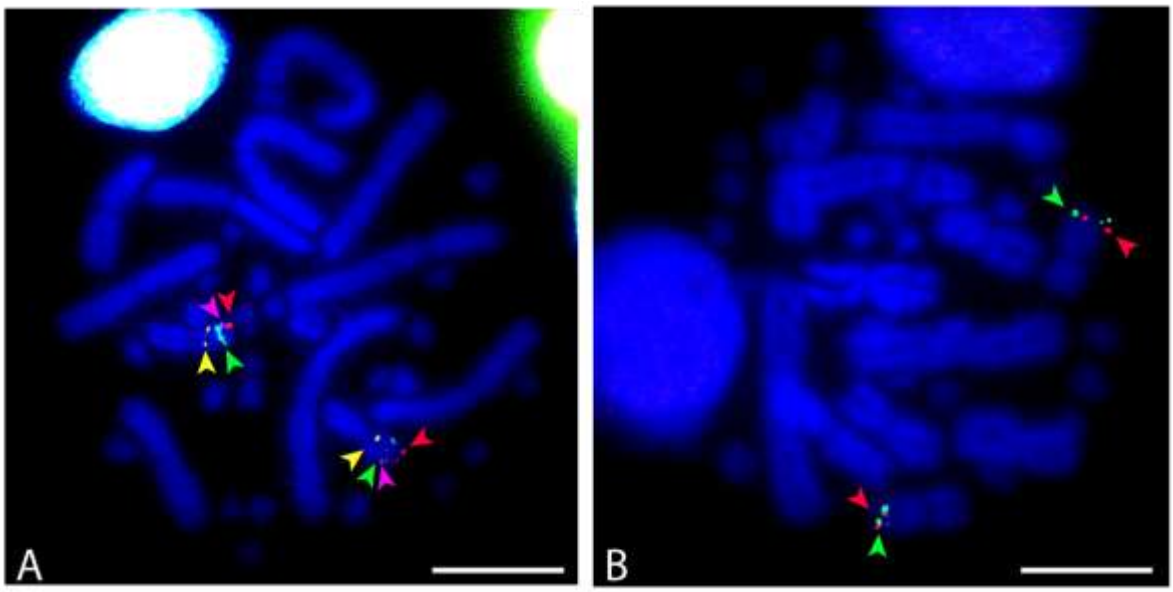

Figure 6. FISH images of chromosome 6 BACs. (A) 198N24 (red), 168D8 (magenta), 129O15 (green), 101M20 (yellow); (B) 200O10 (green) and 200H5 (red).

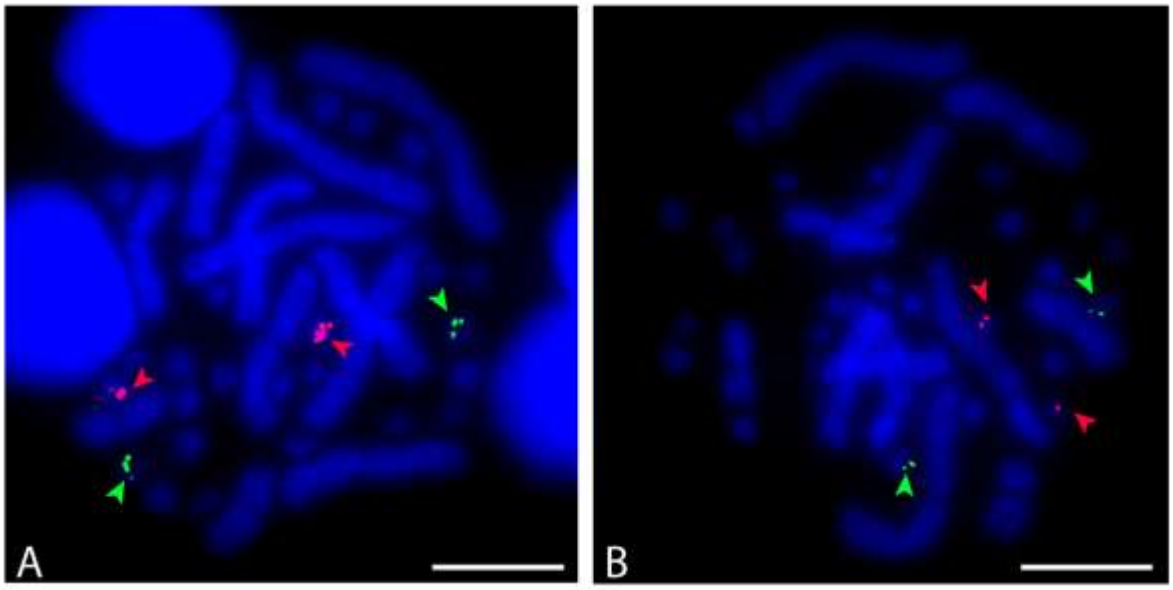

Figure 7. FISH images of microchromosome BACs. (A) 197P21 (red), 230K11 (green); (B) 16A10 (red) and 221B16 (green).

Appendix 5: Male *P. lesueurii* comparative map data (refer to section 3.2.4). Proportional chromosome lengths and relative chromosome sizes. DAPI-stained chromosomes from five male *P. vitticeps* were measured and averaged; chromosome length was calculated as a proportion of the total haploid length, and arm ratio was calculated as the centromeric index (p/total).

Chromosome	*Male*					
	p	Range	*q*	Range	Centromeric index	% Haploid length
Macrochromosomes						
1	7.98 ± 0.21	6.99-8.95	9.23 ± 0.25	7.87-10.01	46.39	17.22
2	4.46 ± 0.15	4.02-5.29	11.56 ± 0.52	9.13-14.01	27.86	16.02
3	6.15 ± 0.18	5.22-7.21	6.31 ± 0.16	5.36-6.87	49.38	12.46
4	5.42 ± 0.08	5.07-5.89	5.77 ± 0.09	5.42-6.25	48.44	11.19
5	4.21 ± 0.06	3.93-4.54	4.94 ± 0.05	4.70-5.16	46.01	9.16
6	2.78 ± 0.06	2.54-3.10	3.67 ± 0.11	3.15-4.18	43.12	6.45
Microchromosomes			*Total*			
7			2.70 ± 0.1	2.43-3.31		2.70
8			2.59 ± 0.08	2.26-3.04		2.59
9			2.51 ± 0.08	2.18-2.91		2.51
10			2.44 ± 0.08	2.10-2.79		2.44
11			2.37 ± 0.07	2.02-2.70		2.37
12			2.30 ± 0.07	1.97-2.55		2.30
13			2.27 ± 0.06	1.97-49		2.27
14			2.22 ± 0.04	1.86-2.30		2.22
15			2.15 ± 0.04	1.85-2.20		2.15
16			2.11 ± 0.04	1.71-2.09		2.11
17			2.00 ± 0.04	1.61-2.03		2.00
18			1.86 ± 0.05	1.35-1.88		1.86

± Following value indicates standard error of the mean.